1964

Conductivity of silver chloride single crystals containing copper(I) or cadmium ions

Henry Cornelis Abbink
Iowa State University

CONDUCTIVITY OF SILVER CHLORIDE SINGLE CRYSTALS CONTAINING COPPER(I) OR CADMIUM IONS

by

Henry Cornelis Abbink

A Dissertation Submitted to the
Graduate Faculty in Partial Fulfillment of
The Requirements for the Degree of
DOCTOR OF PHILOSOPHY

Major Subject: Physical Chemistry

Approved:

Signature was redacted for privacy.

In Charge of Major Work

Signature was redacted for privacy.

Head of Major Department

Signature was redacted for privacy.

Dean of Graduate College

Iowa State University
Of Science and Technology
Ames, Iowa

1964

TABLE OF CONTENTS

TABLE OF CONTENTS (continued)

I. INTRODUCTION

A. Purpose and Nature of this Investigation

Any real crystal at temperatures above absolute zero exhibits departures from perfection in the form of misplaced or missing atoms or ions which are called lattice imperfections or defects. Ionic crystals have been favorable media for the study of lattice defects since the defects are generally charged. Since in most ionic crystals electron conduction is negligible, the study of mobile defects through measurements of the conductivity has contributed much to the present knowledge of lattice defects.

Basic to the study of any phenomenon in which defects are important is the knowledge of the kind of defects present, their concentration, and their mobility. It is now well established that Frenkel defects (interstitial ion plus a vacancy) predominate in silver chloride. The concentration of defects and their mobilities have been determined from an evaluation of the isotherms of conductivity as a function of concentration of a divalent ion additive. However, available values for these parameters were open to question both on experimental and theoretical grounds. One purpose of this investigation was to determine better values for these parameters by the provision

of reliable experimental data and an improved interpretation of the data.

The greatest concern with past experimental data was two-fold: 1) uncertainty of the purity of the pure silver chloride starting material and 2) uncertainties in the concentration of added divalent ion. Since as little as 10 ppm of divalent ion residual impurity in the starting material can significantly affect the results, it is imperative to have pure starting material. In the present investigation, silver chloride was vacuum distilled to yield material with about 0.1 ppm polyvalent impurity. The divalent ion (cadmium) concentration was determined by analysing the actual crystals by activation analysis and atomic absorption spectrophotometry.

The determination of the number of defects and their mobilities from the conductivity data is complicated by the fact that the added cadmium interacts with the vacancies present in the crystal. Past efforts to account for this have not been completely successful. In the present investigation, an attempt has been made to include the Debye-Hückel theory of electrolytes in the description of the interactions. It was anticipated that a successful application of the Debye-Hückel theory would permit a more realistic evaluation of the concen-

trations of defects and their mobilities. The proper description of the interactions between defects and impurities is of course, important in itself.

Earlier work on the conductivity of Cu(I)-doped silver chloride (1) and silver bromide (2) seemed to indicate that an appreciable fraction of the Cu^+ ions went into the crystal interstitially. In order to provide more reliable data on which to base a description of this phenomenon, conductivity measurements were made on vacuum distilled silver chloride which had been doped by a method known to produce only Cu(I), and analyses were performed on the actual crystals.

B. Evidence for Frenkel Defects in Silver Chloride

Most ionic salts conduct charge by the transport of ions through the crystal. Since it was impossible to account for the transfer of charge by ions on the basis of the perfect crystal lattice, it was quite natural for the early workers to suppose that there were intrinsic lattice disorders.

Frenkel (3) proposed that under the influence of thermal agitation, an ion can occasionally acquire enough energy to leave its normal lattice position and occupy an interstitial position. With this model, the intersitital ion under further thermal agitation can acquire enough energy to jump to another

interstitial position. Similarly, a lattice ion next to the vacancy may acquire enough energy to jump into the vacant lattice site, which in effect is a movement of the vacancy. This leads to a mixing of the ions and accounts for diffusion. Such defects also account for the ionic conductivity since in an electric field the positive interstitial has a higher probability of jumping in the field direction; and the vacancy, with a virtual negative charge, has a higher probability of jumping in the opposite direction.

The Frenkel model is not the only one which explains ionic conductivity and diffusion. Schottky (4) proposed that defects may occur by the simultaneous formation of both positive ion and negative ion vacancies by diffusion of the ions to the surface of the crystal. These vacancies can diffuse and respond to an electric field by an argument analogous to the one used for the Frenkel defect.

Both types of defects occur in various ionic systems. In sodium chloride, both the positive and negative ions contribute to the conductivity so transport data (5) alone provided strong evidence for the existence of Schottky-type defects in this system.

In the silver halides, the current is carried entirely by

the silver ion (5, 6). This fact does not distinguish between the two possible types of defects, for Schottky defects with immobile anion vacancies would account for this as well as Frenkel defects in the silver ion sublattice.

The preponderance of evidence now supports the Frenkel model in the silver halides. Strong evidence has long been available from the conductivity measurements by Koch and Wagner (7) on silver bromide. Their work was supported later by the work of Teltow (8) and Kurnick (9) on silver bromide, and Ebert and Teltow (1) on silver chloride. These workers varied the concentration of added divalent halide and found a minimum in the conductivity versus concentration isotherms.

An explanation for the minimum in the conductivity isotherms was possible only on the basis of Frenkel defects. A simple thermodynamic argument (Chapter II) has shown that the product of the vacancy and interstitial concentrations must be constant. When a divalent ion replaces a silver ion, the energetically most feasible method of maintaining electrical neutrality is the creation of a vacancy. The conductivity initially decreases as vacancies are injected with the divalent ions since the more mobile interstitials are suppressed. A minimum is observed since at high concentrations the conduc-

tivity is controlled by the overwhelming number of vacancies, and the conductivity rises in proportion to the number of vacancies.

Nevertheless, a search for Schottky defects in the silver halides was encouraged by Mitchell's (10) postulation of a major role for this type of defect in the photographic process. Lawson's (11) analysis of Strelkow's (12) thermal expansion data and Stasiw's (13) spectral data indicated Schottky defects in silver bromide. However, Christy and Lawson (14) interpreted the temperature dependence of the specific heat of silver bromide in terms of the heat of formation of defects. They concluded from the agreement of their results with the conductivity data of Teltow that Frenkel defects were predominate. Kurnick was able to evaluate the volume change associated with the formation of defects in silver bromide from the pressure dependence of his conductivity data. The volume change was consistent with Frenkel defects.

The most direct method of distinguishing between Frenkel and Schottky defects is the comparison of the macroscopic thermal expansion with that calculated from X-ray data. Since Frenkel defects add no new unit cells in the formation of defects, the thermal expansion coefficients should be identical.

The agreement of the thermal expansion coefficient by both methods was shown for silver bromide by Berry (15) who concluded that Schottky defects could not be present in concentrations higher than ten per cent of the total defects. He was also able to point out a source of error in Lawson's work.

There still was the problem of the anomalous rise in conductivity near the melting point of the silver halides (Fig. 26). It has been thought that this was due to the onset of Schottky defects. For silver chloride, supporting evidence was supplied by the heat capacity measurements by Kobayashi (16) and the thermal expansion data of Zeiten (17). They suggested a Schottky defect concentration of the order of 0.1 mole per cent near the melting point. Layer and Slifkin (18) attributed the enhanced conductivity of silver chloride quenched from near the melting point to frozen-in Schottky defects. However, the comparison of the expansion coefficients determined by X-ray diffraction and dilatation measurements by Nicklov and Young (19) and Fouchaux (20) precluded any appreciable concentration of Schottky defects even near the melting point. The accurate measurements of Fouchaux limited the concentration of Schottky defects to less than 0.045 mole per cent.

C. Review of Related Studies of Defects in Silver Halides

Considered here are experimental methods which provide information on the thermodynamics and the motion defects. Many of the references already cited fall in this category. With a few exceptions, only work pertaining to the intrinsic defect temperature range has been included. This has excluded a large amount of work done at room temperature and very low temperatures where the defects arise primarily from impurities in the sample.

The application of radiotracers to the determination of diffusion coefficients has proved enlightening in several facets of defect studies. Perhaps most important was the verification of the interstitialcy or "indirect interstitial" mechanism proposed by Koch and Wagner (7).

Compton (21) and Compton and Maurer (22) found that in order to have the Nernst-Einstein equation predict the observed relation between the conductivity and diffusion coefficient in silver chloride, it had to be modified by a factor, f,

$$\frac{\sigma}{D} = f \frac{Ne^2}{kT} . \qquad (1)$$

Their value of f was about 1.7. Similar results were obtained by Friauf (23), Miller (24), and Miller and Maurer (25) for silver bromide.

For conductivity by direct interstitial jumps only, the Nernst-Einstein equation would be expected to hold without modification. McCombie and Lidiard (26) pointed out that for the interstitialcy mechanism, the diffusion coefficient is less than calculated by the Nernst-Einstein equation because 1) the charge moves twice the distance of a tracer jump and 2) tracer jumps are not always random so a correlation factor, first proposed by Bardeen and Herring (27), must be introduced. (Often the factor to express the combination of these two effects is called the correlation factor.) For a collinear jump, McCombie and Lidiard calculated a factor of 3.00 for the interstitialcy and 1.25 for the vacancy. Using Teltow's (1) mobility ratio, Lidiard (28) calculated a net factor of 2.3. Calculations by Compaan and Haven (29), Friauf (23, 30), and Lidiard (31) showed that the experimental factor could be explained by assuming contributions from both collinear and noncollinear jumps, but Hove (32) calculated a much higher activation energy for the noncollinear jump. This problem notwithstanding, the evidence clearly supported an interstitialcy mechanism. The factor of 1.25 for the vacancy correlation factor was confirmed by the work of Miller and Maurer (25) on silver bromide doped with cadmium bromide.

Measurement of the anion self-diffusion coefficient in silver chloride by Compton (21), Reade and Martin (33), and Noetling (34); and in silver bromide by Murin and Taush (35) and Tannhauser (36) confirmed the early transport data of Tubandt (5). In all cases the diffusion coefficient of the anion was at least three orders of magnitude less than that of the silver ion.

Before considering diffusion of divalent cations in the silver halides, it is necessary to introduce the concept of "complexes" between divalent ions and vacancies. In the silver halide crystal, a substitutional divalent ion has an excess charge of +1 and the vacancy has an excess charge of -1. If it were not for the thermal energy, every divalent ion would have a vacancy for a nearest neighbor. A vacancy and divalent ion so situated are called a complex and presumably have no charge. At finite temperatures, some of the complexes dissociate into free vacancies and divalent ions. The extent of dissociation depends on the binding energy of the complex.

According to the definition of a complex, a divalent ion must be complexed in order to make a diffusion jump. The problem has been treated theoretically by Lidiard (37), Schone, Stasiw, and Teltow (38), and Teltow (39). Lidiard suggested

that the binding energy of a complex could be evaluated from the dependence of the diffusion coefficient of a given divalent ion tracer on the concentration of that ion in the crystal. Hanlon (40) measured the diffusion coefficient of carrier free Cd^{109}. He found agreement with Lidiard's theory if the mobility was considered a function of concentration. Chemical diffusion measurements (38) could not provide a quantitative test.

Dielectric loss measurements and paramagnetic resonance studies have provided the most direct observation of complexes.

The divalent ion-vacancy complex behaves as an electric dipole. The dielectric loss has been studied by a host of workers, primarily on the alkali halides. Much of the early work was done using low frequencies at low temperatures. Watkins (41) pointed out that any bound vacancy would give a loss peak of some sort, and that some early workers probably observed vacancies bound to precipitated phases. Watkin's own work was done on manganese(II) doped sodium chloride at relatively high temperatures at megacycle frequencies. Unfortunately, work of this caliber has not been done on the silver halides.

Paramagnetic resonance studies are based on the fact that the resonance spectrum of a paramagnetic ion is sensitive to

its immediate surroundings. Again most of the work has been done on the alkali halides. Watkins (42) was able to observe five distinct species of Mn(II) in sodium chloride: 1) manganese chloride aggregates, 2) free manganese ions, 3) manganese ion with a vacancy in a nearest neighbor site, 4) manganese ion with a vacancy in a next-nearest neighbor site, 5) manganese ion located next to a divalent anion impurity.

Paramagnetic resonance of Cu(II) (43) and Mn(II) (44, 45) in silver chloride has been studied. Daehler (45) calculated a binding energy for the Mn(II)-vacancy complex of 0.52 ev.

Measurements of the thermoelectric power of the silver halides doped with various concentrations of divalent halides, have permitted an independent determination of somewhat the same parameters which are determined from conductivity measurements of such samples. Howard and Lidiard (46) and Haga (47, 48, 49) have treated the problem theoretically. Thermoelectric power measurements have been made on silver bromide by Patrick and Lawson (50) and Christy, et al. (51), and on silver chloride by Suzuki, Endo, and Haga (52) and Christy (53). Christy found that the sum of the heats of transport for vacancies and interstitials were surprisingly large and temperature dependent.

It should be apparent from the foregoing that ionic solids

are ideal media for studying defects in solids. Furthermore, the subject of defects in ionic solids is properly regarded as part of the broad study of imperfections in all solids. Defects have been found to be important in a number of phenomena such as chemical reactions in solids, reaction between a solid and gas, and radiation damage. Principles learned from the study of defects in ionic solids can at least be a general guide to the study of defects in other systems such as metals and semiconductors which are of immense practical importance.

D. Activation Analysis

The number of reports of applications of activation analysis to analytical problems has increased dramatically in the last few years. Advancing technology has presented analytical problems which could not be solved readily by conventional chemical methods. Research reactors and other neutron sources have become available to a large number of workers with the result that activation analysis has been successfully applied to more of these problems.

Review articles and bibliographies are numerous. Among the most recent are a review article by Leddicotte (54) and a bibliography by Raleigh (55). Cadmium and copper have been

determined in a number of materials (54, 55). The only application of activation analysis to the simple halides has been the determination of trace impurities in zone refined potassium chloride and potassium bromide (56).

In the present investigation, it was necessary to determine from 20 to 7,000 mole ppm of copper or cadmium in silver chloride, hopefully with an accuracy close to the one per cent with which the conductivity measurements were made. The data in Table 1 indicate the feasibility of the application of activation analysis to this problem.

Table 1. Isotopes useful for activation analysis for cadmium and copper

	Cu^{64}	Cd^{115}
Per cent abundance of target isotope[a]	69.1	28.86
Cross section (barns)[a]	4.1	1.1
Best gamma ray (Mev)[a]	1.02[b]	0.52
Half life (hours)[a]	12.8	53
Disintegrations per minute expected 24 hours after 24 hour irradiation at 10^{12} n/cm^{2}sec of 50 mg of silver chloride doped to 20 mole ppm.	1.2×10^4[c]	1.5×10^4

[a]Data from Trilinear Chart of Nuclides (57).

[b]Positron annihilation sum peak counted with high geometry.

[c]The branching ratio for positron emission is 0.19 (57).

Activation analysis, as generally practiced, involves the simultaneous irradiation of unknowns and standards which are physically similar to the unknowns. The samples are dissolved in a solution containing a known amount of carrier and the interferring radioactivities due to the matrix are removed. After counting, the amount of carrier recovered is determined and the counting rate is corrected. The comparison of the counting rates of the standards and unknowns permits calculation of the amount of element present in the unknown. This general procedure was used in the present investigation.

II. THEORY

The initial portion of this presentation of theory follows closely several sections of the article by Lidiard (28). In some instances, the development here is little more than a catalog of the basic relations necessary to this investigation. For more detail, Lidiard's article or the cited references are recommended.

A. Thermodynamics of Defects and Kinetics of Defect Motion

The formation of Frenkel defects can be represented by the reaction

$$\underset{(N)}{\text{lattice silver ion}} + \underset{(N')}{\text{empty interstitial position}} \overset{K''}{\rightleftharpoons} \underset{(n)}{\text{vacancy}} + \underset{(n)}{\text{interstitial}}, \tag{2}$$

where the quantities in parentheses represent concentrations in no./cc. Chemical thermodynamics gives immediately

$$\frac{n^2}{NN'} = K''(T) = \exp\left(\frac{-\Delta G^o}{RT}\right), \tag{3}$$

where ΔG^o is the standard Gibbs free energy for the reaction. Since in the equilibrium state $n \ll N$ or N', a good approximation for Equation 3 is

$$n^2 = K'(T). \tag{4}$$

A statistical thermodynamic treatment (58, pp. 65-67) gives essentially the same result as Equation 3

$$\frac{n^2}{NN'} = \exp\left(\frac{\Delta S^o_{th}}{k} - \frac{\Delta h^o_f}{kT}\right). \tag{5}$$

Here ΔS^o_{th} is the thermal (vibrational) entropy change and Δh^o_f the enthalpy change due to the formation of a Frenkel defect.

If the number of vacancies and interstitials are not equal, the "solubility product" relation of Equation 4 becomes

$$K'(T) = n_v n_i, \tag{6}$$

where n_v and n_i are the number per unit volume of vacancies and interstitials respectively. A statistical thermodynamic treatment would analogously alter the n^2 factor in Equation 5. Finally, since the mole fraction of defects is small, Equation 6 can be written in terms of the mole fractions of vacancies, x_v, and interstitials, x_i, as

$$K(T) = x_v x_i = x_o^2, \tag{7}$$

where x_o is the mole fraction of either defect in pure silver chloride.

Let us now consider the atomistic theory of the mobility of defects. Fig. 1a shows a schematic representation of the potential of an interstitial ion. It vibrates in the well with frequency, ν, but occasionally acquires enough energy to

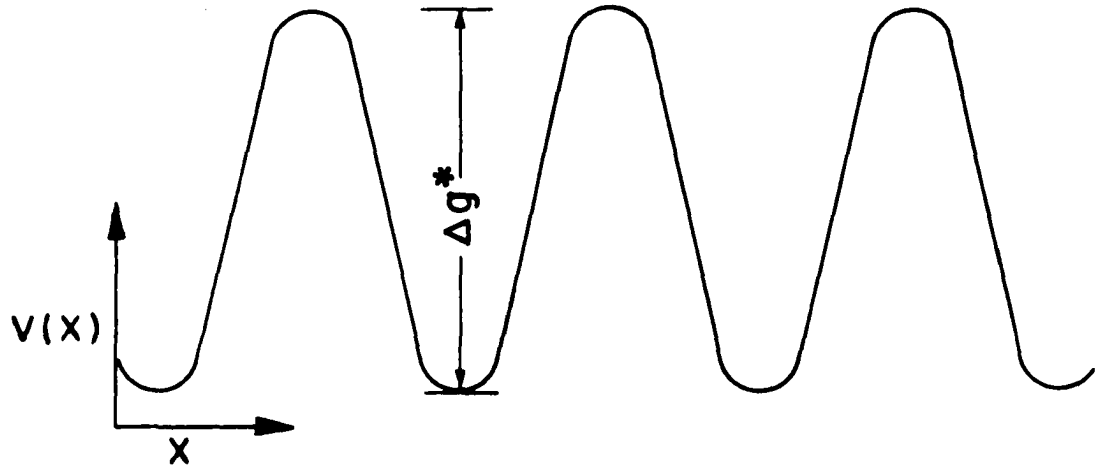

Fig. 1a. Schematic representation of potential of interstitial ion

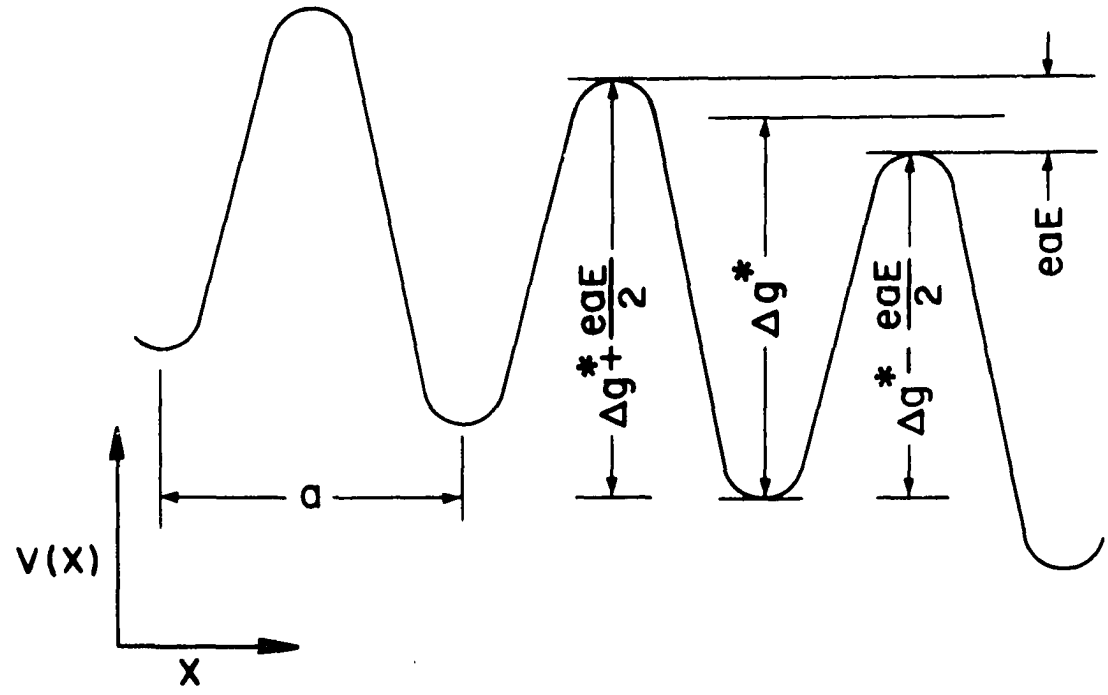

Fig. 1b. Schematic representation of potential of interstitial ion with applied electric field

jump. The frequency of jumps, w, is given by the Boltzman factor times ν (28, p. 277)

$$w = \nu \exp\left(-\frac{\Delta g^*}{kT}\right) . \tag{8}$$

This result is familiar in chemical kinetics. With an applied electric field, E, the potential is altered as shown in Fig. 1b. The net frequency for jumps in the direction of the field is (59, p. 549)

$$p_n = \frac{waeE}{kT} , \tag{9}$$

so the mobility is (28, p. 279)

$$\mu = \frac{a^2 ew}{kT} , \tag{10}$$

or from Equation 8,

$$\mu = \frac{a^2 e\nu}{kT} \exp\left(-\frac{\Delta g^*}{kT}\right) . \tag{11}$$

The temperature dependence of the mobility yields the activation energy for the jump.

An analogous set of relations serves for the motion of the vacancies.

B. Application of Divalent Impurities

1. Simplest theory

Since both the vacancy and interstitial are mobile, the conductivity, σ, at a given temperature is given by

$$\sigma = e(n_v\mu_v + n_i\mu_i), \tag{12}$$

where μ_v and μ_i are the mobilities of the vacancy and interstitial respectively. If N is the number of ion pairs of silver chloride per unit volume, Equation 12 becomes

$$\sigma = Ne(x_v\mu_v + x_i\mu_i). \tag{13}$$

The conductivity of pure silver chloride, σ_o, is

$$\sigma_o = x_o\, Ne(\mu_v + \mu_i). \tag{14}$$

Clearly the concentration of defects must be varied in a controlled manner if x_o, μ_v, and μ_i are to be evaluated.

When a substitutional divalent impurity ion is added, a vacancy is created to maintain electrical charge neutrality. If c is the mole fraction of added divalent impurity, electrical neutrality requires that

$$x_v = c + x_i. \tag{15}$$

Equations 7 and 13 yield

$$x_v = \frac{c}{2}\left(1 + \sqrt{1 + \frac{4x_o^2}{c^2}}\right). \tag{16}$$

Introduction of the mobility ratio $\phi \equiv \mu_i/\mu_v$ and the manipulation of Equations 13, 14, and 16 gives

$$\frac{\sigma}{\sigma_o} = \sqrt{\left(\frac{c}{2x_o}\right)^2 + 1} - \frac{c}{2x_o}\,\frac{(\phi - 1)}{(\phi + 1)}\,. \tag{17}$$

The ratio σ/σ_o is called the relative conductivity.

The general features of Equation 17 are now considered.

At high impurity concentrations, $c \gg x_o$, a linear dependence on c is predicted,

$$\frac{\sigma}{\sigma_o} = \frac{c}{x_o\ (1 + \phi)} \ . \tag{18}$$

The slope as $c \to 0$ is

$$\left[\frac{d(\sigma/\sigma_o)}{dc}\right]_{c \to 0} = \frac{1 - \phi}{2x_o\ (1 + \phi)} \ , \tag{19}$$

which is negative when $\phi > 1$. When $\phi > 1$, there is a minimum in the relative conductivity versus c curve at

$$c_{min} = \frac{x_o\ (\phi - 1)}{\sqrt{\phi}} \tag{20}$$

$$\left(\frac{\sigma}{\sigma_o}\right)_{min} = \frac{2\sqrt{\phi}}{1 + \phi} \ . \tag{21}$$

This simple theory gives at best only semiquantitative agreement with experiment. It does predict the observed minimum and a linear relation between conductivity and concentration when c is large.

2. Simple association theory

The foregoing treatment is naive in neglecting the attraction between the (virtually) oppositely charged divalent cation and vacancy. The concept of a complex between vacancies and divalent ions has already been discussed. As it is applied here, the complexes are neutral and not affected by the electric field. Vacancies which are not complexed are

considered entirely free. The number of free and complexed vacancies is governed by the equilibrium constant for the formation of complexes

$$\text{free vacancy} + \text{free divalent ion} \overset{K_2}{\rightleftharpoons} \text{complex}. \tag{22}$$

The equilibrium constant for this reaction is

$$K_2 = \frac{x_k}{x_v(c - x_k)}, \tag{23}$$

where x_k is the mole fraction of complexes, x_v is the mole fraction of <u>free</u> vacancies, and c is the mole fraction of total divalent ion as before. Equations 7 and 13 are unchanged, but the electrical neutrality condition becomes

$$c - x_k + x_i = x_v. \tag{24}$$

Introducing $\xi \equiv x_v/x_o$ and $H \equiv x_o K_2$, equations 7, 23, and 24 give

$$\frac{c}{x_o} = \left(\xi - \frac{1}{\xi}\right)(1 + H\xi). \tag{25}$$

With $\phi \equiv \mu_i/\mu_v$ as before, Equations 7, 13, and 14 yield

$$\frac{\sigma}{\sigma_o} = \frac{\xi + \phi/\xi}{1 + \phi}. \tag{26}$$

Differentiation of the above equation gives

$$\left(\frac{\sigma}{\sigma_o}\right)_{min} = \frac{2\sqrt{\phi}}{1 + \phi}. \tag{27}$$

Equations 21 and 27 are identical; association does not affect the determination of ϕ from the minimum in the conductivity

versus concentration curve. With ϕ determined by Equation 27, ξ can be calculated as a function of c by the use of Equation 26. Then according to Equation 25, x_o is the intercept and $x_o H$ is the slope of a plot of $c/(\xi - 1/\xi)$ versus ξ. The simple association theory incorrectly predicts a $c^{\frac{1}{2}}$ dependence of conductivity on concentration at large concentrations.

3. Application of Debye-Hückel theory

It is well known that aqueous solutions of electrolytes exhibit departures from ideality, even at very low concentrations, due to the coulombic attraction between oppositely charged ions. The Debye-Hückel theory has been applied to these solutions with considerable success in dilute solutions.

Analogously, charged lattice defects can be regarded as dissolved in the silver chloride which is considered to be a uniform dielectric with dielectric constant D. Equations 7 and 23 must be altered by the addition of activity coefficients. Equation 7 becomes

$$\gamma_v x_v \gamma_i x_i = K, \tag{28}$$

where γ_v and γ_i are the activity coefficients of the vacancy and interstitial respectively. The interaction between defects in the pure silver chloride is not neglected. For this

case, Equation 28 becomes

$$\gamma_o^2 x_o^2 = K = x_{oo}^2, \tag{29}$$

where γ_o is the activity coefficient, x_o the mole fraction of defects in the pure material, and x_{oo} is the hypothetical mole fraction of defects in the absence of interactions. Equation 23 becomes

$$\frac{x_k}{\gamma_v x_v \gamma_c (c - x_k)} = K_2, \tag{30}$$

where γ_c is the activity coefficient of free divalent ions and the activity coefficient of the neutral complex is taken to be unity.

A theoretical formula for the activity coefficient in solutions of electrolytes in which the ions are uniform, rigid spheres of diameter, R, is given by Debye and Hückel (60) as

$$\ln \gamma = - \frac{e^2}{2DkT} \frac{\kappa}{(1 + \kappa R)}, \tag{31}$$

where κ is the Debye-Hückel screening constant. R is effectively a distance of closest approach of ions. Since vacancies which come within the nearest neighbor distance of the divalent ion are considered to be complexed, R must be chosen to be equal to this distance. The screening constant is given by

$$\kappa^2 = \frac{4\pi e^2 (x_i + x_v + c - x_k)}{VDkT} = \frac{8\pi e^2 x_v}{VDkT}, \tag{32}$$

where V is the volume per ion pair. Furthermore,

$$\ln\gamma_i = \ln\gamma_v = \ln\gamma_c = \ln\gamma \tag{33}$$

Numerical values can be inserted into Equations 31 and 32 to give

$$\log_{10}\gamma = - \frac{1.1363 \times 10^7 \sqrt{x_v}}{(DT)^{3/2} (1 + \kappa R)} \tag{34}$$

and, in cm^{-1},

$$\kappa = \frac{3.1322 \times 10^{10} \sqrt{x_v}}{\sqrt{DT}} \tag{35}$$

The mobilities are assumed to be unaffected by the Debye Hückel charge cloud. Equations 28, 29, and 30 are used instead of Equations 7 and 23 in the derivation of the relations of the association theory. With the redefinitions of $\xi \equiv x_v/x_{oo}$ and $H \equiv x_{oo}K_2$, it is easily shown that

$$\frac{c}{x_{oo}} = \left(\gamma^2 \xi - \frac{1}{\xi}\right)\left(H\xi + \frac{1}{\gamma^2}\right) \tag{36}$$

and

$$\frac{1}{\gamma_o}\left(\frac{\sigma}{\sigma_o}\right) = \frac{\xi + \phi/\xi\gamma^2}{1 + \phi} \tag{37}$$

These relations are formally the same as Equations 25 and 26 with the addition of activity coefficients. But since γ is a function of x_v which is in turn a complicated function of H, x_{oo} and c, these equations are solvable only by a numerical method.

The Debye-Hückel theory has its limitations. In addition, some valid objections can be raised to the adaptation presented

here. Both these problems are discussed later.

C. Theory of Conductivity of Cu(I) Doped Silver Chloride

1. Omission of Debye-Hückel interactions

It is assumed that there is an equilibrium distribution of copper between substitutional lattice sites and interstitial sites. Since a vacancy must be formed with an interstitial copper ion, the reaction is:

$$\underset{(C_\ell)}{\text{substitutional copper ion}} \overset{K_I}{\rightleftharpoons} \underset{(C_i)}{\text{interstitial copper ion}} + \underset{(x_v)}{\text{vacancy}}. \tag{38}$$

The quantities in parenthesis are the concentrations of the species in mole fraction. The equilibrium constant is

$$K_I(T) = \frac{x_v C_i}{C_\ell} \tag{39}$$

The product of the concentration of vacancies and (silver) interstitials is still constant as given by Equation 7. Electrical neutrality requires that

$$x_v = x_i + C_i. \tag{40}$$

Substitution for x_i from Equation 7 with the use of $\xi \equiv x_v/x_o$ gives

$$C_i = x_o \left(\xi - 1/\xi \right). \tag{41}$$

Since a substitutional copper ion plays the role of a normal silver ion, its mobility is assumed to be negligible.

An interstitial copper ion presumably is mobile with mobility μ_c. The conductivity is then given by

$$\sigma = Ne(x_v\mu_v + x_i\mu_i + C_i\mu_c). \tag{42}$$

With σ_o given by Equation 14, $\xi \equiv \mu_i/\mu_v$ as before, $\chi \equiv \mu_c/\mu_v$, and the use of Equation 41; one finds

$$\frac{\sigma}{\sigma_o} = \frac{1}{1+\phi}\left[\xi + \frac{\phi}{\xi} + \chi\left(\xi - \frac{1}{\xi}\right)\right] \tag{43}$$

By setting $\frac{d(\sigma/\sigma_o)}{d\xi} = 0$, one obtains

$$\chi = \frac{\phi - \xi_{min}^2}{1 + \xi_{min}^2}, \tag{44}$$

where the subscript indicates evaluation at the minimum in the conductivity isotherms. Substitution from Equation 44 into Equation 43 gives

$$\xi_{min} = \frac{1 + \sqrt{1 - (\sigma/\sigma_o)_{min}^2}}{(\sigma/\sigma_o)_{min}}, \tag{45}$$

i.e., only $(\sigma/\sigma_o)_{min}$ and ϕ are necessary for the evaluation of χ. Although independent data are required to evaluate it, an equilibrium constant for the formation of complexes between the vacancy and copper interstitial is included. The reaction for the formation of complexes is

$$\text{copper interstitial} + \text{vacancy} \overset{K_C}{=} \text{complex}. \tag{46}$$

Then

$$K_C = \frac{C_c}{C_i x_x}. \tag{47}$$

If the mole fraction of copper added to the crystal is C

$$C = C_\ell + C_i + C_c. \tag{48}$$

The combination of Equations 39, 41, 47, and 48 gives

$$K_I = \frac{1}{f(C,\sigma/\sigma_o) - K_C}, \tag{49}$$

where

$$f(C,\sigma/\sigma_o) = \frac{C}{x_o^2\,(\xi^2 + 1)} - \frac{1}{x_o\xi} \tag{50}$$

and ξ is determined by rearrangement of Equation 42,

$$\xi = (\sigma/\sigma_o)(1 + \phi) \pm \frac{\sqrt{(\sigma/\sigma_o)^2(1 + \phi)^2 + 4(1 + \chi)(\chi - \phi)}}{2(1 + \chi)}. \tag{51}$$

The negative sign is taken at concentrations less than the minimum and the positive sign at higher concentrations.

The constancy of $f(C, \sigma/\sigma_o)$ serves to test the model. With insufficient information, K_C is taken to be zero.

2. Inclusion of Debye-Hückel interactions

As before, the activity coefficient γ, is defined by Equation 31 and κ is given by

$$\kappa^2 = \frac{4\pi e^2(x_i + C_i + x_v)}{VDkT} = \frac{8\pi e^2 x_v}{VDkT}. \tag{52}$$

Equation 39 becomes

$$K_I = \frac{\gamma^2 x_v C_i}{C_\ell}, \tag{53}$$

Equation 47 becomes

$$K_C = \frac{C_c}{\gamma^2 C_i x_v} \tag{54}$$

and the product of vacancies and interstitials is

$$\gamma^2 x_v x_i = x_{oo}^2 \tag{55}$$

as before. Equation 41 becomes

$$C_i = x_{oo}\left(\xi - \frac{1}{\gamma^2 \xi}\right) . \tag{56}$$

Starting with Equation 42 and making use of Equations 14, 29, 55, and 56; one finds in place of Equation 42,

$$\frac{\sigma}{\sigma_o} = \frac{1}{(1+\phi)}\left[\xi(1+\chi) + \frac{1}{\gamma^2 \xi}(1-\chi)\right] . \tag{57}$$

Now $f(C, \sigma/\sigma_o)$ is given by

$$f(C, \sigma/\sigma_o) = \frac{C}{x_{oo}^2(\xi^2\gamma^2 - 1)} - \frac{1}{\gamma^2 \xi x_{oo}} \tag{58}$$

and Equation (49) is not changed. Since γ is a function of ξ, the solution is not simple.

III. EXPERIMENTAL

A. Introductory Comments

1. Light sensitivity of silver chloride

This property of silver chloride is well-known. Copper (I) enhances this sensitivity; scraps of the copper-doped material changed from a yellow-green to a faint grey color in less than a minute exposure under fluorescent lighting. Although the pure and the cadmium-doped material did not show any visible changes even under long exposure, all operations involving silver chloride were performed under red light, except for final handling of the analysis samples. The exposure of the copper-doped material even to red light was kept to a minimum.

2. Reactivity of silver chloride

Since the silver ion has a rather low reduction potential, silver chloride readily reacts with all metals except the noble metals to form silver and metal halide, even in the solid state. This reaction with metals could have had a detrimental effect on both equipment and the purity of the silver chloride, so silver, platinum, and quartz were used in the handling of silver chloride and in the construction of some of the equipment. Use of these materials will be

described without further explanation or justification.

3. Reagents

There are several references to "double distilled water" which actually refers to vacuum-distilled, ion-exchanged water. The laboratory "distilled water" is ion-exchanged water. It was distilled under 20 mm pressure to remove dissolved resin fragments. The conductivity of the water was decreased from 1×10^{-6} to 4×10^{-7} $ohms^{-1}$ cm^{-1}.

Except where otherwise noted, all other reagents used were Bakers "Analyzed" analytical reagents.

B. Preparation of Pure and Doped Silver Chloride Single Crystals

1. Preparation of pure silver chloride

In order to obtain silver chloride with the requisite low divalent impurity content, a two step process was required. First, silver chloride powder was prepared by precipitation from solution. The conductivity at 25°C of crystals grown from this material indicated a divalent impurity level of about 20 ppm. Second, a subsequent vacuum distillation of this material reduced the impurities to about 0.1 ppm.

a. Preparation of silver chloride powder Silver chloride was precipitated in batches of 250 grams each by

reaction of silver nitrate and hydrochloric acid. Doubly distilled water was used throughout this procedure. The required amounts of reagents were dissolved in sufficient water to give solutions of 500 ml each. Filtration was necessary to remove insoluble particles from the silver nitrate solution.

Precipitation was accomplished in a test-tube-shaped vessel 45 cm high by 10 cm diameter which was covered with a lucite disc to minimize dust contamination. Holes were provided in the disc for a glass, propeller-type stirrer, and leads from two separatory funnels containing the reactants. Three liters of water in the vessel were heated to about 60°C; the reactants were then added at about 20 ml per minute.

The well-coagulated precipitate which resulted was washed five times with 200 ml of 1:200 nitric acid. The precipitate was then placed back into the reaction vessel and stirred for an hour in three liters of water without heating. This served to break up small clumps and the result was a finer, denser, more easily washed precipitate. The precipitate was washed 20 more times with 200 ml of water with no added electrolyte.

The precipitate was dried in a filter funnel of five cm diameter which was modified by the addition of a 50/50 standard taper outer joint which received a matching cap.

This permitted the silver chloride to be dried under vacuum at room temperature. Most of the resultant silver chloride was powdery although some batches clumped badly and had to be ground by a glass mortar and pestle. Clumping was reduced by washing the precipitate with acetone prior to drying and this procedure was used for later batches.

b. Vacuum distillation of silver chloride. The distaillation apparatus is diagrammed in Fig. 2. In brief, with the left furnace and left half of the curved tube at 850°C and the right half of the curved tube and the right furnace at 475°C, silver chloride was distilled from the container on the left and collected as a liquid in crucibles at the right under a pressure of 0.02 mm Hg.

1) Discussion From available vapor pressure data for a number of metal chlorides, it was possible to estimate purification factors for a distillation of silver chloride.

For a single plate calculation, consider a melt containing n_1 moles of silver chloride and n_2 moles of impurity chloride. The corresponding mole fractions are

$$x_i = \frac{n_i}{n_{total}} = \frac{n_i}{n_1 + n_2} \tag{59}$$

If an ideal solution is assumed, Raoult's law gives the vapor

Fig. 2. Vacuum distillation apparatus

▲. Thermocouple junction

■. End of heater winding

●. Tap on heater winding

⊕. Main tap on heater winding

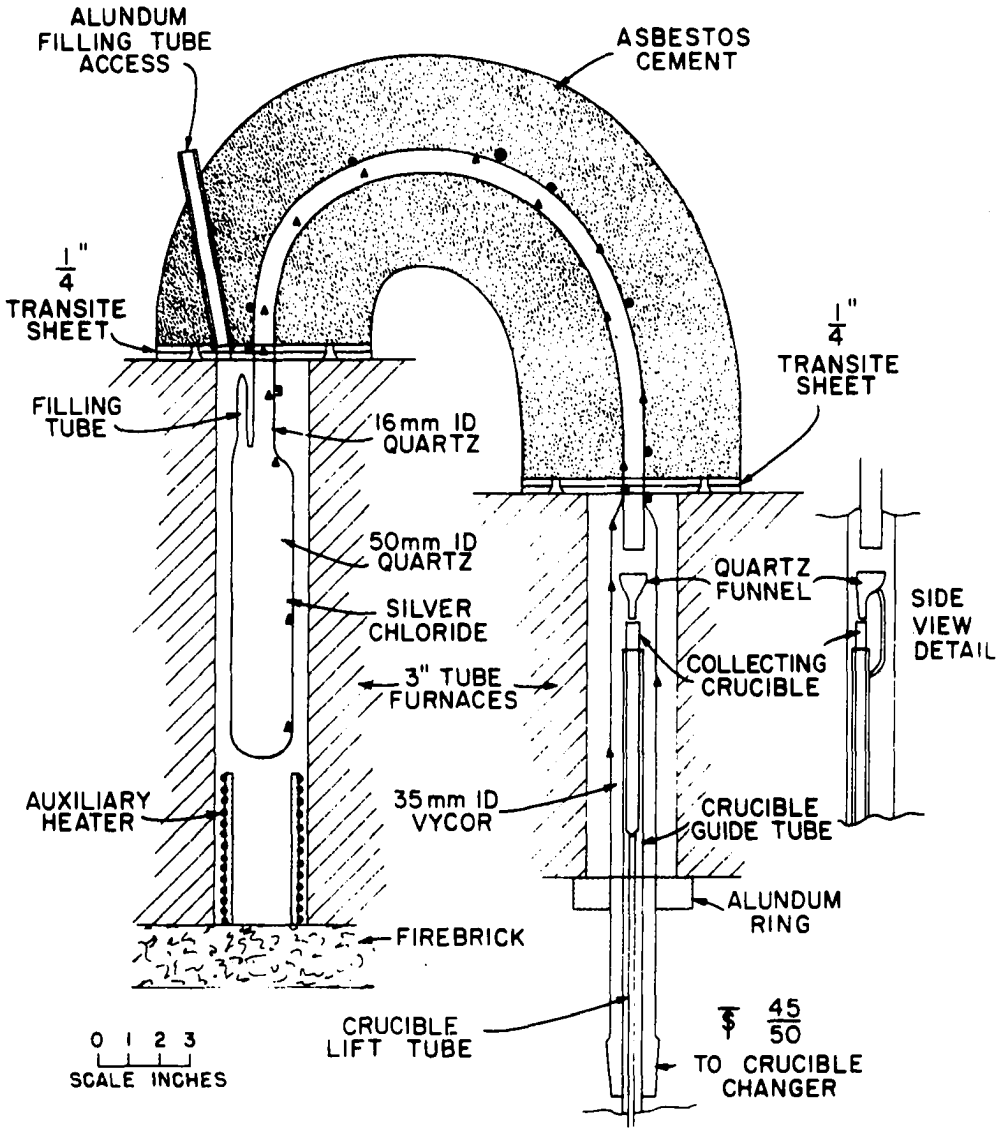
ALUNDUM
FILLING TUBE
ACCESS
ASBESTOS
CEMENT
1/4"
TRANSITE
SHEET
1/4"
TRANSITE
SHEET
FILLING
TUBE
16mm ID
QUARTZ
50mm ID
QUARTZ
SILVER
CHLORIDE
3" TUBE
FURNACES
QUARTZ
FUNNEL
SIDE
VIEW
DETAIL
COLLECTING
CRUCIBLE
AUXILIARY
HEATER
35mm ID
VYCOR
CRUCIBLE
GUIDE TUBE
ALUNDUM
RING
FIREBRICK
CRUCIBLE
LIFT TUBE
45/50
TO CRUCIBLE
CHANGER
0 1 2 3
SCALE INCHES

pressure of each component by

$$p_i = p_i^o x_i, \tag{60}$$

where p_i and p_i^o are the vapor pressure over the mixture and the vapor pressure of the pure substance respectively. The number of moles of each component to leave the melt, dn_i, is proportional to the vapor pressure over the melt, hence

$$\frac{dn_1}{dn_2} = \frac{p_1^o x_1}{p_2^o x_2} = \frac{p_1^o n_1}{p_2^o n_2} \tag{61}$$

which can be rearranged and integrated to give

$$\ln \frac{n_2}{n_{2_o}} = \frac{p_2^o}{p_1^o} \ln \frac{n_1}{n_{1_o}} , \tag{62}$$

where n_{1_o} refers to the number of moles at the beginning of the distillation.

Since the vapor was condensed to give the product, the purification factor is indicated by x_2^v/x_{2_o}, the ratio of the concentration of impurity in the vapor to the concentration in the starting material. Since $n_1 >> n_2$, $n_{total} \simeq n_1$, and $x_1 \simeq 1$; then $x_2^v \simeq x_2 p_2^o/p_1^o$ and Equation 62 gives

$$\ln \frac{x_2^v}{x_{2_o}} = \left(\frac{p_2^o}{p_1^o} - 1 \right) \ln \frac{n_1}{n_{1_o}} + \ln \frac{p_2^o}{p_1^o} . \tag{63}$$

Thus, x_2^v/x_{2_o} may be calculated as a function of the fraction of silver chloride yet to be distilled. These factors are tabulated in Table 2 for various substances for two cases:

Table 2. Vapor pressure and purification factor for various halides

Substance	Vapor pressure[a] at 850°C (mm Hg)	x_2^v/x_{2_o} 0.8 AgCl left	x_2^v/x_{2_o} 0.4 AgCl left	Vapor pressure[a] at 475°C (mm Hg)
AgCl	0.37	---	---	2×10^{-5}[b]
$CaCl_2$	0.0014[c]	4.71×10^{-3}	9.41×10^{-3}	---[d]
NaCl	0.8	1.5	7.3×10^{-1}	3×10^{-4}[b]
KCl	1.7	1.78	1.7×10^{-1}	4×10^{-4}[b]
$MgCl_2$	3.2	1.58	8.1×10^{-3}	7×10^{-4}[b]
$MnCl_2$	28	6.7×10^{-2}	5.0×10^{-10}	2×10^{-2}[b]
CuCl	45	2.5×10^{-3}	---[e]	2.3×10^{-1}

[a]By interpolation or extrapolation of data from Handbook of Chemistry and Physics (61, pp. 2151-2173).

[b]Uncertain due to long extrapolation.

[c]Extrapolation from the data of Hildenbrand and Potter (62).

[d]Very small.

[e]Extremely small; figures are meaningless.

Table 2. (Continued).

Substance	Vapor pressure[a] at 850°C (mm Hg)	x_2^v/x_{2o} 0.8 AgCl left	x_2^v/x_{2o} 0.4 AgCl left	Vapor pressure[a] at 475°C (mm Hg)
$NiCl_2$	80	1.5×10^{-6}	---[e]	1×10^{-3}[b]
$CoCl_2$	105	9×10^{-9}	---[e]	1.6×10^{-1}
$FeCl_2$	105	9×10^{-9}	---[e]	5×10^{-2}[b]
$CdCl_2$	200	---[e]	---[e]	1.3×10^{-1}
$PbCl_2$	250	---[e]	---[e]	1.6×10^{-1}
$ZnCl_2$	>760	---[e]	---[e]	4.5
$SnCl_2$	>760	---[e]	---[e]	6.6×10^{1}
$FeCl_3$	>>760	---[e]	---[e]	>760
$AlCl_3$	>>760	---[e]	---[e]	>760

0.8 and 0.4 of the silver chloride left. Calculations are based on the vapor pressure at 850°C, the distillation temperature. Very favorable decreases are indicated for most dihalides even when only 0.2 of the silver chloride has been distilled away.

In the derivation of the purification factor expression, equilibrium between the vapor and melt was assumed. To justify this assumption, the following argument is given.

The mean free path of a gas molecule is given by

$$\lambda = \frac{1}{\sqrt{2}\,\pi n \sigma^2} \tag{64}$$

Where n and σ are the number of molecules per unit volume and the collision diameter respectively. If σ is taken as 5Å, the mean free path at 850°C is $\simeq$ 0.03 cm for the vapor pressure of 0.37 mm and 0.5 cm at the ambient pressure of 0.02 mm. It is reasonable that if the pressure were close to the vapor pressure for a distance of at least a few cm above the melt, equilibrium would be approached. This would be the case if evaporation were faster than transfer of the gas away from the distillation section. Rather than attempt to show from basic principles that this must be so, it is shown that this situation was achieved in practice.

The argument is based on the fact that the average

pressure $\bar{p}$ in the curved tube between the distillation section and the condensing section can be estimated from the experimental rate of mass transfer. From the ideal gas equation, the pressure necessary to sustain the mass flow is

$$\bar{p} = \frac{n'RT}{C} , \tag{65}$$

where n' is the number of moles of silver chloride transferred per unit time, R is the gas constant, T is the absolute temperature, and C is the conductivity of the curved tube (volume/unit time). The conductivity of a curved tube is not more than that of a straight one of equal length for which the conductivity is given by Guthrie and Wakerling (63, p. 27),

$$C = \frac{D^4\bar{p}}{128\eta L} + \left(\frac{1}{6}\sqrt{\frac{2\pi kT}{m}}\frac{D^3}{L}\right)\left(\frac{1 + \sqrt{m/kT}\, D\bar{p}/\eta}{1 - 1.24\sqrt{m/kT}\, D\bar{p}/\eta}\right) , \tag{66}$$

where D is the tube diameter, L is the tube length, m is the mass of the molecule, k is the Boltzman constant, and η is the viscosity of the gas. This equation is valid providing 1) the flow is not turbulent and 2) the pressure difference between the ends is not so great that the mechanism (viscous or molecular) of flow changes along the tube. In the present application, condition 1 is satisfied, condition 2 may not be but errors due to this should not harm the argument. In principle, Equations 65 and 66 could be solved simultaneously to

yield a cubic equation in $\bar{p}$. However, a rough but painless solution presents itself. Following Guthrie and Wakerling (63, pp. 28-30), Equation 66 reduces to

$$C = 12.1\ D^3/L\ (J) \tag{67}$$

for air at 20°C, where D and L are in cm, $\bar{p}$ in microns, and C in liters/sec. J is given by

$$J = \frac{1 + 0.271\ D\bar{p} + 0.00479\ (D\bar{p})^2}{1 - 0.316\ D\bar{p}} \tag{68}$$

which is tabulated as a function of $D\bar{p}$ by Guthrie and Wakerling. Surprisingly, this treatment for air should hold fairly well for silver chloride at 850°C. Silver chloride vapor is approximately 75 per cent monomer (64). In Equation 66, m and T always appear as m/T, which for silver chloride monomer at 850°C is within 25 per cent of the value for air at 20°C. Furthermore, η is given by the kinetic theory by

$$\eta = \frac{1}{\pi^{3/2}} \sqrt{\frac{mkT}{\sigma^2}}\ . \tag{69}$$

Here the increase in mT is largely cancelled by the increase in σ^2.

In practice, 65 grams of silver chloride were distilled in 15 hours, which is equivalent to 8.4×10^{-6} moles/sec. The tube diameter was 1.6 cm and the length from the distilling section to the condensing section was 40 cm. In anticipation

of the result, J is taken to be 3.8 and $\bar{p}$ is found to be 125μ.

This value of $\bar{p}$ is considerably higher than the 20μ ambient pressure, and since the condensing end must have been at about 20μ, it was concluded that in the distilling end the pressure approached the vapor pressure of 370μ.

Finally, there are two factors which tend to increase the purity further than the x_2^v/x_{20} factors would indicate. First, if there were appreciable pressure up into the curved tube, some degree of reflux would be possible. This would increase the number of theoretical plates, possibly by one. Second, reference to the vapor pressure data for 475°C in Table 2 reveals that many of the impurity chlorides have vapor pressures higher than the ambient pressure and would have little tendency to condense. Although no attempt is made to estimate its magnitude, this effect might be quite important.

2) Construction The entire apparatus was mounted in a slotted angle iron frame 7'6" high by 2'3" wide by 1'9" deep and mounted on casters for mobility. The first step of construction was to mount the two tube furnaces which received the parallel portions of the distilling loop.

For the purpose of constructing the curved furnace around the curved portion of the distilling loop, the quartz loop was

clamped into a construction rack of aluminum rod which reproduced the position of the two tube furnaces. First, chromel-alumel thermocouples, in 1/8" alundum tubes were attached to the loop with chromel wire. Two layers of wet 1/16" asbestos paper, cut to fit between the thermocouples, were added. A third layer covered the thermocouples and the two layers below it to form the core for the winding. The #20 chromel wire winding, presprung to the proper diameter, was spaced uniformly on the core. Taps were provided at the points shown in Fig. 2. The winding was covered with an alundum cement, baked, and covered with several layers of asbestos paper. The transite discs, which carried the thermocouple and winding leads in slots between them, were placed in position. Several loops of wire attached to the inner transite rings were imbedded in the asbestos cement to hold them in place. Also imbedded in the asbestos were two hooks which allowed the completed assembly to be hoisted off the construction rack and eased onto the two tube furnaces.

Temperature was adjusted by means of four 7.5 amp Variacs. One was used for each tube furnace. Each half of the curved furnace was controlled by its own Variac; the crossover point was at the main tap (Fig. 2).

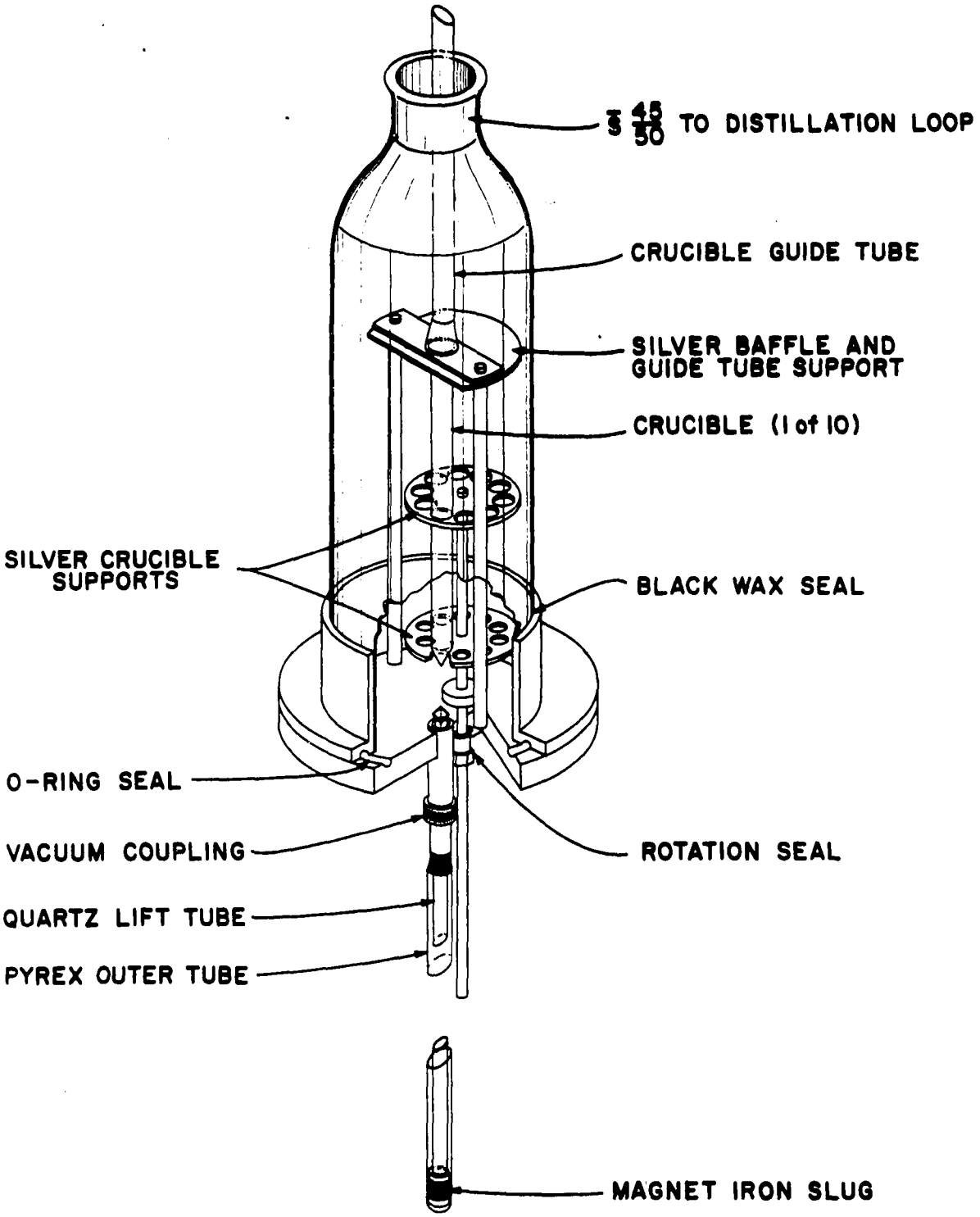

Fig. 3. Crucible changer

To eliminate the necessity of shutting down and opening the system each time a crucible had to be changed, a crucible changer (Fig. 3) was constructed which stored ten crucibles inside the vacuum system for injection, one by one, into the receiving end of the distillation loop. The circular crucible support was rotated until the crucible to be injected was directly under the crucible guide tube. A 2000 gauss cold cathode gauge magnet was placed so that the cylindrical magnet iron slug inside the vacuum system was between the poles. Then, by raising the magnet vertically, the crucible was forced up the crucible guide tube by the quartz lift tube which rested on the magnet iron slug. Total travel was 21 inches. The baffle protected the stored crucibles from occasional drippings from above.

Before it was charged with silver chloride, the distillation loop was cleaned with concentrated nitric acid and rinsed with doubly distilled water. The system was assembled, evacuated to 10^{-6} mm of Hg, and brought to normal operating temperature. Hot spots in the curved furnace were removed with external resistors across the appropriate winding taps. A cold spot at the junction of the distilling furnace and the curved furnace was not completely eliminated, but this would

only have the beneficial effect of a cold finger.

The still was charged with 1.3 kg of silver chloride. Crucibles were cleaned in hot, concentrated sulfuric acid with some nitric acid added. They were soaked and rinsed thoroughly with doubly distilled water and dried in a clean, empty desiccator under vacuum. After reassembly, the system was evacuated and heated. When operating temperatures were approached, helium which had been scrubbed by a hot calcium trap and liquid nitrogen trap was introduced to approximately one mm Hg pressure to prevent distillation until a proper temperature distribution had been established. Power to the auxiliary heater was adjusted to keep the bottom of the charge hotter than the top and the container was mounted radially off-center to the tube furnace, so the charge should have been stirred by convection, if not by boiling. The pressure was then dropped and held at 0.02 mm Hg for distillation by a throttling valve which balanced a helium leak against the pumps. Distillation of a fraction of 65 grams required 12-18 hours depending on variations in temperature from run to run. During the crucible changing operation, distillation was halted by increasing helium pressure.

2. Method of doping crystals with $CdCl_2$ and CuCl

The metal chloride was introduced into the silver chloride by the reaction of the metal with silver chloride according to the following equation

$$\begin{aligned} 2AgCl_{molten} + Cd &\rightarrow CdCl_2 + 2Ag \\ AgCl_{molten} + Cu &\rightarrow CuCl + Ag \end{aligned} \qquad (70)$$

where the metal chloride produced is dissolved in the molten silver chloride. The metals used for doping were of 99.999+ per cent purity, obtained from American Smelting and Refining Company. Copper was introduced as turnings cut from a copper rod with a carbide tool bit. Cadmium was introduced as fragments broken from splatters of the metal with forceps. These very high purity materials were used primarily to prevent interferences to the activation analysis by trace materials.

The following procedure was used for doping crystals. A pointed quartz crucible seven inches long by ten mm I.D. was cleaned and dried as described in the previous section. With the required amount of metal in the bottom of the crucible, a vacuum-distilled silver chloride ingot was introduced after it was bent slightly to prevent it from sliding to the bottom of the crucible and contacting the metal. The crucible was placed in the single crystal furnace (Fig. 4), with the silver rod

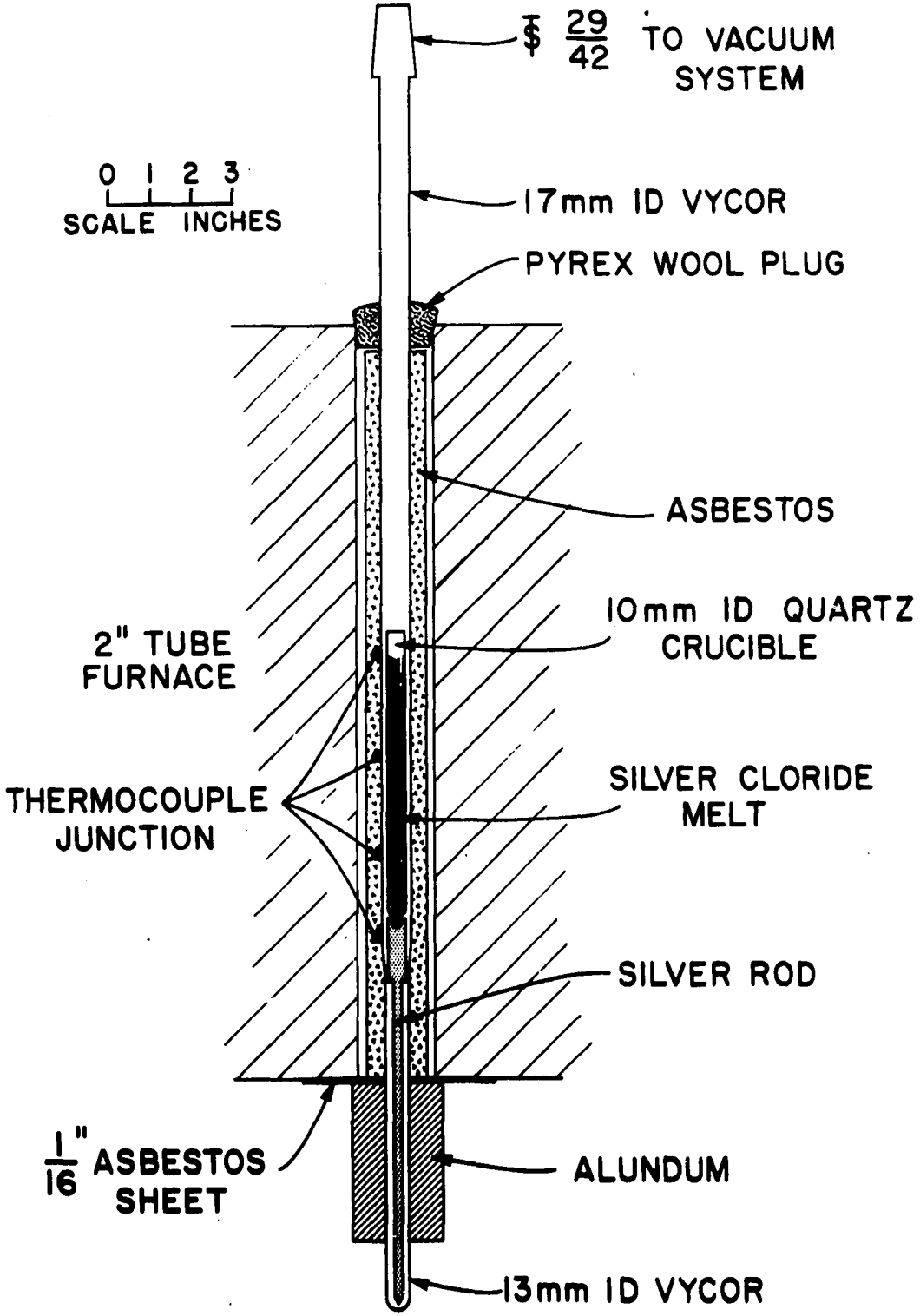

Fig. 4. Single crystal furnace

replaced by a quartz tube of equal length. After a vacuum of 10^{-5} to 10^{-6} mm Hg was attained, the furnace was heated. To prevent volatilization of the impurity chloride, helium which was scrubbed as before was introduced to a pressure of 1.05 atmospheres when the melting point was approached. After a 24 hour reaction time at 500°C, the furnace was cooled at 50°/ hour.

The silver which was formed in the reaction precipitated to the bottom. To prevent the silver from interfering with the crystal growth, the bottom of the crystal was cut off with a jeweler's saw. The end was shaved with a knife and then with a sharp piece of quartz to remove contamination.

To avoid contamination of several crystals in the event one accidentally became contaminated, a dilution method was not used to achieve the various concentrations. Rather, each crystal was doped in the same manner with the amount of added metal varied.

3. Growth of single crystals

The principle of growing single crystals in a stationary crucible by providing cooling from the bottom appears to have been first used by Stöber in 1925 (65) and the method sometimes bears his name. Since then, the method has been used in a

number of modifications but because the principle is so simple, no attempt is made to enumerate them.

For this investigation, crystals one cm in diameter and 15 cm long were prepared. They were grown in quartz crucibles with pointed bottoms in order to start growth from a single nucleation center. Growth of the doped crystals produced concentration gradients. Ideally, the gradient is determined by the distribution coefficient which is the ratio of impurity concentration in the solid phase to the concentration in the melt. It is also influenced by the rate of growth. Copper had a distribution coefficient of about 0.2 and concentrated at the top of the crystal while cadmium had a distribution coefficient of about 1.5 and concentrated at the bottom. These concentration gradients permitted four conductivity samples of different concentration to be obtained from one crystal.

The apparatus used in this investigation is diagrammed in Fig. 4. The following procedure was used to grow all crystals. The system was evacuated to at least 10^{-5} mm Hg; then the furnace was heated at a rate of 75°C/hour. When the sample reached the melting point, helium which was scrubbed as previously described was introduced slowly to a pressure of 1.05 atmospheres. When the bottom thermocouple reached 475°C, the

upper one read 680°C. At this point, a motor-driven Variac was started which lowered the temperature 10-15°C/hour. The temperature gradient was far from linear; the top two thermocouples differed by only 25°C. This situation was improved somewhat by gradually increasing an air stream at the bottom of the Vycor tube after the crystal was about half grown. An insufficient gradient would allow appreciable cooling through the side of the crucible. This would cause a paraboloid-shaped interface solid and melt and result in radial concentration gradients.

C. Preparation of Conductivity and Analysis Samples

1. Crystal cutting

The doped single crystal was scribed at 10.0 mm intervals along its length and cut into four sections of about 20 mm length with a jeweler's saw. Each section was cut as follows. About an eight mm length of the section was clamped into the chuck of a Unimat lathe. With a speed of 155 or 375 rpm, a tool bit fashioned from quartz rod, and with light, slow cuts, the diameter was reduced to about 8-8.5 mm. Occasionally, severe bubbling along the outside of the crystal necessitated smaller diameters than this. About 0.5 mm was removed in facing cuts. The position of the faced end of the crystal was

measured relative to one of the scribed lines, and a one mm thick slice was cut off with a jeweler's saw. This became an analysis sample. After the crystal was refaced and remeasured, a three to four mm thick conductivity sample was cut. Finally, after the crystal was again refaced and remeasured, another analysis sample was cut.

2. Conductivity samples

The faced side of a conductivity sample was glued to the polishing block (Fig. 5) with Duco cement. The unfaced side was ground flat with 400 grit silicon carbide paper, wet with absolute alcohol, on a plate of glass. This was accomplished by gradually advancing the inner block as material was ground away. Hopefully, this method did not greatly strain the sample. The sample was removed by solution of the Duco cement in acetone. After the thickness was measured, the faced side of the sample was ground in a similar manner. About 0.3 mm was removed to eliminate a slight widening of the diameter which occurred when the sample was faced in the lathe.

After the sample was cleaned with acetone, the thickness and diameter were measured with a micrometer to 0.001 mm with platinum discs placed on each side of the crystal to prevent corrosion of the micrometer. An average of readings on five

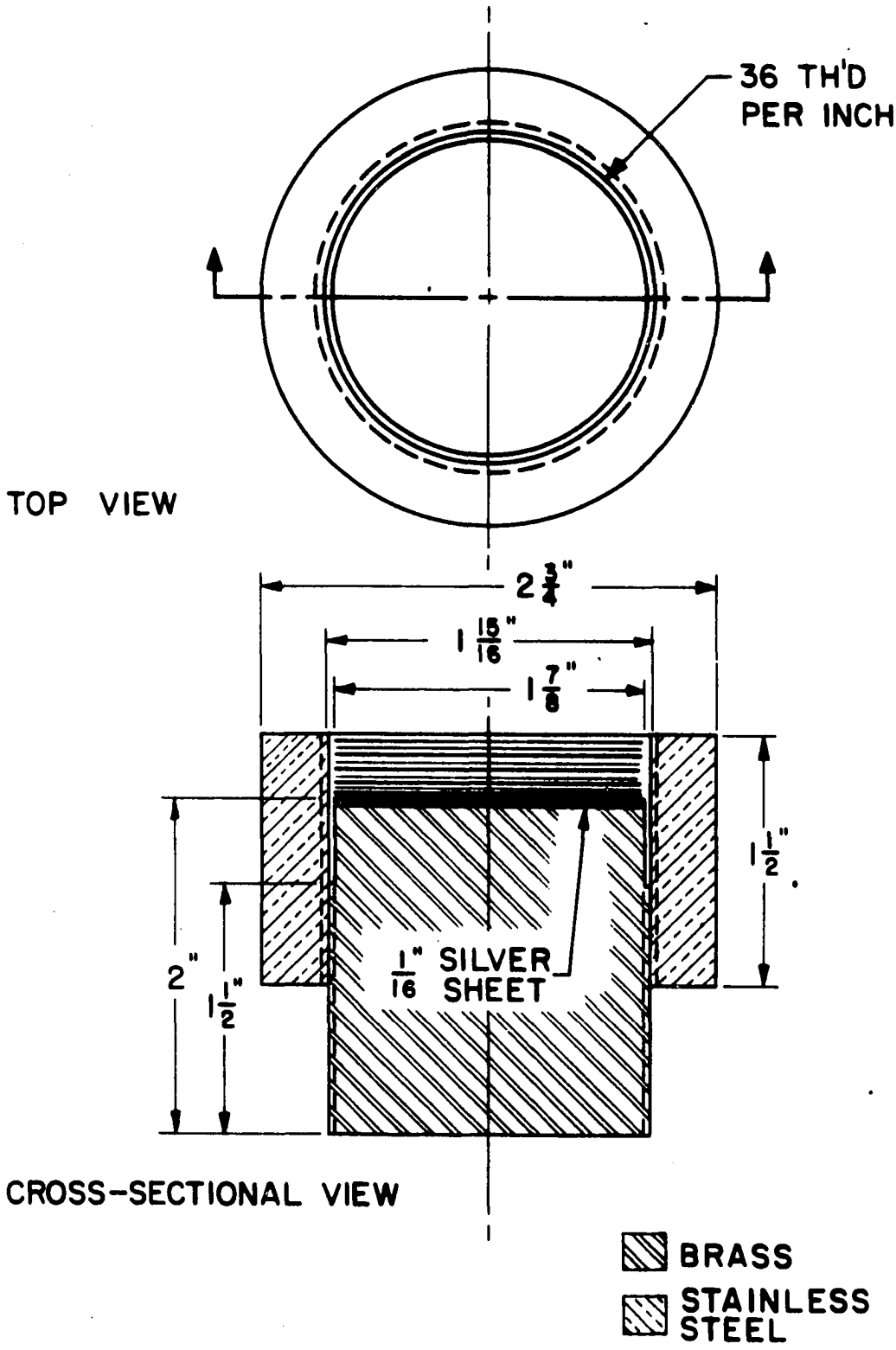

Fig. 5. Polishing block

different diameters was taken. The sample was weighed and the density calculated. Deviations were never greater than 0.2 per cent of the average of 5.555 grams/cm^3, values of 0.1 per cent or less were common.

A thin film of silver was reduced on each face with a concentrated solution of Kodak Dektol developer. A large drop of the solution placed on the surface spread to the edges and was allowed to react for one minute. After the solution was removed, the film was polished with Kleenex and washed with acetone. Examination of a few samples under a microscope showed they had good, square corners and the film covered the entire area of the sample. The faces were painted with Microcircuits SC-12 silver conducting paint to insure good electrical contact between the film and the sample holder electrodes.

3. Analysis samples

Because of the requirements of the activation analysis, the analysis samples had to be thin (0.2 mm) with close tolerance (±0.01 mm). Both faces of the sample were ground in the manner of the conductivity samples. However, on grinding the second side, the thickness of the sample was determined by micrometer from the difference between the distance from the end of the grinding block to the face of the sample and the

thickness of the block.

D. Conductivity Measurements

1. Sample holder

The sample holder shown in Fig. 6 held one pure and two doped conductivity samples so that the relative conductivity of the doped samples could be calculated from the conductivity of a pure sample at an identical temperature.

Although the figure should be self-explanatory, a few remarks are in order. The aluminum ring (P) successfully leveled the temperature gradient so that with the sample holder absent, the temperature one inch above and below the sample position was less than one degree from that at the sample position at 375°C. No radial gradient was detected.

The inconel overlay (J) had two functions. First, grounded to the sample holder body, it served as an electrical shield to minimize noise from the furnace winding. Second, with black tape covering the gap between the inconel overlay and sample holder body (D), it excluded light.

The quartz capillary seal (E) was the result of several attempts to obtain a seal with a high leakage resistance. When new, leakage resistance was greater than 10^{12} ohms but deteriorated to the lowest value of 7×10^{9} ohms for which corrections

Fig. 6. Conductivity sample holder

A. Type BNC connector
B. Platinum, platinum-13% rhodium measuring thermocouple
C. Number 20 platinum wire
D. Apiezon W, wax seal
E. Quartz capillary tube
F. 1/8" alundum thermocouple tube
G. Stupekoff seal
H. O-ring seal
I. Cooling tube
J. 11 mil inconel overlay
K. Vitreous quartz outer tube
L. Quartz tubing
M. Light spring
N. Transite furnace top
O. Alundum furnace tubes
P. Cylindrical aluminum ring
Q. Furnace winding
R. Type K control thermocouple
S. Stainless steel support rod
T. Nickel electrodes, platinum faced
U. Sample

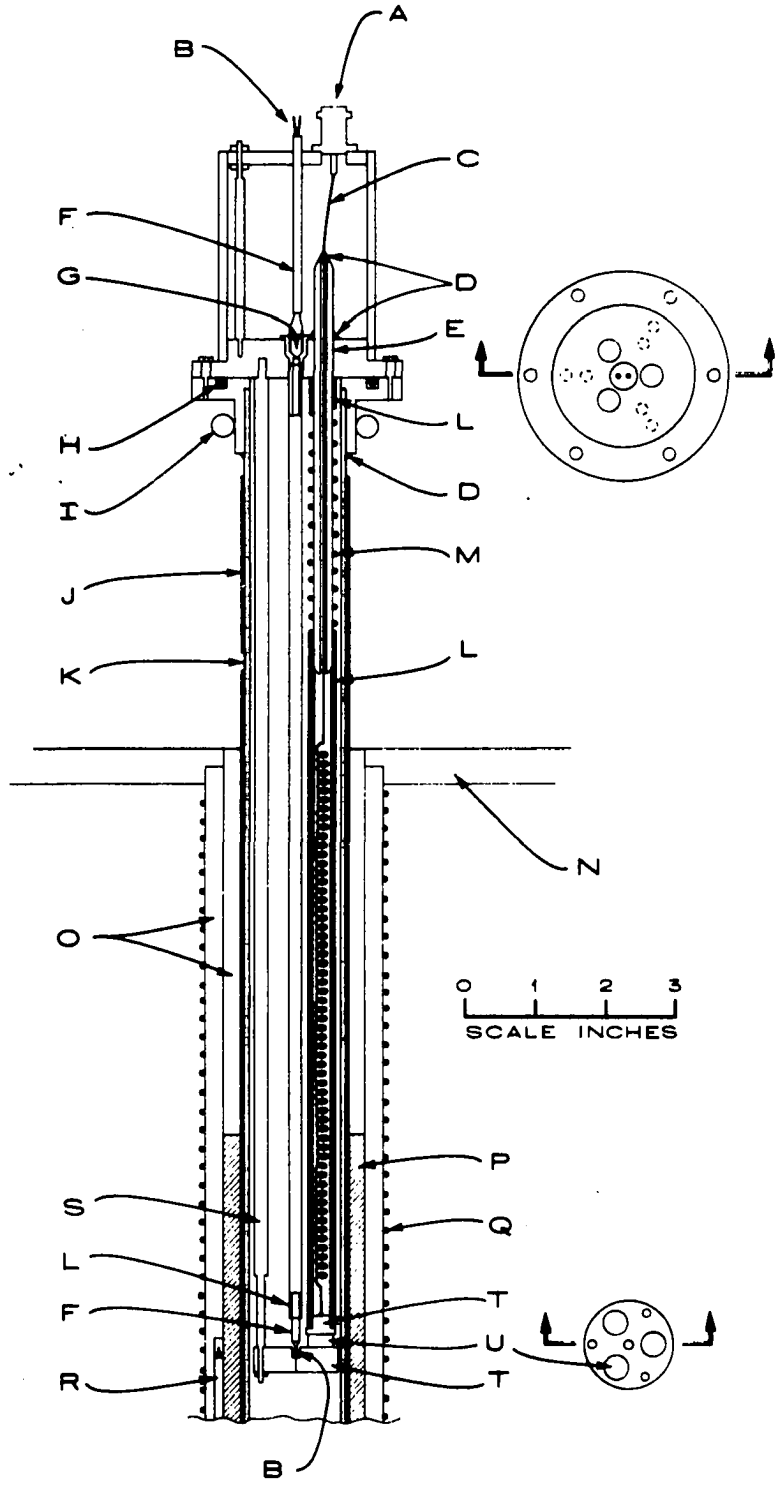
A
B
C
F
G
D
E
L
H
I
D
M
J
K
L
N
O
0 1 2 3
SCALE INCHES
P
S
Q
L
T
F
U
T
R
B

were made where necessary.

Although the nickel electrodes had a layer of platinum sheet silver-soldered to their faces, it was necessary to interpose discs of one mil platinum between these electrodes and the sample since the samples invariably stuck.

Finally, the samples were held under a helium atmosphere during the measurements. The helium was cleaned by passing through a column of powdered active uranium prepared by decomposition of the hydride (66).

2. Measurements

The alternating current conductivity was determined by means of a General Radio Type 716-C capacitance bridge for the entire range of resistances encountered.

When resistances were larger than 110,000 ohms, they were calculated from the capacitance, dissipation factor, and frequency with the assumption that the crystal was equivalent to a resistor and capacitor in parallel. A substitution method was used to minimize errors. At the highest resistance values, a frequency of one Kc/sec was used. When the resistance decreased sufficiently, 10 Kc/sec was used to keep dissipation factor values below 0.2. Signals of about 0.1 volt rms were generally used when feasible. Occasionally signals as

high as one volt were required for the highest resistances.

When resistances were less than 110,000 ohms, the crystals were balanced directly against decade resistors and capacitors. It was found that the conductivity went through a maximum (however slight), as the frequency was varied, at all but the highest temperatures. The maximum conductivity was considered to be the best value.

The frequency at the maximum varied from one to 20 Kc/sec as the temperature was raised. At the two highest temperatures, 20 or 50 Kc/sec were used. Signals of 0.04 to 0.1 volts were used.

After the high resistances were corrected for the leakage resistance of the sample holder and the low resistances for residual resistance in the leads and sample holder, the conductivity was calculated by the relation

$$\sigma = \frac{\ell}{AR} \tag{71}$$

where ℓ, A, and R are the thickness, area, and resistance of the sample, respectively.

Temperature was measured by means of a platinum, platinum-13 per cent rhodium thermocouple which was calibrated against the ice and steam points and N.B.S. melting point standards of tin, lead, zinc, and aluminum. Corrections were 0.4°C or less.

3. Equipment

As previously mentioned, the General Radio Type 716-C bridge was used. The signal generator was a Hewlett Packard 200CD. Output signals were amplified by a Tektronix Type 122, battery powered, low level preamplifier. Detection was by means of a General Radio Type 1231-B amplifier and null detector, with Type 1231-P5 interstage filter. Balancing resistors were General Radio Type 1432 (five decades, one ohm/step to 10 K ohms/step) supplemented by General Radio Type 510 decades of 0.01 and 0.1 ohm/step. Balancing capacitors were General Radio Type 980N and 980M decades of 0.001 and 0.01 uf/step, respectively.

The thermocouple emf was measured by a Rubicon Type B potentiometer and Rubicon 3414 galvanometer. The standard cell was calibrated periodically against a N.B.S. certified cell.

Temperature was controlled by a Minneapolis Honeywell Boston Division OMM-2HCT-2 current proportioning controller, Minneapolis Honeywell Model 365345-1 magnetic amplifier, and a two KVA saturable core reactor. A variac in the power line to the reactor gave a better match between reactor and furnace. With a change of set point of 10-20 degrees, temperature

oscillations settled down to 0.1-0.2 degrees after 20 minutes and to 0.02 degrees after 30-40 minutes.

E. Activation Analysis

1. Preparation of standard samples

The same procedure was used for preparing standards doped with copper or cadmium. As previously described, 125 grams of undried silver chloride precipitate was prepared. The reagent grade MCl_2 hydrate (M = Cu or Cd) was recrystallized once and the required amount was dissolved in about two ml of water. This solution was thoroughly mixed with the damp silver chloride and rough dried under vacuum in a desiccator without desiccant. The product was then transferred to a vacuum system and pumped to 10^{-6} mm Hg for 24 hours. Small clumps were ground in a glass mortar and pestle. The product was sieved through a platinum disc which was perforated with approximately 0.4 mm holes.

It was hoped that by this procedure the MCl_2 would be uniformly deposited over the silver chloride particles. The final standard weighed only about 60 mg so uniformity on a small scale was imperative. The powder probably contained about 0.2 per cent water as water of hydration to the M^{++} ion. This would not cause a noticeable difference in the neutron

flux attenuation between standards and unknowns. The fact that the copper in the standard occurred in the divalent state as opposed to the monovalent state in the unknowns was of no consequence, since calculations were made on a weight basis before conversion to mole per cent.

In order to fashion standards, the silver chloride-metal chloride powder was pressed under 18,000 psi into pellets 1/2 inch in diameter and approximately one mm thick. The diameter was reduced to approximately nine mm, and the pellets were ground to 0.20 mm thickness in the same manner as the analysis samples.

In order to analyse the powder, eight gram samples were weighed and dissolved in concentrated ammonia solution. An aliquot of Cu^{64} or Cd^{115} solution was added and the silver chloride was precipitated by addition of nitric acid. The M^{++} in solution was titrated with EDTA using NAS indicator (67) supplied by Dr. J. S. Fritz of this laboratory.

To correct for coprecipitation, the silver chloride precipitate was redissolved and M^{++} carrier was added. The solution was acidified to reprecipitate the silver chloride. The carrier in solution was precipitated as the sulfide and prepared for counting, as described later for the activation

analysis samples. The ratio of the counting rate of this sample to the counting rate of an equal aliquot of the original solution gave the loss due to coprecipitation. This correction was two to three per cent for cadmium and 0.05 to 0.1 per cent for copper.

The copper standard was also analysed by a spectrophotometric method using neocuproine reagent. The results agreed with the titration method to within 0.6 per cent.

2. Sample irradiation

Sample holders were constructed from 1/16 inch polyethylene sheet as shown in Fig. 7. Each accommodated 14 samples. Six of these were standards; four were located in the end-most positions and two at the center-most positions. The eight analysis samples from one crystal were placed in the remaining positions. Since there was usually about a 0.01 to 0.02 mm spread in the thickness of analysis samples, an attempt was made to choose standard samples of thickness within 0.005 mm of the analysis sample immediately next to it. With the weighed samples in place, the three sheets were tacked together along the edges by melting with a heated scribing tool.

The sample holder was wrapped in three layers of aluminum foil and sealed in quartz capsules, 24 mm inside diameter and

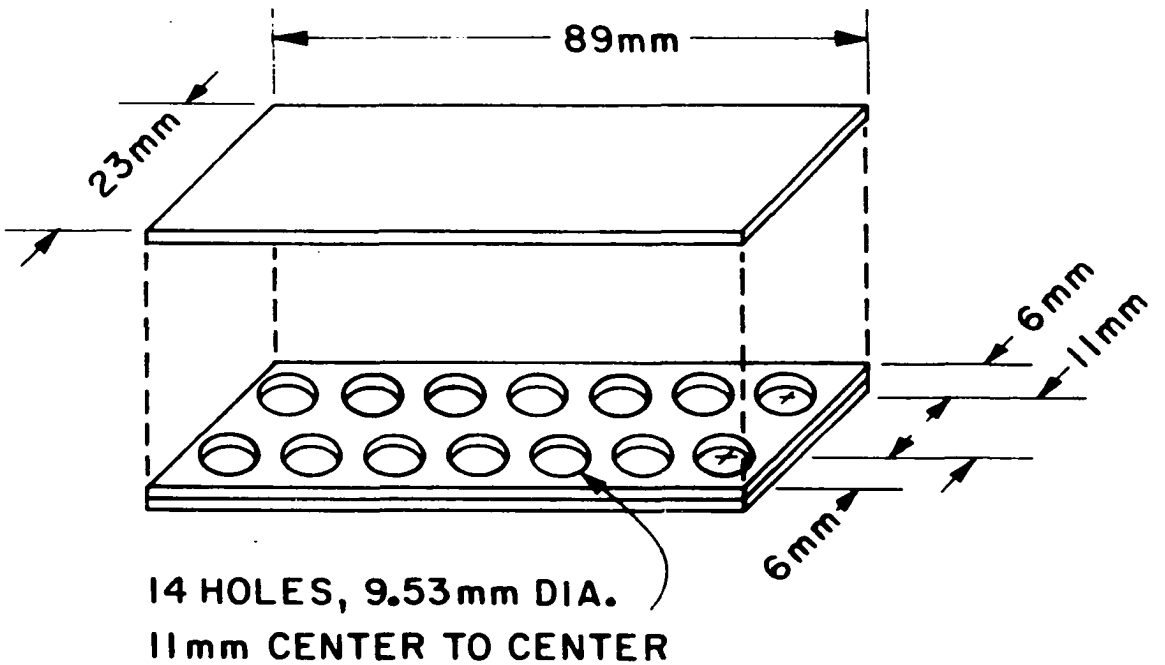

Fig. 7. Sample holder for activation analysis samples

125 mm long. They were irradiated in the isotope tray of the CP-5 reactor at the Argonne National Laboratory for 24 hours at fluxes from 5×10^{10} to 5×10^{12} neutrons/cm^2 sec depending on the particular sample. Samples were available within ten hours of the end of the irradiation.

3. Isolation and counting of activity

The cadmium and copper doped samples were carried through the same general procedure. Into a 250 ml tall form beaker was pipetted a 20 ml aliquot of carrier containing 10 mg of copper as the nitrate or 20 mg of cadmium as the chloride. After 10 ml of concentrated ammonia were added, the sample was introduced and the solution was stirred until the sample was dissolved. One ml of chlorine water was added and the solution was boiled until silver chloride first appeared. About 40 ml of water and some filter pulp were added, followed by two drops of hydrochloric acid and sufficient 1:4 nitric acid added dropwise to make the solution acidic. The solution was filtered through a filter paper disc in a chimney-type filter assembly to remove the silver chloride. This decreased the silver activity to about 0.1 per cent of its original level. A factor of 10^{-6} was necessary to eliminate contamination of the counting samples.

Except for the standards for the lowest concentration crystals of copper and cadmium (Cu 3 and Cd 4), the carrier was precipitated as the sulfide using thioacetamide in a 250 ml centrifuge bottle. After the sample was centrifuged and the supernate was removed, the precipitate was dissolved in about one ml of nitric or hydrochloric acid for the copper or cadmium sulfide, respectively. The solution was heated almost to dryness. The sample was then transferred to an ion exchange column by rinsing with two five ml portions of the eluent to be used.

For the exception noted above, the sample was filtered directly into a 100 ml volumetric flask. After the solution was diluted to volume, a 10 ml aliquot was introduced to the ion exchange column.

Kraus and Nelson (68) present graphically the distribution coefficient versus concentration of hydrochloric acid for a number of elements on Dowex 1-X8 anion exchange resin. These data predicted good separations of silver from copper and cadmium.

Columns one cm inside diameter and 15 cm long were used. Cu(II) was eluted readily with 0.5 M hydrochloric acid while silver remained adsorbed on the resin. When 5 M hydrochloric

acid was used as eluent, the silver elution peak was at 60 ml but the cadmium did not begin to elute until after 200 ml. Cadmium was stripped from the column with 1:20 ammonia solution.

In both cases, the carrier was eluted into a 40 ml pointed-centrifuge tube and precipitated with thioacetamide from ammoniacal solution. The precipitate was dissolved in a few drops of nitric or hydrochloric acid and the solution was evaporated almost to dryness. A few drops of water were added and the solution was transferred to a 3/8 inch diameter cellulose nitrate counting tube by means of a micropipet. All tubes were filled to a standard height of 1/2 inch. This was approximately 0.75 ml in volume.

Each sample was counted in a 3 inch sodium iodide crystal-photomultiplier tube detector. The gamma ray spectrum was analysed by a Model 201 Nuclear Data 256 channel analyser. Only occasionally were less than 100,000 counts under the desired peak accumulated. Counting times were usually 5 to 20 minutes. Each sample was counted twice; usually at least 12 hours elapsed between the first and second determination.

After counting, the sample was quantitatively rinsed into a 400 ml beaker. The solution was titrated with 0.05 M EDTA

at pH 5 to 5.5. Pyridine was used for a buffer. The end point was detected with NAS (67) indicator.

Coincidence corrections were determined by counting aliquots of 100, 200, 250, and 500 λ of a solution of either Cu^{64} or Cd^{115}. An actual counts per minute per λ was determined by extrapolation to zero volume. A coincidence correction versus counting rate curve was constructed for each isotope.

4. Processing of counting data

In order to handle the large number of spectra which resulted from the activation analysis, a program was written to process these data on the Iowa State University IBM 7074 computer.

For each spectrum, the computer located the channel number of the peak (the channel with the highest number of counts) and integrated over a given number of channels. The beginning and end of the integration range was specified in terms of a given number of channels from the peak channel. The live time stored in the first and last channels of the spectrum was used to calculate the counting rate.

A number of corrections to the counting rate were made as follows:

Background correction Up to ten background spectra could be stored. On the basis of the clock time at which the backgrounds and the spectrum were taken, the closest background (multiplied by the ratio of the live times) was subtracted channel by channel from the spectrum.

Zeroing correction The Cd^{115} and Cu^{64} spectra are shown in Fig. 8. The shoulders at the base of the peaks lead to at least two errors in the integration. First, if the peak shifts appreciably to higher channels, it also broadens, and the integration range must be chosen sufficiently wide to include the entire peak. But if for some samples the peak shifts to lower channels, a positive error results since more of the shoulder is included in the integration range.

The second error results from peak shifts of a fraction of a channel and is due to the shoulders being greater on one side of the peak than on the other. Suppose on one determination a peak is located exactly at an integral channel number. If on a subsequent determination the peak (and to a good approximation the whole spectrum in the area of the peak) shifts a fraction of a channel, f, the integration is in error by f times the difference in the shoulder height on each side of the peak since the integration range moves only in integral channel

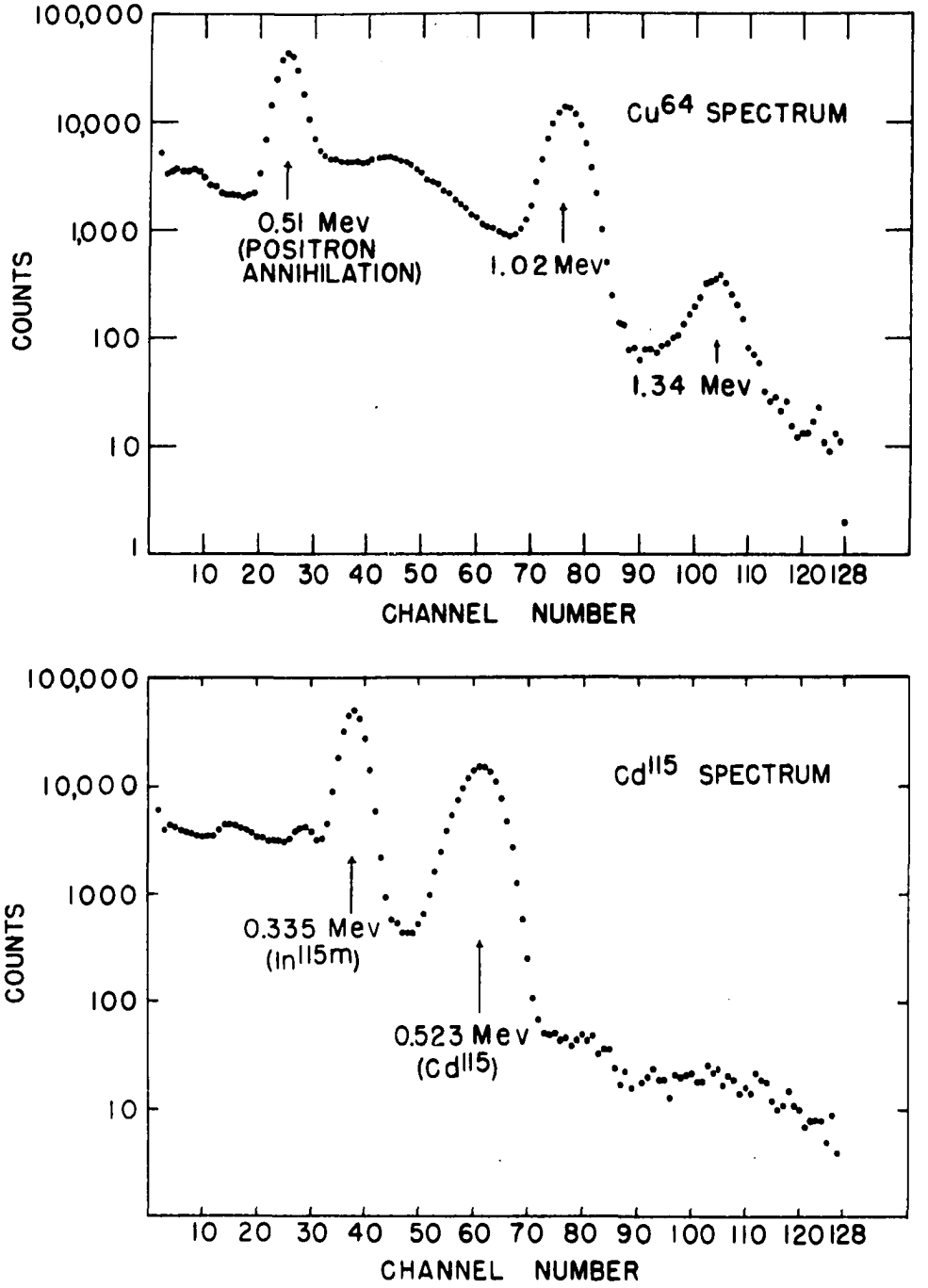

Fig. 8. Typical Cu^{64} and Cd^{115} spectra

steps. A greater error would result if the peak channel was incorrectly located due to statistics at the top of the peak.

Since both of these errors would not occur if there were no shoulders, the peak was "zeroed" by subtracting from the spectrum a third degree polynomial which was determined by a least squares fit to the shoulders on either side of the peak.

In practice, the uncertainty in fitting the polynomial was of the same order as the peak shift error. However, this procedure does have the advantage of partially correcting for any monotonic contributions from other isotopes and was used for the copper analysis. It was not used for the cadmium analysis because the proximity of the In^{115m} daughter peak to the Cd^{115} peak did not allow a sufficient shoulder for the curve fitting.

Coincidence correction The counting rate was multiplied by a second degree expansion in counting rate which represented the experimental coincidence correction.

Decay correction This was made in the usual manner.

Analyser efficiency correction In order to correct for changes in the counting efficiency of the analyser, one of the standards in each irradiation was counted periodically to monitor any changes. The activity of this standard, after all the other corrections, was assumed to be constant and the counting rate of all the other samples was corrected accordingly.

Corrections were usually not more than one per cent.

F. Alternate Methods of Analysis

1. Neocuproine analysis of copper

The electrodes were removed from the conductivity samples by grinding on 400 grit silicon carbide paper. Less than 0.1 mm of crystal was removed in the process. Each sample was weighed and dissolved in 20 ml of concentrated ammonia solution. When solution of the sample was complete, one ml of chlorine water was added and the solution was heated to drive off ammonia until silver chloride appeared. Then 40 ml of doubly distilled water were added, followed by several drops of hydrochloric acid and sufficient 1:4 nitric acid, added drop-wise, to make the solution acidic. The silver chloride was removed by filtration and the solution was transferred to a 250 ml separatory funnel. For the four most concentrated samples, an aliquot of the solution was used.

Since the tracer determination of the fractional coprecipitation of copper with silver chloride, which was carried out for the activation analysis standards, indicated only 0.05 to 0.1 per cent coprecipitation for 500 ppm material, coprecipitation probably was not a serious error even at the lowest concentrations.

The general procedure for neocuproine determination of copper outlined by Diehl and Smith (69, pp. 28-29) was followed closely.

To the copper solution in the separatory funnel were added five ml of ten per cent hydroxylamine hydrochloride and ten ml of 30 per cent sodium citrate solution. The pH was adjusted to about five and five ml of 0.2 per cent neocuproine in ethanol were added. The copper was extracted with 30 ml of chloroform which was drained into a 100 ml volumetric flask. An additional one ml of neocuproine solution was added to the separatory funnel and two more 20 ml extractions were carried out. Twenty ml of ethanol were added and the solution was made to volume with chloroform. For the four least concentrated samples, the volume of extractant was reduced by a factor of two and the solutions were made to 50 ml.

The absorbance of these solutions and of standards covering the concentration range of 50 to 200 μg per 100 ml was measured in one cm quartz cells against a blank solution at 459 mμ with a Beckman DU spectrophotometer. Absorbance readings ranged from 0.03 to 0.28. A Beers Law plot of the standards was slightly curved and was used as a working curve for the determination of the unknowns.

2. Atomic absorption spectrophotometric determination of cadmium

The electrodes were removed from the conductivity samples as above. The samples were weighed and dissolved in 15 ml of concentrated ammonia solution in 100 ml volumetric flasks except the five least concentrated samples which were dissolved in 50 ml flasks. Since both ammonia and silver chloride affected the intensity of the cadmium line, standards were made by dissolving pieces of vacuum distilled silver chloride the same size as the conductivity samples in 15 ml of ammonia and adding aliquots of standard cadmium solutions. The solutions were made to volume with doubly distilled water. A separate series of standards were used for the samples in the 50 ml flasks.

Measurements were made on the Perkin Elmer Model 214 atomic absorption spectrophotometer with a cadmium Osram lamp source. Since the solutions clogged the aspirator, they were injected into the flame with a constant speed, motorized syringe. A reading of only 3.5 per cent absorption was obtained for the lowest concentration. The highest reading used was 89 per cent.

IV. ANALYSIS OF CRYSTALS: RESULTS AND DISCUSSION

A. Results

The concentration of cadmium determined by activation analysis and by atomic absorption spectrophotometry is plotted in Fig. 9 as a function of the position of the sample in the original crystal. A similar presentation is given in Fig. 10 for the concentration of copper by activation analysis and by neocuproine reagent.

The results for the activation analysis were disturbing. For example, the points for the Cd 3 and Cd 4 profiles seemed to be badly scattered and the shape of the Cd 2 and Cu 3 curves was not expected. In view of this, independent analyses on the conductivity samples were in order.

For the cadmium analysis, the activation analysis seems to be exonerated, although there is a consistent disagreement with the atomic absorption results by about ten per cent for Cd 1 and Cd 2. For the copper analysis, the activation analysis seems to fail completely for the lowest concentrations.

The results of analysis by the various methods are presented in Tables 3 and 4.

Fig. 9. Concentration profiles of cadmium doped crystals

The dashed lines are to tie together points for a given crystal and are not intended to represent the concentration gradient in the crystal. The numbering system corresponds to the one in Table 3

Δ . Atomic absorption analysis

O . Activation analysis

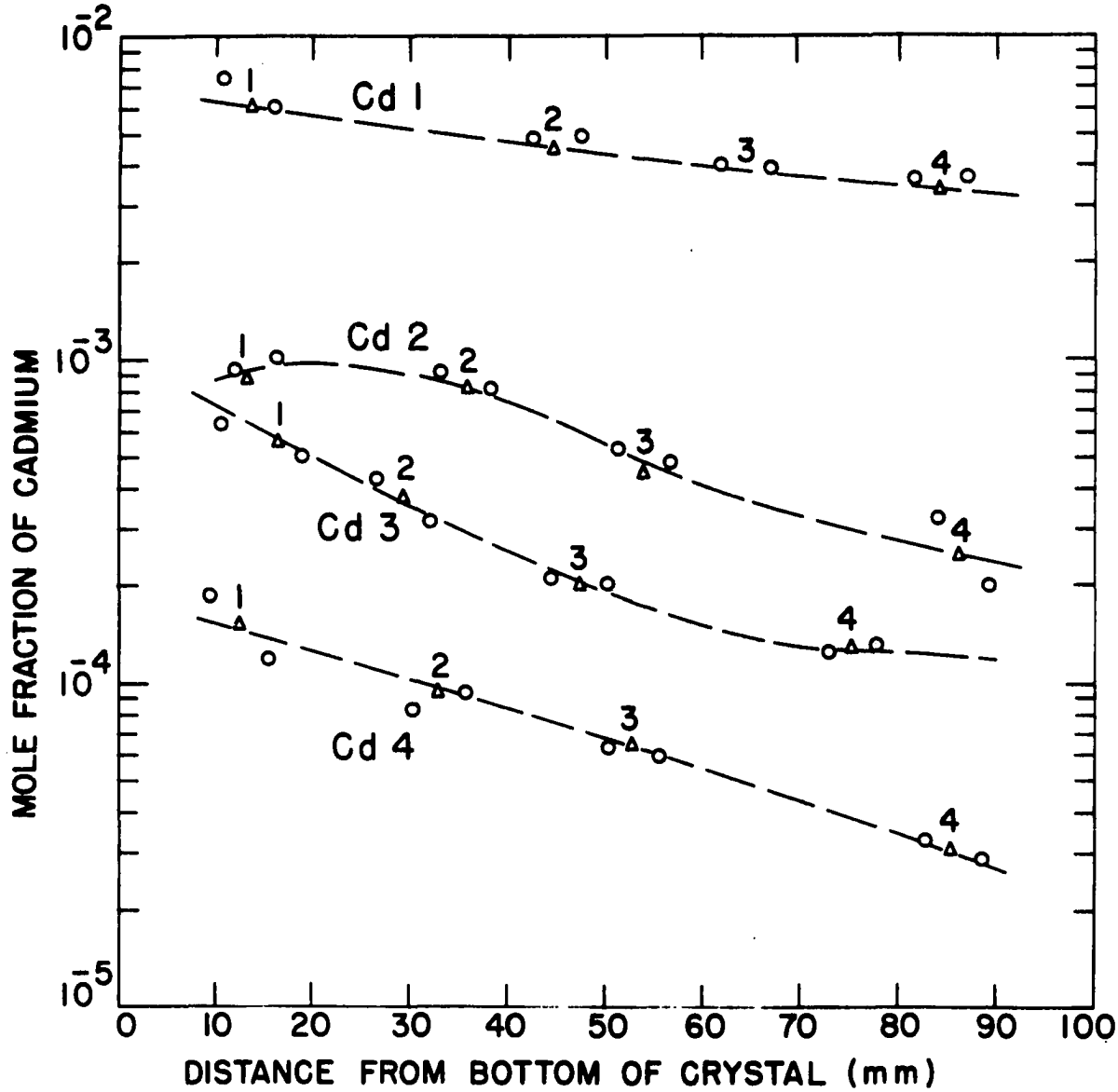
MOLE FRACTION OF CADMIUM
10^{-2}
10^{-3}
10^{-4}
10^{-5}
Cd 1
Cd 2
Cd 3
Cd 4
1
2
3
4
0
10
20
30
40
50
60
70
80
90
100
DISTANCE FROM BOTTOM OF CRYSTAL (mm)

Fig. 10. Concentration profiles of copper doped crystals

The numbering system corresponds to the one in Table 4.

△. Neocuproine analysis

○. Activation analysis, Argonne CP-5 Reactor

□. Activation analysis, Iowa State University Training Reactor, UTR-10 (an early experiment using copper foil as a standard)

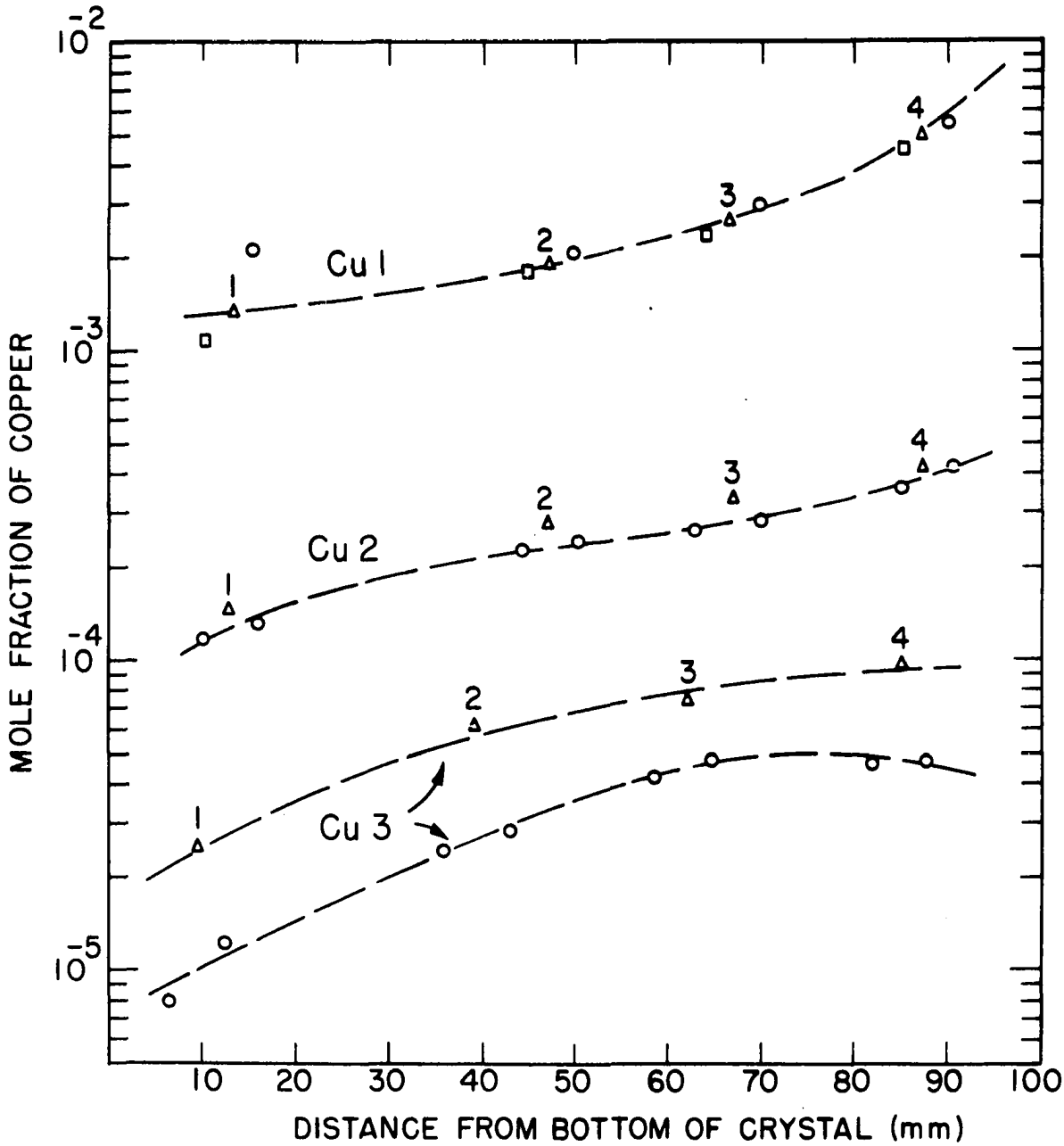
MOLE FRACTION OF COPPER
10^{-2}
10^{-3}
10^{-4}
10^{-5}
Cu 1
Cu 2
Cu 3
1
2
3
4
10
20
30
40
50
60
70
80
90
100
DISTANCE FROM BOTTOM OF CRYSTAL (mm)

Table 3. Mole fraction of cadmium in conductivity samples

Sample number	Results by activation analysis	Results by atomic absorption
Cd 4-4	3.15×10^{-5}	3.01×10^{-5}
Cd 4-3	6.05×10^{-5}	6.41×10^{-5}
Cd 4-2	8.56×10^{-5}	9.32×10^{-5}
Cd 4-1	1.39×10^{-4}	1.51×10^{-4}
Cd 3-4	1.13×10^{-4}	1.28×10^{-4}
Cd 3-3	2.02×10^{-4}	1.98×10^{-4}
Cd 3-2	3.72×10^{-4}	3.73×10^{-4}
Cd 3-1	5.7×10^{-4}	5.54×10^{-4}
Cd 2-4	2.65×10^{-4}	2.45×10^{-4}
Cd 2-3	4.91×10^{-4}	4.41×10^{-4}
Cd 2-2	8.7×10^{-4}	8.14×10^{-4}
Cd 2-1	1.00×10^{-3}	8.54×10^{-4}
Cd 1-4	3.60×10^{-3}	3.33×10^{-3}
Cd 1-3	3.95×10^{-3}	---
Cd 1-2	4.86×10^{-3}	4.43×10^{-3}
Cd 1-1	6.52×10^{-3}	6.03×10^{-3}

Table 4. Mole fraction of copper in conductivity samples

Sample number	Results by activation analysis	Results by neocuproine
Cu 3-1	1.034×10^{-5}	2.52×10^{-5}
Cu 3-2	2.66×10^{-5}	6.14×10^{-5}
Cu 3-3	4.54×10^{-5}	7.42×10^{-5}
Cu 3-4	4.71×10^{-5}	9.61×10^{-5}
Cu 2-1	1.245×10^{-4}	1.463×10^{-4}
Cu 2-2	2.34×10^{-4}	2.759×10^{-4}
Cu 2-3	2.75×10^{-4}	3.333×10^{-4}
Cu 2-4	3.82×10^{-4}	4.194×10^{-4}
Cu 1-1	1.45×10^{-3}	1.346×10^{-3}
Cu 1-2	1.91×10^{-3}	1.898×10^{-3}
Cu 1-3	2.60×10^{-3}	2.629×10^{-3}
Cu 1-4	4.87×10^{-3}	4.943×10^{-3}

B. Discussion of Methods of Analysis

1. Activation analysis

a. Errors

1) Self-shielding Both silver and chlorine have a high neutron absorption cross-section so absorption is appreciable even in a thin sample.

Let A_o be the expected induced activity from a sample if there were no self-shielding. The actual activity, A, is less than A_o by a factor, f, i.e.,

$$A = A_o f. \tag{72}$$

For an infinite slab, where $n\sigma x$ is small, Gilat and Gurfinkel (70) have given

$$f = 1 + \frac{n\sigma x}{2} \ln (n\sigma x) - \frac{n\sigma x}{2} (3/2 - \gamma) - \frac{(n\sigma x)^2}{6} \tag{73}$$

where

n = number of absorbing nuclei per cc

σ = neutron cross-section

x = thickness of the slab

γ = Euler's constant = 0.5772.

For a slab of silver chloride 0.2 mm thick, about nine per cent (f = 0.91) absorption was calculated. Since the thickness of both standards and unknowns was constant to $\pm$ 0.01 mm, an uncertainty of about 0.5 per cent was indicated for both the cadmium and copper analyses. For the cadmium standards (0.1 per cent Cd) about 0.2 per cent additional attenuation due to the cadmium was calculated so the very low concentration unknowns should have been high by this factor. The highest concentration unknown was expected to be low by about one per cent.

2) Flux variation in the sample holder The six standards included with each irradiation were to monitor and correct for small flux gradients and possible shielding of the inner samples by the outer ones. The results of the counting rate per unit weight for the standards are outlined in Figs. 11 and 12. With the exception of Cd 1 and perhaps Cd 2, the data were consistent. This is illustrated more clearly if the data are plotted as in Fig. 13. For each unknown, a value for the counting rate per unit weight appropriate to its position in the sample holder was used. Values were taken from a smooth curve drawn as in Fig. 13. For most samples, the uncertainty in this value caused an uncertainty in the results of one to three per cent.

If there were any shielding of the inner samples by the outer ones, the effect was too small to be noticed in the presence of the flux gradients.

3) Counting errors For a given number of accumulated counts, C, the relative standard error due to the statistical nature of radioactive decay processes is given by

$$\sigma = \frac{\sqrt{C}}{C} . \qquad (74)$$

Since usually 10^5 counts were accumulated, the statistical standard error was about 0.3 per cent.

Fig. 11. Counting rate per unit weight of cadmium standards

Each of the four rectangles corresponds to a sample holder for one irradiation. Each square represents a sample position in the sample holder. In each square representing a position occupied by a standard is given the counting rate per unit weight for two series of determinations. The upper number refers to the first determination; the lower number to the second. The data is arbitrarily scaled to per cent of the lowest value for each irradiation. The standards marked with an asterisk were used to monitor the counting efficiency of the analyser and were assumed to be constant after corrections for decay were made. All other samples were corrected according to the observed counting rate of that standard. It, in fact, did not vary by more than approximately one per cent. The abbreviation, n. c., indicates that the sample was not counted on that series.

Cd 1 115 hrs. between series

130.5 130.0			145.0 144.8			100.0 n.c.
126.8 *			111.6 111.8			120.3 120.0

Cd 2 35 hrs. between series

105.0 105.1			104.1 104.0			104.2 *
110.3 110.2			103.9 104.0			100.2 100.0

Cd 3 20 hrs. between series

100.9 100.8			119.7 119.8			126.7 *
100.1 100.0			120.3 120.8			127.8 127.6

Cd 4 20 hrs. between series

127.4 127.0			124.5 123.4			106.3 106.2
118.7 *			113.7 n.c.			100.0 100.0

Cu 1 — 24 hrs. between series

103.3 *			lost		104.3 104.7
102.9 n.c.			104.1 103.9		100.0 101.4

Cu 2 — 7 hrs. between series

110.4 110.4			103.2 102.5		100.0 *
110.2 110.6			104.5 105.1		102.4 100.6

Cu 3 — 12 hrs. between series

116.0 114.8			n.c. 107.1		104.7 104.0
116.6 117.3			109.3 *		100.0 103.3

Fig. 12. Counting rate per unit weight of copper standards; see facing page for Fig. 11

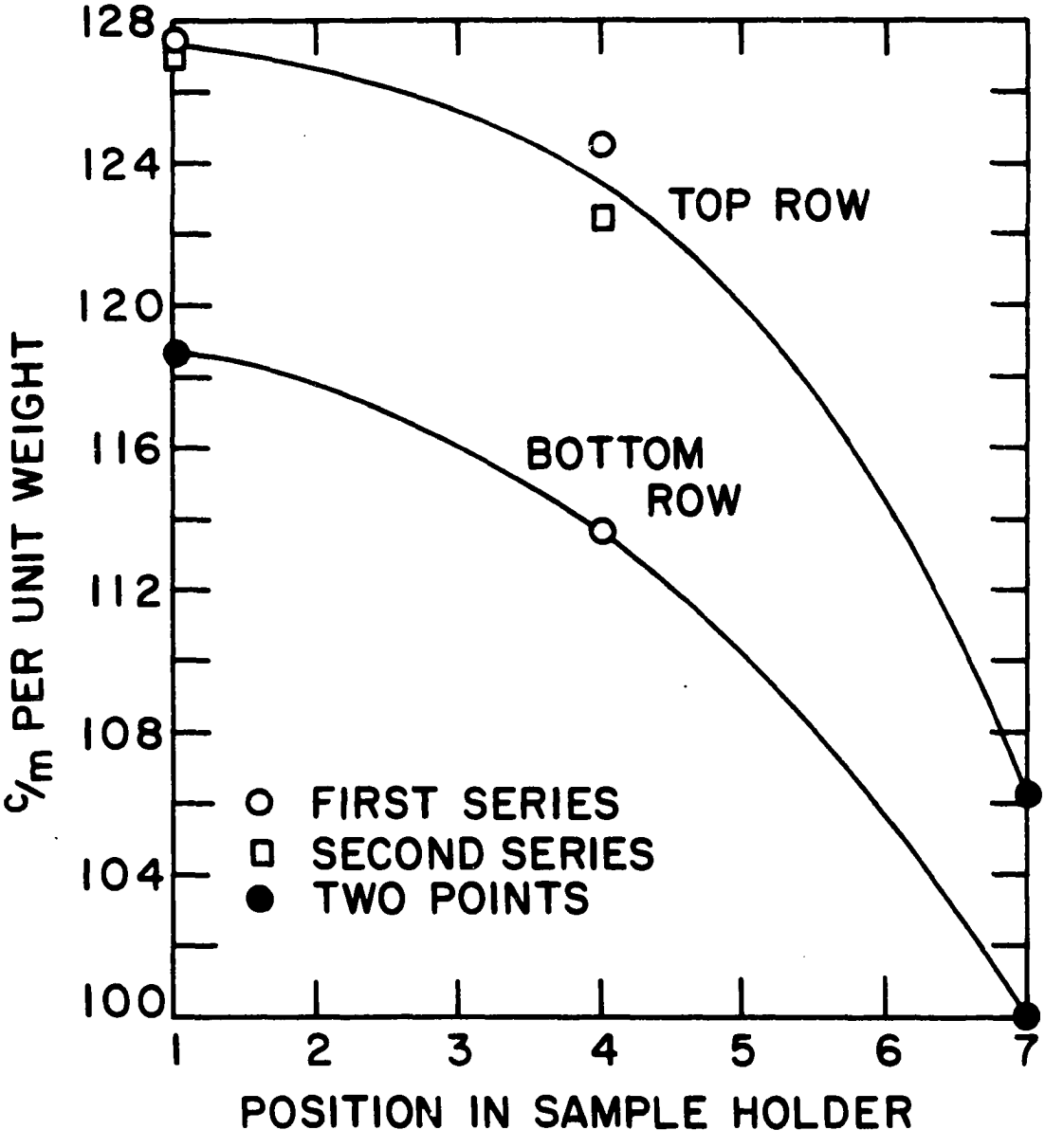

Fig. 13. Flux variation throughout sample holder for Cd 4

Ordinate in arbitrary units of Fig. 11.

Uncertainties in the counting rate due to peak drift or the "zeroing" correction, coincidence correction, or the analyzer efficiency correction were about 0.5 per cent each.

4) Recovery factor error This was determined largely by the accuracy of the EDTA titration of the carrier after counting. An error of not more than 0.3 per cent was expected for the titration. Additional errors due to non-uniform delivery by pipets, etc., could have caused an error of about 0.2 per cent.

The total standard error calculated by

$$\sigma_{\text{total}} = \sqrt{\sum_{1} \sigma_{1}^{2}} \qquad (75)$$

was 1.9, 2.5, or 3.4 per cent depending on whether the uncertainty due to flux gradients was 1.0, 2.0, or 3.0 per cent, respectively. Included in these figures are the uncertainties in the counting rate of the standard samples. If the errors listed above are the only appreciable ones, the accuracy could be increased substantially by irradiating the samples in a uniform neutron flux.

b. Failure of copper analysis In light of the above error analysis, some other sources of error must be sought to explain the apparent failure of the copper activation analysis.

Interference by an impurity in either the standards or unknowns is considered first. Since the results for the lowest concentrations were low, it must be presumed that the impurity was in the standard and decaying with a half life shorter than Cu^{64}. The irradiations were done in order of decreasing concentration in the crystals. Each time, the period between the end of the irradiation and the counting of samples was shortened. There would then have been the possibility that by the time the standards for Cu 1 were counted, the impurity had decayed out, but it had not decayed out for the other two. But, for all cases, the activity decayed with the Cu^{64} half-life as indicated by the agreement between the two series of counting rate determinations. Furthermore, no isotope can be found that would survive the chemical separation procedure, decay with a one Mev gamma ray, and have a half-life close to 12.8 hrs.

An equally unlikely explanation is the possibility that in the lower concentration samples, the Cu(I) in the crystal was not converted completely to Cu(II) upon solution in ammonia and some was lost in the subsequent precipitation of silver chloride. However, Cu(I) is oxidized to Cu(II) in ammonia solution by the silver ion, if not by atmospheric

oxygen or added chlorine water. Also, this explanation cannot explain why there would be loss from the lowest concentration crystals but not from the highest concentrations.

The disagreement between the activation analysis and neocuproine reagent determinations is thus unexplained. The activation analysis was assumed to be the one in error because the procedure was complex compared to the neocuproine determination and the probability of unknown sources of error was higher.

2. Neocuproine determination

Neocuproine is a well-established reagent for the determination of copper. Spectrophotometric measurements are usually accurate to about one per cent. For the lowest concentration samples, which gave a low absorbance, the error was probably about two per cent.

Based on the fact that for a 500 ppm sample there was 0.05 to 0.1 per cent copper coprecipitated in the silver chloride precipitation, it was estimated that for the lowest concentration samples coprecipitation errors should not have been more than about two per cent. Total error for the determination should have been less than four per cent.

Chemical trace analysis is subject to contamination

errors. However, contamination did not appear to be a factor since a blank carried through the entire procedure did not contain copper.

3. Atomic absorption spectrophotometry

Preliminary experiments showed that ammonia enhanced the intensity of the cadmium line and silver chloride decreased its intensity. It is estimated that variations in ammonia and silver chloride concentrations caused errors of one to two per cent.

Two series of atomic absorption determinations were made. The deviation from the average of the two series averaged about four per cent. The results of this method are probably accurate to about five to six per cent.

C. Implications

The cadmium activation analysis was successful although further study of the systematic difference between the two methods of analysis for the two highest concentration crystals would be desirable. For the two lowest concentration crystals, the disagreements seem to arise from local concentration gradients. Certainly Cd 4 has an undulating concentration profile. This behavior points up a weakness in the crystal

growing procedure used in this investigation.

In view of the cadmium results, there is probably no reason that the copper analysis cannot be made to work successfully. An investigation is now underway for this purpose.

Both the atomic absorption and the neocuproine methods approached the limit of their sensitivity with the lowest concentration samples. However, samples ten times less concentrated than the lowest concentration used in this work could be handled by activation analysis with a decrease in accuracy of less than one per cent with no increase in counting time.

V. CONDUCTIVITY DATA

A. Presentation of Data

1. Experimental data

The thermal expansion corrected conductivity at the temperatures of measurement are presented for all the pure and doped samples in Fig. 14.

2. Relative conductivity isotherms for doped samples

The experimental temperatures usually varied from the isotherm temperatures by one or two degrees so the data had to be corrected accordingly. The relative conductivity isotherms were obtained by two methods.

By the direct method, the relative conductivity was calculated by dividing the conductivity of the doped sample by the conductivity of the pure sample in that run. The relative conductivity for the isotherms was taken from a plot of relative conductivity versus temperature.

The indirect method was done by computer. The conductivity of all samples was calculated for each isotherm temperature from a parabola fitted to the logarithm of the conductivity versus reciprocal temperature for the three temperatures closest to the isotherm temperature. This was a valid procedure since usually one of the experimental points was

Fig. 14. Results of conductivity measurements

In each of the two tables on a page is presented the conductivity of the pure sample and two doped samples for a conductivity run. Temperature is in ^{o}C; conductivity is in $\Omega^{-1}cm^{-1}$ and has been corrected for thermal expansion with the data of Fouchaux (20). In the heading the sample number is given which corresponds to the number in Fig. 9 and 10 and in Tables 3 and 4. Directly above the sample number of the doped samples is given the concentration in mole fraction. These tables have been prepared by computer; thus 3.005E-05 = 3.005×10^{-5}.

TEMP.	PURE SAMPLE	CADMIUM DOPED SAMPLES 6.030E-03	4.430E-03
	P-12	CD1-1	CD1-2
24.23	2.307E-09	1.015E-06	9.963E-07
50.15	7.261E-09	7.984E-06	7.443E-06
69.20	2.130E-08	3.531E-05	3.379E-05
95.58	2.099E-08	2.119E-04	1.962E-04
108.90	6.420E-07	4.276E-04	3.103E-04
123.64	1.729E-06	6.635E-04	4.658E-04
131.36	2.753E-06	8.026E-04	5.624E-04
141.64	4.832E-06	1.015E-03	7.123E-04
151.17	7.867E-06	1.242E-03	8.729E-04
160.13	1.211E-05	1.490E-03	1.048E-03
171.14	1.994E-05	1.835E-03	1.293E-03
181.33	3.083E-05	2.196E-03	1.550E-03
192.17	4.846E-05	2.637E-03	1.861E-03
203.24	7.522E-05	3.144E-03	2.222E-03
214.39	1.153E-04	3.714E-03	2.627E-03
226.78	1.820E-04	4.420E-03	3.128E-03
239.14	2.819E-04	5.211E-03	3.689E-03
252.49	4.447E-04	6.157E-03	4.364E-03
263.77	6.434E-04	7.040E-03	4.995E-03
275.14	9.082E-04	7.964E-03	5.663E-03
282.76	1.169E-03	8.724E-03	6.211E-03
298.39	1.856E-03	1.033E-02	7.384E-03
315.05	3.022E-03	1.235E-02	8.924E-03
332.48	4.693E-03	1.491E-02	1.094E-02
353.79	8.349E-03	1.923E-02	1.449E-02
371.87	1.388E-02	2.453E-02	1.919E-02

TEMP.	PURE SAMPLE	CADMIUM DOPED SAMPLES 3.950E-03	3.330E-03
	P-13	CD1-3	CD1-4
24.40	3.220E-09	8.964E-07	8.843E-07
60.62	1.516E-08	1.972E-05	1.909E-05
81.50	6.751E-08	7.162E-05	6.856E-05
94.72	2.135E-07	1.639E-04	1.513E-04
108.65	6.434E-07	2.631E-04	2.409E-04
121.92	1.557E-06	3.843E-04	3.532E-04
131.68	2.795E-06	4.899E-04	4.505E-04
142.09	5.003E-06	6.211E-04	5.713E-04
150.06	7.521E-06	7.376E-04	6.785E-04
162.20	1.338E-05	9.409E-04	8.653E-04
172.07	2.069E-05	1.132E-03	1.041E-03
182.22	3.226E-05	1.362E-03	1.253E-03
193.12	5.064E-05	1.638E-03	1.508E-03
203.74	7.690E-05	1.937E-03	1.783E-03
214.13	1.142E-04	2.265E-03	2.085E-03
226.80	1.824E-04	2.709E-03	2.496E-03
240.32	2.945E-04	3.249E-03	2.991E-03
254.58	4.760E-04	3.887E-03	3.576E-03
268.05	7.370E-04	4.563E-03	4.208E-03
282.62	1.162E-03	5.408E-03	4.990E-03
297.96	1.850E-03	6.464E-03	5.977E-03
315.70	3.089E-03	7.949E-03	7.385E-03
328.24	4.336E-03	9.265E-03	8.569E-03
342.04	6.284E-03	1.118E-02	1.039E-02
351.38	8.227E-03	1.286E-02	1.212E-02
371.83	1.426E-02	1.796E-02	1.725E-02

TEMP.	PURE SAMPLE	CADMIUM DOPED SAMPLES	
		8.720E-04	8.140E-04
	P-15	CD2-1	CD2-2
22.61	2.124E-09	9.017E-07	9.155E-07
49.87	6.922E-09	5.354E-06	5.197E-06
60.79	1.208E-08	8.984E-06	8.683E-06
71.31	2.384E-08	1.563E-05	1.491E-05
82.09	5.774E-08	2.935E-05	2.737E-05
96.34	2.199E-07	4.733E-05	4.395E-05
110.70	7.001E-07	7.213E-05	6.702E-05
125.90	1.944E-06	1.077E-04	9.995E-05
135.19	3.389E-06	1.350E-04	1.252E-04
144.35	5.536E-06	1.661E-04	1.541E-04
150.84	7.677E-06	1.908E-04	1.771E-04
161.54	1.274E-05	2.362E-04	2.191E-04
170.99	1.945E-05	2.823E-04	2.619E-04
181.63	3.110E-05	3.430E-04	3.182E-04
192.56	4.904E-05	4.135E-04	3.833E-04
205.06	8.014E-05	5.044E-04	4.673E-04
216.14	1.221E-04	5.953E-04	5.514E-04
228.66	1.931E-04	7.122E-04	6.598E-04
240.03	2.872E-04	8.324E-04	7.716E-04
249.43	3.906E-04	9.461E-04	8.782E-04
260.79	5.755E-04	1.105E-03	1.046E-03
271.68	8.097E-04	1.289E-03	1.203E-03
282.16	1.093E-03	1.490E-03	1.396E-03
291.93	1.504E-03	1.765E-03	1.663E-03
302.23	2.039E-03	2.117E-03	2.011E-03
314.53	2.898E-03	2.699E-03	2.597E-03
351.30	7.987E-03	6.504E-03	6.584E-03
373.45	1.448E-02	1.238E-02	1.252E-02

TEMP.	PURE SAMPLE	CADMIUM DOPED SAMPLES	
		4.410E-04	2.450E-04
	P-14	CD2-3	CD2-4
23.37	1.875E-09	1.206E-06	7.910E-07
51.14	6.746E-09	4.881E-06	3.072E-06
60.60	6.077E-08	7.276E-06	4.516E-06
71.71	1.293E-07	1.155E-05	6.945E-06
82.79	5.496E-08	1.713E-05	1.019E-05
96.62	2.242E-07	2.658E-05	1.568E-05
110.96	7.348E-07	4.022E-05	2.355E-05
126.18	1.990E-06	5.961E-05	3.465E-05
134.00	3.213E-06	7.204E-05	4.172E-05
143.32	5.246E-06	8.858E-05	5.107E-05
153.44	8.721E-06	1.096E-04	6.291E-05
162.43	1.331E-05	1.307E-04	7.481E-05
172.37	2.080E-05	1.571E-04	8.965E-05
182.39	3.215E-05	1.875E-04	1.068E-04
192.71	4.937E-05	2.227E-04	1.266E-04
203.98	7.705E-05	2.659E-04	1.516E-04
207.22	8.725E-05	2.794E-04	1.594E-04
217.66	1.292E-04	3.266E-04	1.881E-04
227.71	1.866E-04	3.791E-04	2.221E-04
238.35	2.717E-04	4.437E-04	2.681E-04
247.94	3.766E-04	5.130E-04	3.230E-04
264.04	6.418E-04	6.705E-04	4.680E-04
274.14	8.792E-04	8.087E-04	6.127E-04
285.61	1.246E-03	1.029E-03	8.646E-04
301.04	1.929E-03	1.466E-03	1.383E-03
317.61	3.114E-03	2.363E-03	2.394E-03
333.68	4.798E-03	3.730E-03	3.985E-03
351.76	7.972E-03	6.576E-03	7.045E-03
370.93	1.360E-02	1.202E-02	1.262E-02

Fig. 14 (Continued)

TEMP.	PURE SAMPLE	CADMIUM DOPED SAMPLES 5.540E-04	3.730E-04
	P-16	CD3-1	CD3-2
23.88	1.878E-09	1.388E-06	1.137E-06
51.16	6.540E-09	5.576E-06	4.383E-06
70.64	2.105E-08	1.353E-05	9.619E-06
82.86	5.583E-08	2.082E-05	1.465E-05
95.85	1.947E-07	3.169E-05	2.220E-05
110.83	6.801E-07	4.892E-05	3.414E-05
125.28	1.847E-06	7.134E-05	4.958E-05
132.97	2.932E-06	8.589E-05	5.960E-05
143.02	5.112E-06	1.080E-04	7.472E-05
151.25	7.787E-06	1.286E-04	8.880E-05
160.53	1.212E-05	1.547E-04	1.067E-04
171.29	1.972E-05	1.894E-04	1.302E-04
171.73	2.015E-05	1.910E-04	1.313E-04
182.25	3.178E-05	2.301E-04	1.579E-04
193.58	5.069E-05	2.776E-04	1.901E-04
204.28	7.758E-05	3.291E-04	2.254E-04
215.09	1.171E-04	3.880E-04	2.661E-04
228.21	1.895E-04	4.700E-04	3.243E-04
237.85	2.666E-04	5.400E-04	3.760E-04
247.21	3.665E-04	6.177E-04	4.363E-04
257.72	5.208E-04	7.229E-04	5.234E-04
268.89	7.463E-04	8.642E-04	6.497E-04
272.59	8.389E-04	9.210E-04	7.033E-04
284.36	1.208E-03	1.145E-03	9.220E-04
298.45	1.834E-03	1.545E-03	1.341E-03
315.50	2.869E-03	2.306E-03	2.200E-03
333.26	4.636E-03	3.684E-03	3.757E-03
351.24	7.691E-03	6.235E-03	6.516E-03
371.35	1.335E-02	1.159E-02	1.210E-02

TEMP.	PURE SAMPLE	CADMIUM DOPED SAMPLES 1.980E-04	1.280E-04
	P-17	CD3-3	CD3-4
23.37	2.372E-09	6.938E-07	4.924E-07
60.40	1.716E-08	3.974E-06	2.755E-06
70.12	2.159E-08	5.723E-06	3.938E-06
82.03	5.392E-08	8.660E-06	5.932E-06
97.98	2.394E-07	1.424E-05	9.664E-06
109.24	6.175E-07	1.955E-05	1.318E-05
124.09	1.717E-06	2.859E-05	1.914E-05
134.65	3.231E-06	3.663E-05	2.439E-05
142.35	4.935E-06	4.333E-05	2.875E-05
151.56	7.847E-06	5.232E-05	3.457E-05
161.14	1.238E-05	6.292E-05	4.143E-05
170.64	1.911E-05	7.495E-05	4.922E-05
181.43	3.048E-05	9.033E-05	5.931E-05
192.42	4.829E-05	1.086E-04	7.156E-05
202.34	7.157E-05	1.275E-04	8.471E-05
213.77	1.113E-04	1.536E-04	1.041E-04
226.87	1.800E-04	1.920E-04	1.355E-04
237.85	2.663E-04	2.361E-04	1.760E-04
247.70	3.722E-04	2.900E-04	2.302E-04
258.19	5.273E-04	3.734E-04	3.194E-04
266.79	6.972E-04	4.729E-04	4.303E-04
278.10	9.957E-04	6.659E-04	6.483E-04
286.95	1.305E-03	8.868E-04	8.980E-04
301.82	2.002E-03	1.430E-03	1.523E-03
316.49	2.990E-03	2.321E-03	2.467E-03
332.08	4.491E-03	3.801E-03	4.001E-03
350.33	7.434E-03	6.632E-03	6.963E-03
371.35	1.343E-02	1.240E-02	1.288E-02

Fig. 14 (Continued)

TEMP.	PURE SAMPLE	CADMIUM DOPED SAMPLES 1.510E-04	9.320E-05
	P-21	CD4-1	CD4-2
24.73	3.323E-09	6.653E-07	4.544E-07
40.34	6.876E-09	1.418E-06	9.528E-07
59.58	1.654E-08	3.234E-06	2.134E-06
71.47	3.566E-08	5.058E-06	3.325E-06
82.85	8.738E-08	7.424E-06	4.840E-06
98.26	3.193E-07	1.195E-05	7.723E-06
109.89	7.455E-07	1.649E-05	1.058E-05
125.00	1.943E-06	2.413E-05	1.534E-05
133.53	3.163E-06	2.946E-05	1.863E-05
142.78	5.155E-06	3.599E-05	2.264E-05
150.09	7.487E-06	4.182E-05	2.621E-05
161.09	1.255E-05	5.161E-05	3.223E-05
171.79	2.034E-05	6.266E-05	3.908E-05
182.55	3.225E-05	7.533E-05	4.709E-05
192.83	4.936E-05	8.938E-05	5.634E-05
204.04	7.690E-05	1.073E-04	6.905E-05
216.08	1.215E-04	1.314E-04	8.810E-05
226.47	1.779E-04	1.587E-04	1.126E-04
240.08	2.876E-04	2.104E-04	1.656E-04
252.03	4.318E-04	2.825E-04	2.477E-04
262.84	6.154E-04	3.849E-04	3.700E-04
272.37	8.322E-04	5.205E-04	5.333E-04
282.97	1.160E-03	7.508E-04	8.051E-04
300.33	1.950E-03	1.387E-03	1.522E-03
316.35	3.089E-03	2.415E-03	2.612E-03
333.73	4.900E-03	4.221E-03	4.454E-03
352.74	7.952E-03	7.477E-03	7.707E-03
372.89	1.398E-02	1.331E-02	1.367E-02

TEMP.	PURE SAMPLE	CADMIUM DOPED SAMPLES 6.410E-05	3.010E-05
	P-25	CD4-3	CD4-4
24.41	3.172E-09	3.400E-07	2.000E-07
50.00	9.845E-09	1.112E-06	6.199E-07
61.50	1.627E-08	1.735E-06	9.468E-07
71.27	3.344E-08	2.462E-06	1.323E-06
82.44	8.560E-08	3.566E-06	1.901E-06
95.42	2.551E-07	5.277E-06	2.762E-06
110.07	7.783E-07	7.827E-06	4.055E-06
124.98	1.959E-06	1.120E-05	5.706E-06
133.88	3.226E-06	1.368E-05	6.922E-06
142.98	5.229E-06	1.651E-05	8.322E-06
151.30	7.930E-06	1.946E-05	9.807E-06
161.15	1.260E-05	2.338E-05	1.187E-05
171.25	1.984E-05	2.806E-05	1.454E-05
181.73	3.116E-05	3.390E-05	1.840E-05
192.57	4.895E-05	4.163E-05	2.461E-05
202.95	7.375E-05	5.158E-05	3.446E-05
215.64	1.198E-04	7.038E-05	5.689E-05
227.63	1.855E-04	1.005E-04	9.721E-05
239.24	2.796E-04	1.516E-04	1.660E-04
251.62	4.258E-04	2.464E-04	2.893E-04
262.60	6.101E-04	3.859E-04	4.582E-04
273.04	8.510E-04	5.888E-04	6.888E-04
285.19	1.240E-03	9.421E-04	1.071E-03
300.27	1.949E-03	1.618E-03	1.774E-03
316.82	3.142E-03	2.786E-03	2.947E-03
333.79	4.986E-03	4.630E-03	4.796E-03
351.76	7.856E-03	7.701E-03	7.787E-03
373.01	1.406E-02	1.375E-02	1.394E-02

Fig. 14 (Continued)

TEMP.	PURE SAMPLE	COPPER DOPED SAMPLES	
		1.346E-03	1.898E-03
	P-1	CU1-1	CU1-2
24.40	4.323E-09	3.199E-09	3.802E-09
49.98	1.087E-08	2.109E-08	2.418E-08
82.83	6.410E-08	2.528E-07	2.828E-07
110.05	6.236E-07	1.058E-06	1.336E-06
122.43	1.325E-06	2.665E-06	3.341E-06
126.78	2.002E-06	2.364E-06	2.939E-06
143.65	5.263E-06	5.044E-06	6.146E-06
150.55	7.572E-06	6.831E-06	8.277E-06
161.99	1.304E-05	1.099E-05	1.319E-05
172.08	2.060E-05	1.657E-05	1.971E-05
182.11	3.183E-05	2.490E-05	2.939E-05
192.74	4.966E-05	3.790E-05	4.424E-05
203.46	7.554E-05	5.688E-05	6.562E-05
213.95	1.128E-04	8.444E-05	9.605E-05
228.24	1.905E-04	1.432E-04	1.595E-04
239.76	2.864E-04	2.182E-04	2.389E-04
254.29	4.681E-04	3.659E-04	3.928E-04
267.22	7.142E-04	5.761E-04	6.087E-04
282.07	1.134E-03	9.527E-04	9.922E-04
297.95	1.829E-03	1.609E-03	1.656E-03
314.88	2.946E-03	2.747E-03	2.809E-03
P-1 REPLACED BY P-11			
319.42	3.402E-03	3.085E-03	3.121E-03
332.38	4.896E-03	4.606E-03	4.580E-03
351.01	8.083E-03	7.832E-03	7.826E-03
372.45	1.424E-02	1.427E-02	1.429E-02

TEMP.	PURE SAMPLE	COPPER DOPED SAMPLES	
		2.629E-03	4.943E-03
	P-2	CU1-3	CU1-4
24.06	3.426E-09	4.376E-09	4.555E-09
50.58	9.280E-09	3.059E-08	3.212E-08
71.00	2.349E-08	1.444E-07	1.473E-07
83.67	6.065E-08	3.417E-07	3.506E-07
96.96	2.026E-07	8.505E-07	8.635E-07
110.85	6.537E-07	1.826E-06	2.207E-06
126.89	1.977E-06	3.728E-06	6.052E-06
143.77	5.251E-06	7.763E-06	1.272E-05
162.51	1.316E-05	1.646E-05	2.612E-05
182.81	3.271E-05	3.622E-05	5.555E-05
205.89	8.296E-05	8.367E-05	1.232E-04
226.53	1.785E-04	1.706E-04	2.414E-04
254.29	4.671E-04	4.317E-04	5.750E-04
268.62	7.436E-04	6.875E-04	8.866E-04
279.51	1.043E-03	9.730E-04	1.225E-03
297.95	1.825E-03	1.738E-03	2.104E-03
316.81	2.849E-03	2.884E-03	3.413E-03
333.54	4.640E-03	4.601E-03	5.243E-03
351.75	7.843E-03	7.918E-03	8.651E-03
372.50	1.371E-02	1.429E-02	1.553E-02
397.05	2.621E-02	2.810E-02	3.044E-02

Fig. 14 (Continued)

TEMP.	PURE SAMPLE	COPPER DOPED SAMPLES	
		1.463E-04	2.759E-04
	P-24	CU2-1	CU2-2
21.81	4.525E-09	7.118E-09	5.714E-09
36.78	7.692E-09	1.323E-08	1.080E-08
49.85	1.267E-08	2.238E-08	2.065E-08
60.40	1.974E-08	3.460E-08	3.597E-08
71.05	3.464E-08	5.614E-08	6.773E-08
81.82	8.051E-08	9.359E-08	1.192E-07
95.32	2.299E-07	1.834E-07	2.359E-07
103.48	4.404E-07	2.800E-07	3.598E-07
109.66	6.862E-07	3.707E-07	4.854E-07
116.62	1.106E-06	5.335E-07	6.859E-07
125.68	2.009E-06	8.588E-07	1.075E-06
133.81	3.137E-06	1.326E-06	1.618E-06
142.52	5.026E-06	2.118E-06	2.480E-06
151.05	7.773E-06	3.337E-06	3.745E-06
160.82	1.229E-05	5.563E-06	5.991E-06
170.93	1.946E-05	9.402E-06	9.722E-06
180.18	2.908E-05	1.504E-05	1.506E-05
181.26	3.048E-05	1.592E-05	1.590E-05
192.06	4.797E-05	2.723E-05	2.634E-05
203.16	7.443E-05	4.604E-05	4.354E-05
214.67	1.153E-04	7.791E-05	7.247E-05
227.17	1.824E-04	1.342E-04	1.237E-04
237.44	2.623E-04	2.050E-04	1.891E-04
247.88	3.746E-04	3.086E-04	2.860E-04
257.36	5.130E-04	4.401E-04	4.109E-04
267.17	7.059E-04	6.267E-04	5.903E-04
278.26	1.000E-03	9.159E-04	8.716E-04
289.26	1.398E-03	1.311E-03	1.260E-03
301.29	1.994E-03	1.912E-03	1.858E-03
315.55	3.005E-03	2.925E-03	2.874E-03
333.02	4.807E-03	4.724E-03	4.698E-03
352.53	7.959E-03	7.844E-03	7.896E-03
372.36	1.371E-02	1.361E-02	1.374E-02

TEMP.	PURE SAMPLE	COPPER DOPED SAMPLES	
		3.333E-04	4.194E-04
	P-23	CU2-3	CU2-4
21.59	3.049E-09	3.800E-09	3.993E-09
40.28	6.922E-09	1.041E-08	1.072E-08
49.26	1.015E-08	1.691E-08	1.757E-08
61.11	1.767E-08	3.334E-08	3.352E-08
70.71	3.122E-08	6.098E-08	6.818E-08
83.53	8.220E-08	1.299E-07	1.463E-07
96.13	2.461E-07	2.600E-07	2.904E-07
109.85	7.031E-07	7.049E-07	7.870E-07
116.35	1.100E-06	7.200E-07	8.015E-07
125.13	1.913E-06	1.115E-06	1.233E-06
134.01	3.195E-06	1.733E-06	1.892E-06
142.50	5.039E-06	2.600E-06	2.818E-06
149.62	7.256E-06	3.673E-06	3.943E-06
160.63	1.221E-05	6.151E-06	6.508E-06
171.02	1.957E-05	1.001E-05	1.044E-05
181.21	3.035E-05	1.599E-05	1.647E-05
192.13	4.783E-05	2.637E-05	2.681E-05
204.57	7.873E-05	4.628E-05	4.642E-05
215.66	1.201E-04	7.513E-05	7.464E-05
227.22	1.830E-04	1.225E-04	1.207E-04
240.81	2.949E-04	2.130E-04	2.088E-04
255.09	4.772E-04	3.715E-04	3.633E-04
268.43	7.351E-04	6.084E-04	5.954E-04
282.77	1.152E-03	1.007E-03	9.881E-04
299.49	1.902E-03	1.745E-03	1.720E-03
317.26	3.169E-03	3.009E-03	2.994E-03
333.95	4.967E-03	4.719E-03	4.680E-03
351.98	7.895E-03	7.592E-03	7.569E-03
371.75	1.358E-02	1.312E-02	1.332E-02

Fig. 14 (Continued)

TEMP.	PURE SAMPLE	COPPER DOPED SAMPLES		TEMP.	PURE SAMPLE	COPPER DOPED SAMPLES	
		2.520E-05	6.140E-05			7.420E-05	9.610E-05
	P-22	CU3-1	CU3-2		P-26	CU3-3	CU3-4
24.31	3.145E-09	3.628E-09	2.288E-09	24.22	4.440E-09	2.231E-09	2.389E-09
49.74	9.705E-09	1.141E-08	9.817E-09	49.36	1.244E-08	9.639E-09	1.075E-08
60.87	1.589E-08	1.831E-08	1.818E-08	60.91	2.094E-08	1.912E-08	2.102E-08
71.31	3.196E-08	3.017E-08	3.343E-08	71.14	3.849E-08	3.599E-08	3.902E-08
82.45	7.872E-08	5.433E-08	6.395E-08	81.87	8.204E-08	6.450E-08	7.008E-08
97.05	2.725E-07	1.275E-07	1.488E-07	92.87	2.082E-07	1.258E-07	1.339E-07
110.49	6.702E-07	2.884E-07	3.199E-07	104.70	5.305E-07	2.512E-07	2.640E-07
124.60	1.873E-06	7.492E-07	7.522E-07	114.45	1.039E-06	4.268E-07	4.484E-07
134.39	3.291E-06	1.436E-06	1.343E-06	125.28	2.009E-06	8.093E-07	8.258E-07
143.24	5.280E-06	2.548E-06	2.273E-06	136.36	3.892E-06	1.593E-06	1.618E-06
151.31	7.883E-06	4.212E-06	3.642E-06	147.30	6.538E-06	2.925E-06	2.901E-06
161.66	1.285E-05	7.781E-06	6.565E-06	159.16	1.151E-05	5.530E-06	5.430E-06
171.39	1.995E-05	1.340E-05	1.124E-05	171.13	1.977E-05	1.059E-05	1.033E-05
182.00	3.146E-05	2.312E-05	1.954E-05	181.90	3.141E-05	1.858E-05	1.805E-05
192.50	4.870E-05	3.850E-05	3.307E-05	191.84	4.750E-05	3.060E-05	2.972E-05
203.63	7.576E-05	6.361E-05	5.584E-05	203.10	7.407E-05	5.204E-05	5.062E-05
216.10	1.217E-04	1.075E-04	9.686E-05	213.72	1.112E-04	8.380E-05	8.205E-05
227.58	1.850E-04	1.691E-04	1.557E-04	228.30	1.900E-04	1.557E-04	1.527E-04
240.51	2.918E-04	2.741E-04	2.582E-04	240.56	2.918E-04	2.523E-04	2.485E-04
254.94	4.742E-04	4.555E-04	4.370E-04	253.36	4.483E-04	4.045E-04	3.996E-04
268.69	7.416E-04	7.219E-04	7.018E-04	268.71	7.395E-04	6.927E-04	6.868E-04
282.90	1.158E-03	1.139E-03	1.117E-03	284.06	1.196E-03	1.147E-03	1.141E-03
298.79	1.862E-03	1.842E-03	1.820E-03	300.97	1.984E-03	1.941E-03	1.933E-03
313.72	2.871E-03	2.853E-03	2.829E-03	315.50	2.972E-03	2.957E-03	2.932E-03
332.47	4.809E-03	4.819E-03	4.782E-03	331.60	4.620E-03	4.658E-03	4.600E-03
351.67	7.892E-03	8.027E-03	7.935E-03	351.30	7.693E-03	7.944E-03	7.791E-03
371.16	1.334E-02	1.334E-02	1.339E-02	371.77	1.330E-02	1.347E-02	1.341E-02

Fig. 14 (Continued)

quite close to the isotherm temperature. The relative conductivity for a given sample and isotherm temperature was calculated by dividing the conductivity by the average of the conductivity of the 14 pure samples at that temperature.

Below 298°C, isotherms which were determined by both methods usually agreed within one per cent. Above this temperature, differences of two to three per cent were noted for some samples. The indirect method was more consistent at these temperatures.

The relative conductivity isotherms are tabulated in Fig. 15 for the cadmium and copper doped samples.

3. Conductivity of pure silver chloride

The average values of conductivity for the 14 pure samples are presented in Table 5. In the temperature range 152-298°C, the deviation from the average for most samples was several tenths of one per cent; for two samples it was just over one per cent. Above this temperature range, the deviation commonly was up to four per cent.

B. Errors

It was estimated that the thickness of the conductivity samples could be measured to $\pm$ 0.003 mm and the diameter to $\pm$ 0.01 mm. The corresponding maximum error due to size

Fig. 15. Relative conductivity isotherms

The first three pages are the isotherms for the cadmium doped samples. The second page is a continuation of the table on the first page. The temperatures used represent equal increments on a reciprocal temperature scale. On the third page, the isotherms given are at the temperatures used by Ebert and Teltow (1). The last three pages follow the same format but are for the copper doped samples. An asterisk following a temperature indicates the results for that temperature were determined by the indirect method (see text). Otherwise, the direct method was used. These tables have been prepared by computer; thus 3.005E-05 = 3.005×10^{-5}.

MOLE FRACTION CADMIUM	TEMPERATURE (DEG. C.) 152.33*	161.58	171.24*	181.35	191.92*	202.99	214.60*	226.80	239.62
3.005E-05	1.2083	0.9330	0.7351	0.5950	0.5054	0.4670	0.4721	0.5195	0.5950
6.409E-05	2.3955	1.8350	1.4186	1.0970	0.8618	0.6990	0.5933	0.5435	0.5425
9.324E-05	3.3085	2.5330	1.9536	1.5085	1.1616	0.9160	0.7383	0.6310	0.5775
1.278E-04	4.2331	3.3000	2.5095	1.9460	1.4864	1.1620	0.9161	0.7545	0.6505
1.510E-04	5.2798	4.0620	3.1333	2.4100	1.8451	1.4270	1.1094	0.8870	0.7360
1.980E-04	6.4182	5.0250	3.8280	2.9670	2.2573	1.7500	1.3493	1.0670	0.8635
2.445E-04	7.4278	5.7300	4.4407	3.4170	2.6182	2.0120	1.5518	1.2110	0.9680
3.734E-04	10.9830	8.5500	6.3245	5.0750	3.8779	2.9920	2.2893	1.7600	1.3640
4.414E-04	12.9676	10.0000	7.7717	6.0000	4.6064	3.5370	2.7019	2.0700	1.5900
5.568E-04	15.9014	12.4100	9.5478	7.4300	5.6618	4.3790	3.3359	2.5520	1.9550
6.062E-04	22.0808	17.1900	13.2992	10.3600	7.9441	6.1100	4.6704	3.5580	2.7100
6.539E-04	23.7970	18.4700	14.3356	11.1000	8.5737	6.5900	5.0430	3.8440	2.9180
3.330E-03	85.9305	66.0000	51.7996	39.7200	30.9679	23.5500	18.1826	13.6800	10.3100
3.620E-03	93.4239	72.8000	56.2817	43.2200	33.6567	25.7000	19.7544	14.8500	11.2000
4.430E-03	108.1442	83.3000	65.4941	50.2600	38.8316	29.7100	22.8204	17.1700	13.1000
6.031E-03	153.9777	119.3000	92.6399	71.1400	55.0129	42.0000	32.2797	24.2900	18.4700

MOLE FRACTION CADMIUM	TEMPERATURE (DEG. C.) 253.12	267.34	282.35	298.23	315.04*	332.86*	351.80*	371.96*
3.005E-05	0.6895	0.7800	0.8525	0.9050	0.9521	0.9810	0.9829	0.9848
6.409E-05	0.5845	0.6575	0.7430	0.8225	0.8981	0.9452	0.9735	0.9737
9.324E-05	0.5760	0.6180	0.6900	0.7700	0.8534	0.9099	0.9461	0.9687
1.278E-04	0.6075	0.6180	0.6690	0.7430	0.8028	0.8587	0.9179	0.9539
1.510E-04	0.6495	0.6225	0.6455	0.7025	0.7878	0.8618	0.9173	0.9436
1.980E-04	0.7365	0.6765	0.6725	0.7020	0.7552	0.8170	0.8751	0.9191
2.445E-04	0.8050	0.7145	0.6920	0.7225	0.7502	0.8145	0.8895	0.9467
3.734E-04	1.0780	0.8865	0.7740	0.7315	0.7398	0.7779	0.8367	0.8975
4.414E-04	1.2420	1.0000	0.8490	0.7670	0.7472	0.7637	0.8305	0.9028
5.568E-04	1.5050	1.1870	0.9690	0.8430	0.7775	0.7642	0.8001	0.8595
8.062E-04	2.0980	1.6100	1.2750	1.0270	0.8947	0.8442	0.8421	0.8711
8.539E-04	2.2350	1.7140	1.3600	1.0850	0.9292	0.8476	0.8318	0.8609
3.330E-03	7.7400	5.8200	4.3190	3.2180	2.4959	1.9107	1.5367	1.2551
3.620E-03	8.4300	6.2800	4.6840	3.4850	2.6863	2.0645	1.6333	1.3098
4.430E-03	9.6900	7.2400	5.3500	3.9000	3.0394	2.3031	1.7753	1.3973
6.031E-03	13.6900	10.2000	7.5300	5.5700	4.2068	3.1388	2.3622	1.7854

Fig. 15 (Continued)

MOLE FRACTION CADMIUM	TEMPERATURE (DEG. C.) 175.00°	200.00°	225.00°	250.00°	275.00°	300.00°	325.00°	350.00°	375.00°
3.005E-05	84.1152	45.4173	25.4866	14.7733	8.7925	5.4572	3.5546	2.4249	1.7147
6.409E-05	59.3742	32.0717	18.0438	10.4683	6.2552	3.9054	2.5882	1.8171	1.3517
9.324E-05	51.0767	27.7714	15.6142	9.0898	5.4653	3.4367	2.3047	1.6682	1.2696
1.278E-04	47.0094	25.5422	14.3906	8.3652	5.0429	3.1809	2.1322	1.5658	1.2186
1.510E-04	13.0115	7.0835	3.9964	2.3582	1.4894	1.0515	0.8796	0.8315	0.8690
1.980E-04	12.0703	6.5589	3.7042	2.1890	1.3918	0.9981	0.8571	0.8411	0.8780
2.445E-04	7.0413	3.8042	2.1510	1.3128	0.9083	0.7414	0.7555	0.8241	0.9136
3.734E-04	4.0195	2.1618	1.2546	0.8357	0.6949	0.6950	0.7864	0.8832	0.9532
4.414E-04	8.7206	4.6779	2.6533	1.5939	1.0641	0.8314	0.7629	0.7959	0.8703
5.568E-04	5.9698	3.1982	1.8261	1.1312	0.8189	0.7277	0.7578	0.8314	0.9066
8.062E-04	3.4630	1.8643	1.0968	0.7570	0.6693	0.7008	0.7895	0.8703	0.9242
8.539E-04	2.2695	1.2358	0.7692	0.6104	0.6408	0.7447	0.8330	0.9135	0.9571
3.330E-03	2.8333	1.5251	0.9127	0.6639	0.6276	0.7118	0.8307	0.9134	0.9448
3.620E-03	1.7671	0.9727	0.6411	0.5722	0.6531	0.7808	0.8865	0.9435	0.9708
4.430E-03	1.2856	0.7340	0.5462	0.5725	0.7042	0.8332	0.9285	0.9722	0.9714
6.031E-03	0.6754	0.4720	0.5099	0.6683	0.8194	0.9132	0.9697	0.9829	0.9850

Fig. 15 (Continued)

MOLE FRACTION COPPER	TEMPERATURE (DEG. C.) 152.33*	161.58	171.24*	181.35	191.92*	202.99	214.60*	226.80	239.62
2.520E-05	0.5415	0.6050	0.6720	0.7320	0.7862	0.8355	0.8769	0.9110	0.9385
6.140E-05	0.4661	0.5110	0.5627	0.6175	0.6739	0.7345	0.7878	0.8400	0.8825
7.420E-05	0.4646	0.4910	0.5379	0.5880	0.6442	0.7015	0.7549	0.8140	0.8620
9.610E-05	0.4581	0.4760	0.5248	0.5700	0.6257	0.6825	0.7393	0.7980	0.8485
1.463E-04	0.4315	0.4550	0.4837	0.5230	0.5661	0.6175	0.6729	0.7320	0.7895
2.759E-04	0.4807	0.4850	0.4995	0.5190	0.5477	0.5850	0.6263	0.6760	0.7310
3.334E-04	0.5044	0.5020	0.5108	0.5280	0.5470	0.5820	0.6225	0.6680	0.7190
4.194E-04	0.5393	0.5325	0.5328	0.5430	0.5564	0.5850	0.6194	0.6575	0.7040
1.346E-03	0.8912	0.8440	0.8099	0.7810	0.7698	0.7520	0.7500	0.7510	0.7620
1.898E-03	1.0781	1.0160	0.9625	0.9220	0.8988	0.8690	0.8521	0.8380	0.8340
2.629E-03	1.3325	1.2615	1.1721	1.0825	1.0633	1.0160	0.9833	0.9550	0.9360
4.943E-03	2.1626	2.0030	1.8327	1.7160	1.6058	1.5090	1.4245	1.3010	1.2600

Fig. 15 (Continued)

MOLE FRACTION COPPER	TEMPERATURE (DEG. C.) 253.12	267.34	282.35	298.23	315.04*	332.86*	351.80*	371.96*
2.520E-05	0.9585	0.9725	0.9825	0.9900	1.0097	1.0211	1.0155	0.9906
6.140E-05	0.9170	0.9440	0.9640	0.9770	1.0016	1.0140	1.0044	0.9953
7.420E-05	0.9020	0.9340	0.9570	0.9735	0.9950	1.0110	1.0160	0.9850
9.610E-05	0.8910	0.9250	0.9515	0.9710	0.9862	0.9984	0.9965	0.9806
1.463E-04	0.8410	0.8875	0.9230	0.9500	0.9826	0.9865	0.9707	0.9794
2.759E-04	0.7845	0.8370	0.8830	0.9240	0.9654	0.9814	0.9767	0.9888
3.334E-04	0.7700	0.8225	0.8720	0.9145	0.9610	0.9617	0.9538	0.9607
4.194E-04	0.7555	0.8065	0.8555	0.9010	0.9561	0.9531	0.9502	0.9752
1.346E-03	0.7800	0.8070	0.8420	0.8800	0.9383	0.9780	1.0104	1.0244
1.898E-03	0.8370	0.8520	0.8750	0.9075	0.9578	0.9751	1.0093	1.0256
2.629E-03	0.9245	0.9245	0.9380	0.9620	0.9357	0.9467	1.0002	1.0241
4.943E-03	1.2195	1.1930	1.1700	1.1530	1.1107	1.0805	1.0929	1.1129

Fig. 15 (Continued)

MOLE FRACTION COPPER	TEMPERATURE (DEG. C.) 175.00°	200.00°	225.00°	250.00°	275.00°	300.00°	325.00°	350.00°	375.00°
2.520E-05	0.7990	0.7586	0.7525	0.7789	0.8308	0.8937	0.9334	1.0083	1.0248
6.140E-05	0.9467	0.8784	0.8418	0.8401	0.8706	0.9181	0.9416	1.0069	1.0263
7.420E-05	1.1509	1.0307	0.9570	0.9280	0.9320	0.9582	0.9376	0.9965	1.0257
9.610E-05	1.7894	1.5345	1.3580	1.2472	1.1861	1.1551	1.0911	1.0915	1.1140
1.463E-04	0.4962	0.6032	0.7237	0.8293	0.9082	0.9544	0.9858	0.9713	0.9827
2.759E-04	0.5055	0.5742	0.6673	0.7702	0.8604	0.9281	0.9756	0.9766	0.9919
3.334E-04	0.5145	0.5730	0.6605	0.7571	0.8493	0.9219	0.9672	0.9541	0.9630
4.194E-04	0.5341	0.5774	0.6519	0.7412	0.8320	0.9090	0.9624	0.9495	0.9813
1.346E-03	0.6942	0.8237	0.9056	0.9514	0.9795	0.9919	1.0168	1.0169	0.9853
1.898E-03	0.5819	0.7175	0.8298	0.9080	0.9570	0.9795	1.0100	1.0053	0.9939
2.629E-03	0.5555	0.6857	0.8041	0.8875	0.9447	0.9798	1.0039	1.0172	0.9777
4.943E-03	0.5411	0.6671	0.7879	0.8761	0.9383	0.9755	0.9936	0.9973	0.9771

Fig. 15 (Continued)

Table 5. Conductivity of pure silver chloride[a]

Temp. (°C)	Conductivity ($\Omega^{-1}cm^{-1}$)	Temp. (°C)	Conductivity ($\Omega^{-1}cm^{-1}$)
20.91	2.886×10^{-9}	253.12	4.484×10^{-4}
60.13	1.830×10^{-8}	267.34	7.124×10^{-4}
83.94	7.344×10^{-8}	282.35	1.137×10^{-3}
97.17	2.385×10^{-7}	298.23	1.830×10^{-3}
111.42	7.723×10^{-7}	315.04	2.935×10^{-3}
126.80	2.093×10^{-6}	332.86	4.770×10^{-3}
143.47	5.299×10^{-6}	351.80	7.929×10^{-3}
152.33	8.275×10^{-6}	371.96	1.375×10^{-2}
161.58	1.279×10^{-5}	200.00[b]	6.582×10^{-5}
171.24	1.979×10^{-5}	225.00[b]	1.692×10^{-4}
181.35	3.070×10^{-5}	250.00[b]	4.040×10^{-4}
191.92	4.773×10^{-5}	275.00[b]	9.050×10^{-4}
202.99	7.399×10^{-5}	300.00[b]	1.926×10^{-3}
214.60	1.154×10^{-4}	325.00[b]	3.859×10^{-3}
226.80	1.806×10^{-4}	350.00[b]	7.551×10^{-3}
239.62	2.840×10^{-4}	375.00[b]	1.495×10^{-2}

[a]Average of 14 determinations.

[b]Longer interpolations were required for these temperatures, used by Ebert and Teltow (1).

measurements was 0.25 per cent.

If the reduced silver electrode did not exactly reproduce the area of the sample, the conductivity would be low. This error could not have been more than the error caused by a 0.02 mm error in the measurement of the diameter, or about 0.3 per cent.

At temperatures above 140°C, for which the resistance of the sample was balanced against resistance boxes, the uncertainty introduced by the bridge and resistance boxes was about 0.1 per cent. The uncertainty in the resistances calculated from the dissipation factor ranged from about three per cent at the lowest resistances determined by this method (100 KΩ) to ten per cent for the highest (200 MΩ).

The frequency dependence of the conductivity of pure silver chloride is shown for several temperatures in Fig. 16. Below 285°C, polarization appeared to be negligible. At 372°C, there was probably a several per cent error due to polarization.

At 298°C and above, the conductivity varied with time. The effect was greater for pure crystals as shown by Table 6. It is believed that this behavior was caused by divalent impurities either from the silver paint or from the Dektol

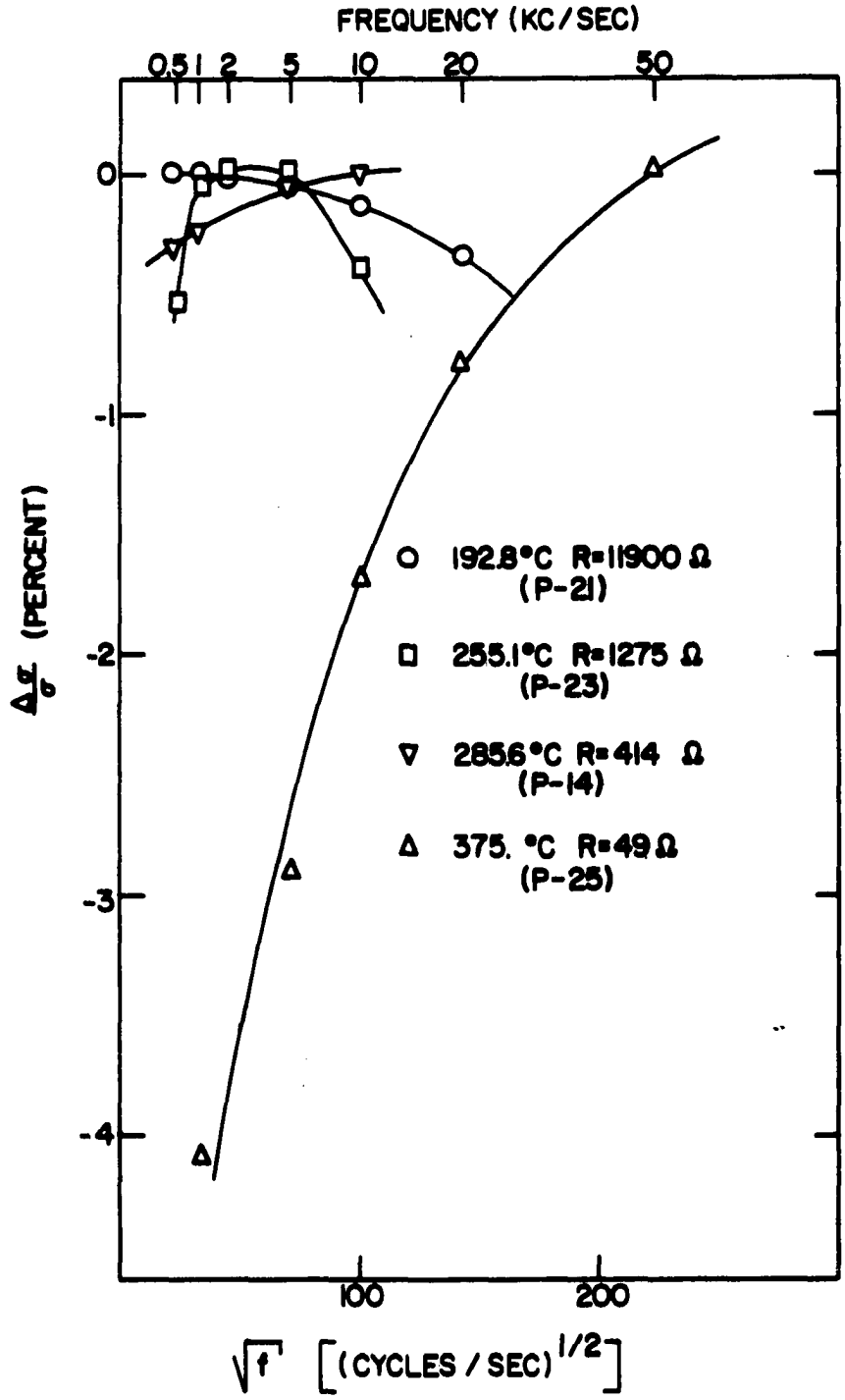

Fig. 16. Frequency dependence of conductivity of pure silver chloride

diffusing into the crystal. This is substantiated by the fact that the room temperature conductivity was about an order of magnitude higher after the conductivity run was completed. A two to five per cent uncertainty in the data above 298°C is caused by this factor.

Table 6. Variation of conductivity with time at 315°C

Δt (min)	$\Delta\sigma/\sigma$ for 0.006 mole fraction Cd doped crystal (per cent)	$\Delta\sigma/\sigma$ for pure crystal (per cent)
0	0.00	
5		0.00
8	-0.06	
15		-0.17
16	+0.03	
24		-0.41

There was a 0.25°C uncertainty in the temperature measurements. The corresponding uncertainty in the conductivity ranged from 0.6 per cent at 375°C to 1.3 per cent at 150°C.

The conductivity is probably accurate to 1.5 per cent in the range 152 to 298°C. Above this range, the uncertainty increases to five to ten per cent at 372°C. Due to partial cancellation of errors, the relative conductivity is probably accurate to less than one per cent in the 152 to 298°C range. Above this range, little cancellation of errors is expected.

VI. RESULTS AND DISCUSSION

A. Cadmium Doped Silver Chloride

1. Method of solution with inclusion of Debye-Huckel interactions

Equations 29, 34, 35, 36, 37, and the relation $\xi = x_v/x_{oo}$ are formally complete; the parameters to be determined are H, x_{oo} and ϕ. By the computer method described below, these parameters were determined by the adjustment of the values to give a calculated conductivity isotherm which best fitted the experimental points.

The experimental isotherm was a set of points $[c_i, (\sigma/\sigma_o)_{i,exp}]$ in which c_i was the concentration and $(\sigma/\sigma_o)_{i,exp}$ was the experimental relative conductivity for the i^{th} point. For each concentration, c_i, Equation 36 was solved with a given x_{oo} and H to yield ξ_i, the value of ξ for the concentration. Since $x_v = x_{oo}\xi_i$, γ was a function of ξ_i given by Equations 34 and 35. Therefore Equation 36 had to be solved numerically.

For a given x_{oo}, γ_o was evaluated by the simultaneous solution of Equation 29 and Equation 34 with $x_v = x_o$ by successive approximation. Then for a given ϕ, a calculated value of the relative conductivity was obtained from Equation

37 for each concentration. The values of H, x_{oo}, and ϕ were adjusted so that (71, Chapter 11)

$$\sum_{i=1}^{n} \left(w_i \left[\left(\frac{\sigma}{\sigma_o} \right)_{i,calc} - \left(\frac{\sigma}{\sigma_o} \right)_{i,exp} \right] \right)^2 = \text{minimum}, \qquad (76)$$

where n was the number of experimental points to be fitted. Curve fitting in this manner is called a least squares method; the summation on the left side of Equation 76 is called the sum of the squares. The weighting factor, w_i, was set by

$$w_i = \frac{1}{\left(\frac{\sigma}{\sigma_o} \right)_{i,exp}} \qquad (77)$$

so that the relative deviation, rather than the absolute deviation, was minimized. H, x_{oo}, and ϕ were varied separately in turn to satisfy Equation 76. The usual order of variation was x_{oo}, ϕ , H, and ϕ ; this cycle was repeated seven to 15 times. ϕ was varied twice each cycle since its variation did not require the solution of Equation 36.

In order to evaluate the ξ_i from Equation 36, a general second degree expansion,

$$y = a_o + a_1 x + a_2 x^2, \qquad (78)$$

was fitted to the three points ($x_1 = g\,\xi_i^o$, y_1), ($x_2 = \xi_i^o$, y_2) and ($x_3 = \xi_i^o/g$, y_3) where

$$y_j = \left(\gamma^2 x_j - \frac{1}{x_j} \right) \left(H x_j + \frac{1}{\gamma_j 2} \right) - \frac{c_i}{x_{oo}} . \qquad (79)$$

ξ_i^o was the estimate for ξ_i and g was a range factor which was made smaller if the solution fell between x_1 and x_3. The approximate solution was obtained from Equation 78 as the value of x closest to ξ_i^o for which y = 0.

The procedure for adjusting H, x_{oo}, or ϕ to satisfy the condition of Equation 76 was similar; H is used for illustration. The sum of the squares, S_j, was calculated for three different values of H: $H_1 = hH^o$, $H_2 = H^o$, and $H_3 = H^o/h$ where H^o was the estimate for H or its value from the previous cycle, and h was a range factor similar in function to g used above. The general second degree expansion, Equation 78, was fitted to the three points ($x_j = H_j$, $y_j = S_j$) where j = 1, 2, or 3. The value of x corresponding to the minimum in the second degree expansion was taken as the new value of H.

The attractive feature of this procedure was that time was not wasted in finding an exact solution for a parameter on each cycle since it changed again after the other two had been varied. Unfortunately, the dependence of the sum of the squares on the value of a parameter was not at all well represented by a second degree equation so proper regulation of h was essential. Furthermore, reasonable initial estimates of H, x_{oo}, ϕ, and the ξ_i were necessary. Even the results

of the simple association theory were not adequate.

To overcome the latter difficulty, Equation 34 was modified by the addition of a factor, s,

$$\log_{10}\gamma = -s \frac{1.1363 \times 10^7 \sqrt{x_v}}{(DT)^{3/2}} \left(\frac{1}{1 + \kappa R}\right) . \qquad (80)$$

This allowed the Debye-Hückel treatment to be "turned on" in steps starting with the simple association theory (s = 0), for which the initial estimates were adequate, to fully on (s = 1). The results of the least squares fit for each step was used for the estimates for the next step.

The variation of H had a relatively smaller effect on the sum of the squares than did the variation of x_{oo} or ϕ. The apparent presence of small, local oscillations in the dependence of the sum of the squares on H as the solution for H was approached often led to difficulties. Better results were obtained when x_{oo} and ϕ were varied while H was held constant. This was done for several values of H. The best value of H was found from a manual plot of the sum of the squares versus H.

Because of the strong dependence of the activity coefficient on the dielectric constant (Equation 34), it was imperative to use reliable values of the dielectric constant at the temperatures for which the data were analysed. The

results of measurements of the temperature dependence of the dielectric constant for silver chloride were kindly provided by G. C. Smith (72) prior to publication.

2. Evaluation and Discussion of Parameters

a. General features of the conductivity isotherms

Several of the isotherms are shown in Figs. 17 and 18. Fig. 17 shows the initial decrease in relative conductivity due to the depression of the concentration of the more mobile interstitials. The roughly linear dependence of conductivity on concentration at high concentration levels due to vacancy conduction is illustrated. This effect appears at lower concentration at lower temperatures since the intrinsic concentration of defects is smaller.

With three variable parameters in both cases, the Debye-Hückel interactions treatment gave a better least squares fit to the isotherms than could be achieved by the simple association theory ($s = 0$ in Equation 77). This is illustrated in Table 7 at temperatures for which data for a direct comparison were available. At other temperatures, H was held constant when $s = 0$, so a fair comparison was not possible. However, the sum of the squares at all temperatures except 202.99°C for the inclusion of the Debye-Hückel interactions was

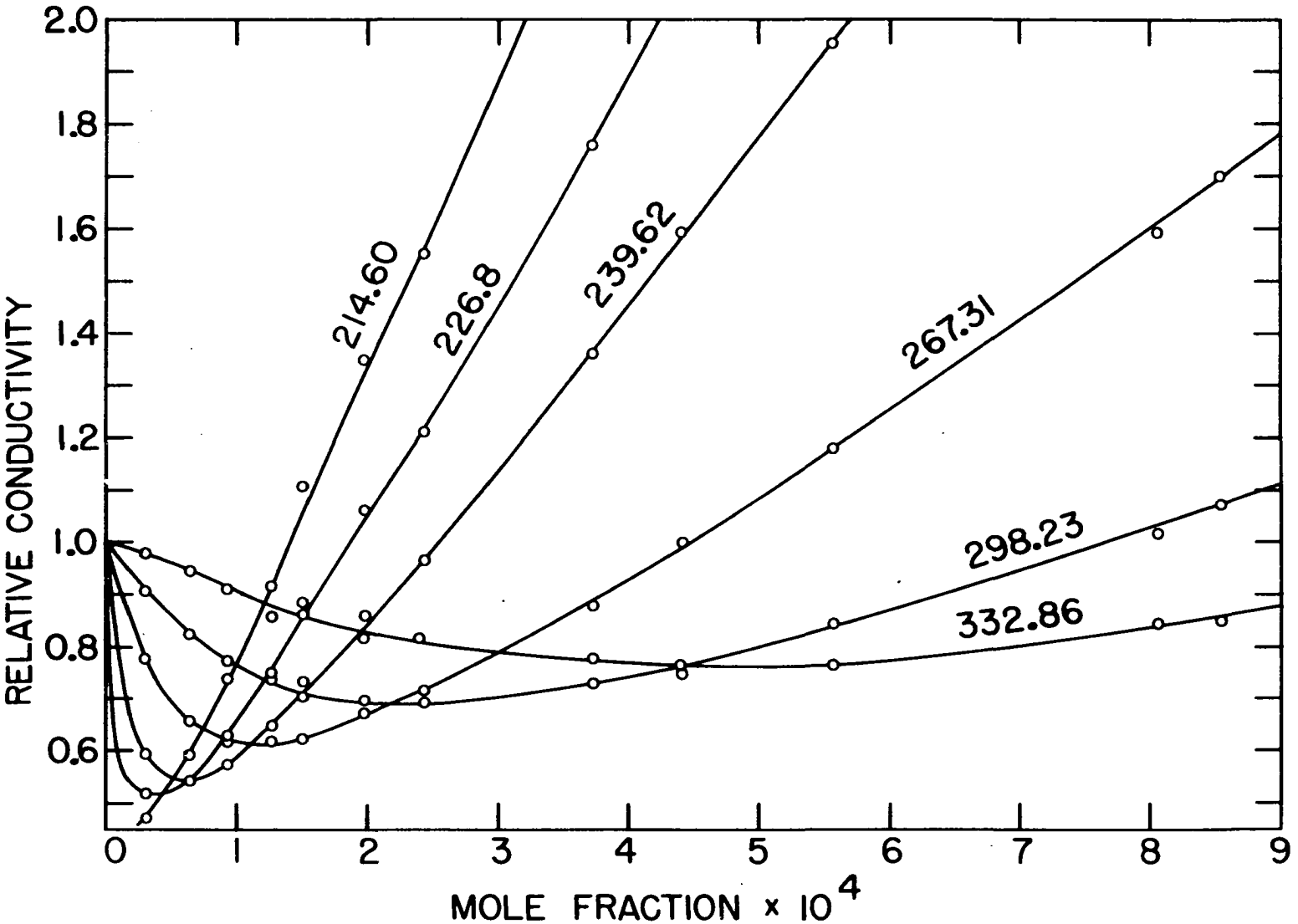

Fig. 17. Relative conductivity isotherms for low concentrations of cadmium for several temperatures (°C)

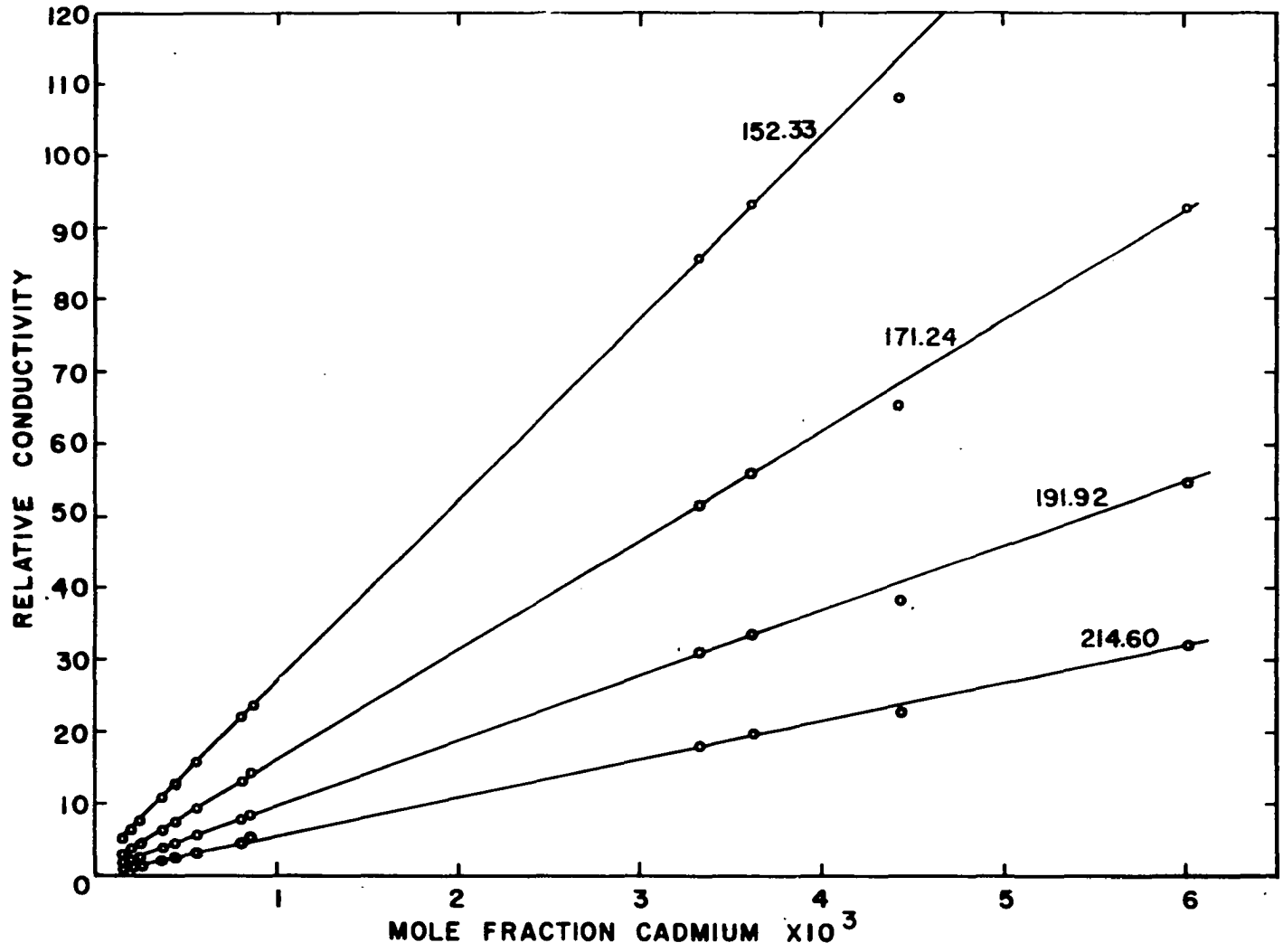

Fig. 18. Relative conductivity isotherms for higher concentrations of cadmium for several temperatures (^{o}C)

3×10^{-3} or less. Isotherms calculated by the least squares fit for both theories are shown with the experimental points in Figs. 19 and 20.

Table 7. Sum of squares for least squares fit to the relative conductivity isotherms[a]

Temperature	Sum of squares simple association theory	Sum of squares Debye-Hückel theory
239.62	1.0×10^{-2}	2.4×10^{-3}
253.12	4.9×10^{-3}	1.1×10^{-3}
267.34	3.1×10^{-3}	8.2×10^{-4}

[a]See facing page, Fig. 19, for details of calculations.

b. Concentration of defects in pure silver chloride

The concentration of defects found by three methods is presented in Table 8. The results of the simple theory are in fair agreement with the values given by Ebert and Teltow (1). The agreement between the results of the simple theory and the simple association theory was most fortuitous since for the three highest temperatures there was bad scatter in the $\frac{c}{(\xi - 1/\xi)}$ versus ξ plots and the placing of the straight line through the points was quite arbitrary.

The values for γ_o indicate that it is important to take into account the Debye-Hückel interactions between the

Fig. 19. Comparison of calculated isotherms with experiment

Both calculated curves were obtained by a least squares fit to the experimental points for the lowest 12 concentrations (8.54×10^{-4} mole fraction or less). All points were weighted inversely proportionally to their relative conductivity in order to minimize the fractional deviation rather than the absolute deivation. R in Equation 34 was taken as 2.9Å. The inclusion of the Debye-Hückel interactions gave a decidedly better fit to the lowest concentration points, and to the highest concentration points (Fig. 20). The four highest points in Fig. 20 were not included in the least squares calculation. The parameters for which the curves were calculated are as follows:

239.6° — — — $\phi = 11.13$, $H = 0.0042$, $x_o = 2.17 \times 10^{-5}$
——— $\phi = 16.29$, $H = 0.011$, $x_{oo} = 1.38 \times 10^{-5}$

267.3° — — — $\phi = 8.63$, $H = 0.012$, $x_o = 4.59 \times 10^{-5}$
——— $\phi = 13.17$, $H = 0.0075$, $x_{oo} = 3.09 \times 10^{-5}$.

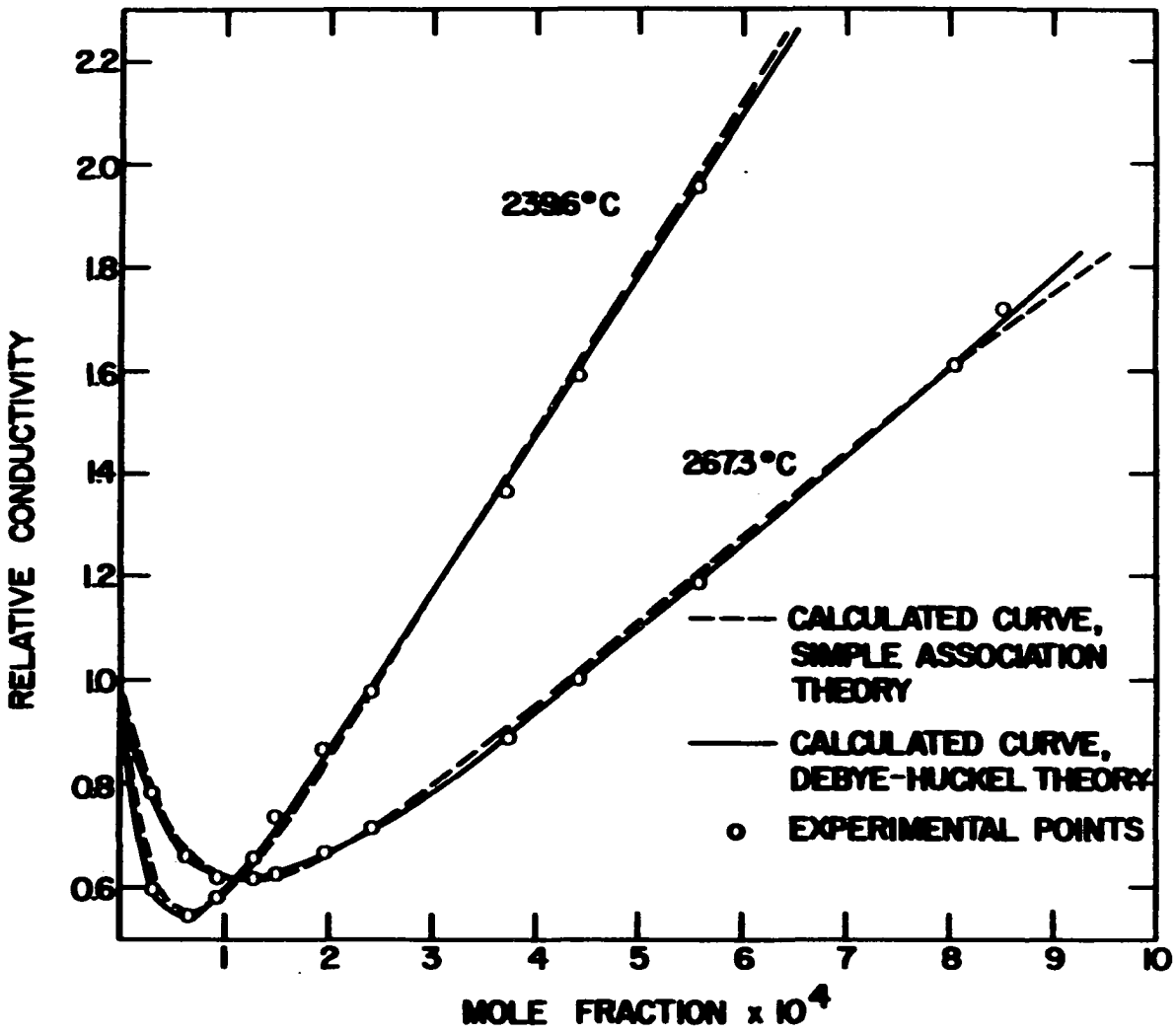
RELATIVE CONDUCTIVITY
2.2
2.0
1.8
1.6
1.4
1.2
1.0
0.8
0.6
1
2
3
4
5
6
7
8
9
10
MOLE FRACTION x 10^4
2396°C
2673°C
CALCULATED CURVE, SIMPLE ASSOCIATION THEORY
CALCULATED CURVE, DEBYE-HUCKEL THEORY
EXPERIMENTAL POINTS

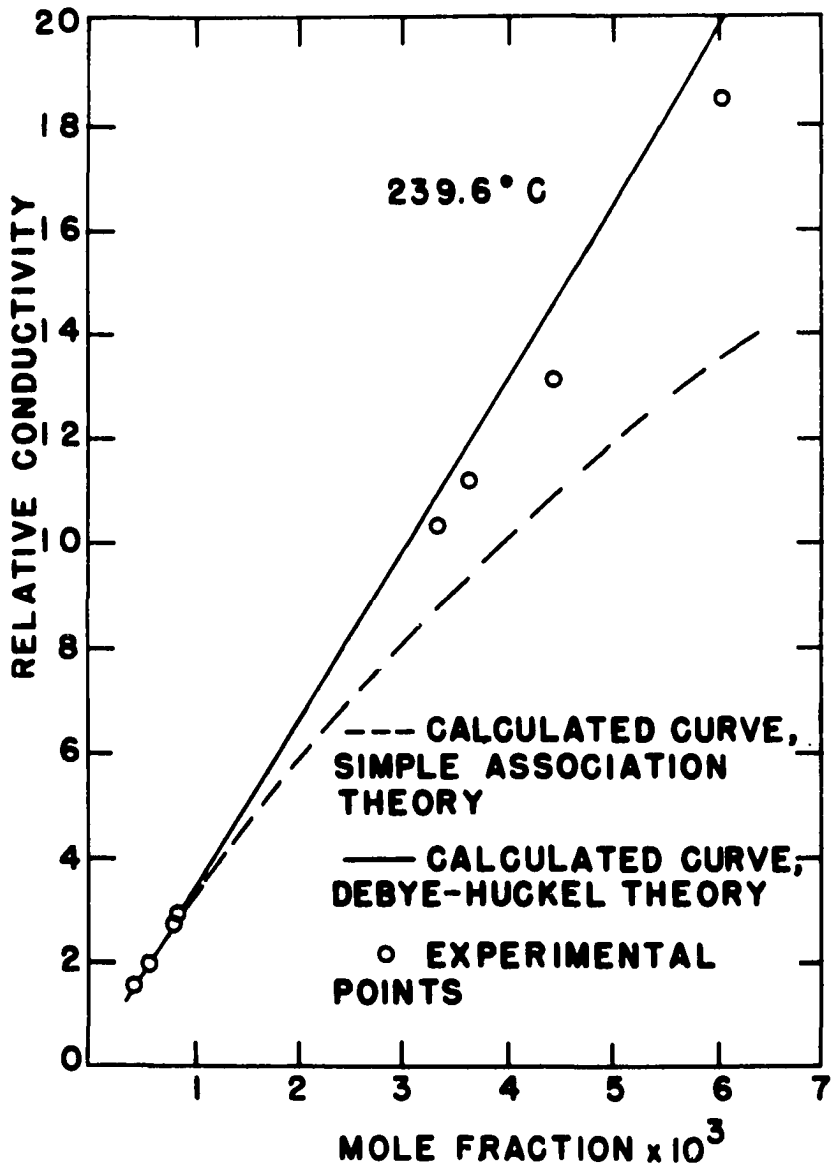

Fig. 20. Comparison of calculated isotherm with experiment; see facing page, Fig. 19

Table 8. Mole fraction of intrinsic defects in silver chloride

Temperature (°C)	x_o^a (mole fraction x 10^5)	x_o^b (mole fraction x 10^5)	$x_{o\delta}^c$ (mole fraction x 10^5)	x_o^c (mole fraction x 10^5)	γ_o^c
202.99	---[d]	---[d]	0.396	0.435	0.910
214.60	---[d]	---[d]	0.565	0.629	0.898
226.80	---[d]	---[d]	0.865	0.980	0.882
239.62	---[d]	---[d]	1.32	1.53	0.864
253.12	2.7	2.5	2.01	2.38	0.845
267.34	3.9	3.8	3.10	3.78	0.821
282.35	6.5	6.6	4.76	5.98	0.795
298.23	9.9	10.	7.05	9.12	0.774
315.04	18.	19.	---	---	---

[a]Simple theory, initial slope method, Equations 19 and 21.

[b]Simple association theory, by plot of $\frac{c}{(\xi - 1/\xi)}$ versus ξ.

[c]By least squares, with Debye-Hückel interactions. Parameters are defined by Equation 29.

[d]Cannot be determined by this method since the minimum in the isotherm did not fall in the range of concentrations used in this investigation.

defects in the pure crystal as well as between the impurity ions and vacancies.

The mole fraction of defects obtained by the Debye-Hückel interactions treatment are plotted logarithmically versus reciprocal temperature in Fig. 21. The enthalpy and entropy change for the formation of a Frenkel defect can be determined from such a plot if Equation 5 is rewritten in terms of mole fraction,

$$x_{oo}^2 = 2 \exp\left(\frac{\Delta s_{th}^o}{k} - \frac{\Delta h_f^o}{kT}\right) \tag{81}$$

The factor of two arises because there are two interstitial sites for every silver ion. A number of values for the enthalpy of formation are given in Table 9.

Table 9. Enthalpy of formation of a Frenkel defect

Method	Δh_f^o (e.u.)
Simple theory, Ebert and Teltow (1)	1.69
Simple association theory, Ebert and Teltow	1.27
Simple theory, present work	1.6
Debye-Hückel interactions treatment, formation of isolated defect (from plot of x_{oo})	1.48
Debye-Hückel interactions treatment, formation of defect in actual crystal at 239°C (from plot of x_o)	1.55
Theoretical value, Yamashita and Kurosawa (73)	1.83

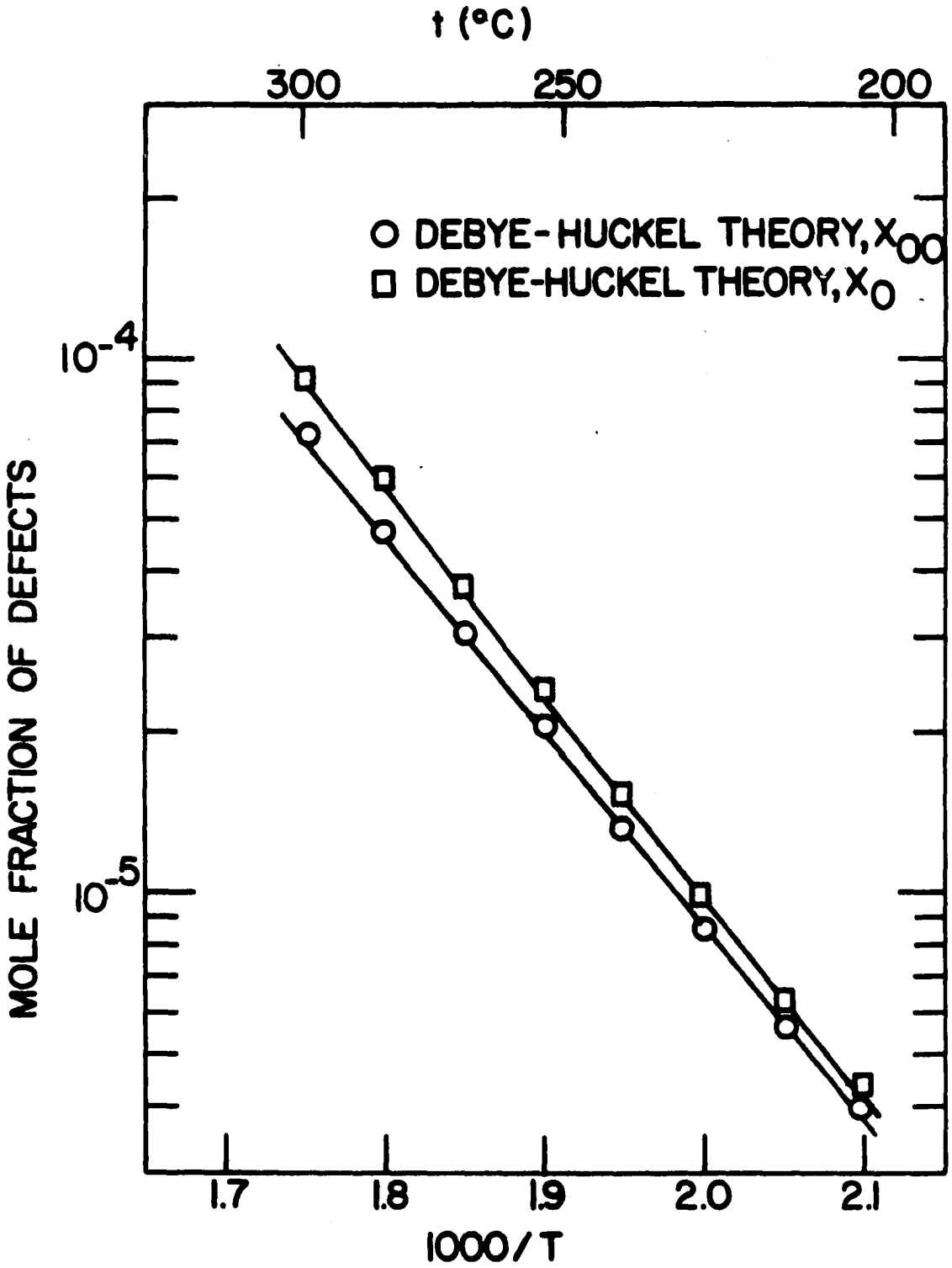

Fig. 21. Temperature dependence of the concentration of Frenkel defects

From the x_{oo} curve of the Debye-Hückel interactions treatment, the entropy of formation was 10.4 e.u. Thus,

$$x_{oo} = \sqrt{2} \exp\left(5.2 - \frac{8588}{T}\right). \qquad (82)$$

c. Divalent ion-vacancy complexes

1) Binding energy The results of the calculations of K_2 by the simple association theory and the Debye-Hückel interactions treatment are given in Table 10. The values determined by the Debye-Hückel interactions treatment are plotted logarithmically versus reciprocal temperature in Fig. 22. Except for the 298.23°C point, which was uncertain since the sum of the squares was insensitive to changes in H, there is a general downward curvature at higher temperatures. The results of the simple association theory displayed a similar strong temperature dependence. No explanation can be offered.

The line drawn in Fig. 22 represents a binding energy of 0.59 ev. This is somewhat larger than the value of 0.14 ev calculated by Bailey (74) and the value of 0.52 ev observed for the manganese(II)-vacancy complex in silver chloride by Daehler (45).

The temperature dependence of K_2 is given by Lidiard (28, p. 299),

Table 10. Complex formation constant, K_2[a]

Temperature (°C)	K_2[b]	K_2[c]
202.99	---	2910
214.60	---	2520
226.80	---	1850
239.62	---	1140
253.12	2200	747
267.34	1700	322
282.35	440 (540)[d]	52.5
298.23	390 (1150)[d]	284
315.04	50 (460)[d]	---

[a]In units of (mole fraction)$^{-1}$.

[b]By simple association theory.

[c]By Debye-Hückel interactions treatment.

[d]In order to check if the rapid drop in K_2 with temperature (corresponding to a binding energy of >1 ev) was real or due to uncertainty in the slope of the $\frac{c}{(\xi - 1/\xi)}$ versus ξ plots, a second line was drawn with what was considered the maximum possible slope. The figures in parentheses are the values of K_2 corresponding to this second line. The minimum binding energy by the simple association theory, using these points, is 0.7 ev.

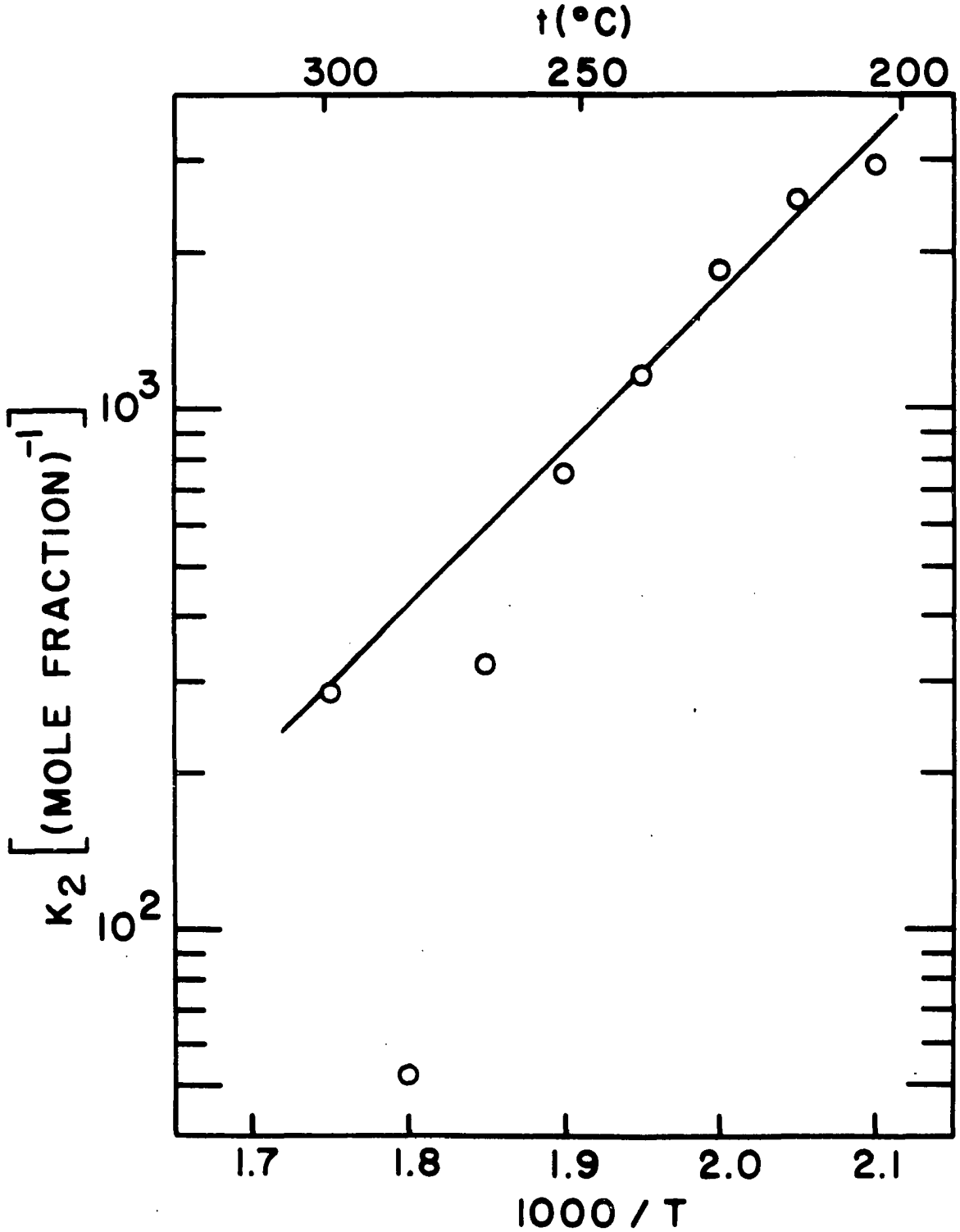

Fig. 22. Temperature dependence of K_2

$$K_2 = z_1 \exp\left(-\frac{\Delta g_a}{kT}\right), \tag{83}$$

where Δg_a is the free energy association and z_1 is the number of distinct orientations of the complex; it is 12 for a sodium chloride type lattice for the nearest neighbor complex. The free energy can be expressed in terms of the enthalpy and entropy of association,

$$\Delta g_a = \Delta h_a - T\Delta s_a. \tag{84}$$

From Fig. 22, $\Delta s_a = -8.8$ e.u. It would be expected that the entropy charge would be considerably less than for the annihilation of a Frenkel defect. This may indicate that the binding energy of 0.59 ev is too high.

2) Degree of association The degree of association as a function of cadmium concentration is shown for three temperatures in Fig. 23.

Lidiard (75) has developed a theory for the conductivity of doped ionic crystals in which both Debye-Hückel interactions and association are taken into account, but in a somewhat different manner than in the present investigation. Lidiard has assumed coulombic interactions at all distances. A single parameter, Δg_a, fixes both the binding energy of the complex and the magnitude of the long range interactions. If Δg_a is chosen as the real free energy of formation of the

Fig. 23. Degree of association versus concentration of cadmium for three temperatures (^{o}C)

The numbers in parentheses represent the quantity $-kT/\Delta g_a$, calculated according to Equation 83.

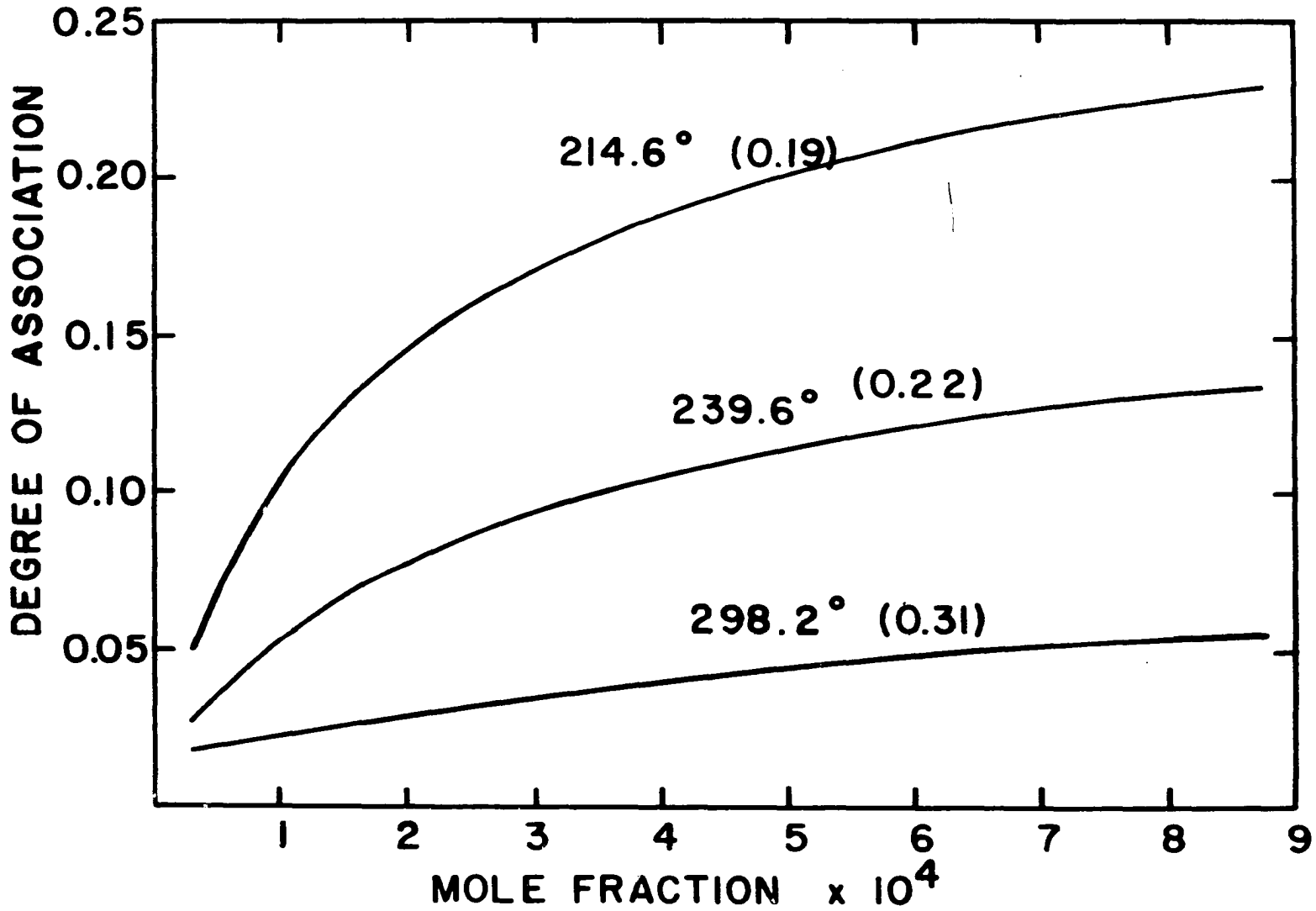
0.25
0.20
0.15
0.10
0.05
DEGREE OF ASSOCIATION
214.6° (0.19)
239.6° (0.22)
298.2° (0.31)
1
2
3
4
5
6
7
8
9
MOLE FRACTION x 10^4

complex, the long range interactions are too small. This is equivalent to activity coefficients which are too large and leads to high values for the degree of association. Lidiard presents graphs similar to Fig. 23 both in the original paper and in the Handbuch der Physik article (28, p. 300). It is not surprising that for a given concentration and Δg_a his values are about a factor of two higher than given in Fig. 23.

In addition, Lidiard has neglected the contribution of intrinsic defects. This is a good approximation for the alkali halides in which the intrinsic defect concentration is small, but is not valid for the silver halides. At very low concentrations of dopant, Lidiard's curves converge on the origin; the ones in Fig. 23 do not.

d. Motion of defects The mobilities of the interstitial and vacancy were calculated by the relation $\phi = \mu_i/\mu_v$ and Equation 14. The results are given in Table 11.

This table illustrates the error in determining ϕ by the minimum in the isotherms for the simple theory and simple association theory. Since the calculation of ϕ is the first step in the treatment of data by these methods, it is surprising that they give as good results as they do.

Equation 11 is an expression of the temperature depend-

Table 11. Mobility of defects

Temperature (°C)	ϕ^a	ϕ^b	$\mu_v^{a,c}$	$\mu_v^{b,c}$	$\mu_i^{a,c}$	$\mu_i^{b,c}$
202.99	--	22.68	--	1.92	--	43.5
214.60	--	20.94	--	2.23	--	46.8
226.80	--	18.37	--	2.54	--	46.6
239.62	--	16.35	--	2.87	--	46.9
253.12	10.08	14.46	4.04	3.26	40.8	47.1
267.34	8.48	12.86	5.15	3.64	43.7	46.8
282.35	7.70	11.34	5.37	4.12	41.4	46.7
298.23	6.20	9.78	6.86	4.98	42.5	48.7
315.04	5.12	--	7.12	--	36.4	--

[a]Simple theory (ϕ calculated by Equation 21).

[b]Debye-Hückel interactions treatment.

[c]Mobility in (cm^2/V sec) x 10^4.

ence of the mobility. It can be rewritten as

$$\mu_s = \frac{\mu_{os}}{T} \exp\left(-\frac{\Delta h_s^*}{kT}\right), \tag{85}$$

where

$$\mu_{os} = \frac{a_s^2 e \nu_s}{k} \exp\left(\frac{\Delta s_s^*}{k}\right). \tag{86}$$

Here Δh_s^* and Δs_s^* are the enthalpy and entropy of activation. The subscript s will be replaced by i or v to denote the various quantities for an interstitial or a vacancy.

The temperature dependence of μ_i and μ_v by the simple theory and the Debye-Hückel interactions treatment is shown in Fig. 24. The quantities calculated according to Equations 85 and 86 by use of this figure are given in Table 12.

Table 12. Mobility parameters

	μ_{ov_o} $\left(\frac{cm^2\ ^oK}{V\ sec}\right)$	Δh_v^* (ev)	μ_{oi_o} $\left(\frac{cm^2\ ^oK}{V\ sec}\right)$	Δh_i^* (ev)
Debye-Hückel interactions treatment	52.5	0.26	6.65	0.045
Ebert and Teltow (1), simple theory	---	0.333	---	0.148
Ebert and Teltow, simple association theory	---	0.371	---	0.139

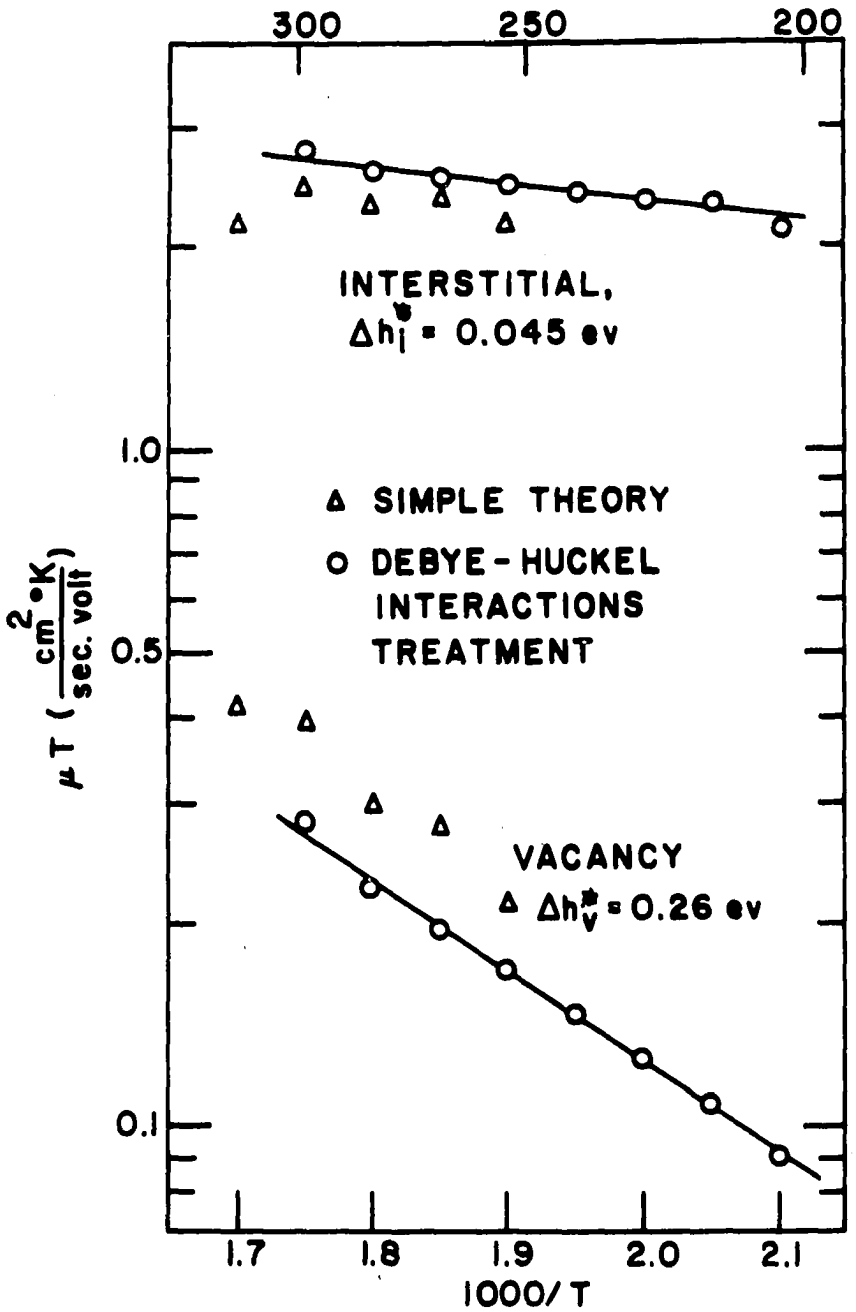

Fig. 24. $\mu_i T$ and $\mu_v T$ versus 1000/T

It is interesting that the results of the simple theory support the very low activation energy for interstitial motion. However, a great deal of confidence cannot be placed in this value; some calculations with R = 2.9 instead of 3.9Å in Equation 34 gave a temperature dependence of interstitial mobility indicating an activation energy of 0.08 ev. Nevertheless, the true value is probably lower than the results of Ebert and Teltow (1) indicate. The low activation energy is in agreement with the calculation by Hove (32) which indicates an activation energy approaching zero for the collinear interstitialcy mechanism.

By analysing the temperature dependence of the correlation factor, Friauf (23, 30) was able to determine the activation energy of the collinear and non-collinear interstitialcy jumps for silver bromide. His values were 0.078 and 0.23 ev, respectively. It was not feasible to treat the existing conductivity and diffusion data for silver chloride in the same manner. If two competing mechanisms of interstitial motion with roughly the above activation energies operated in silver chloride, a curvature in the log $\mu_i T$ versus 1000/T plot should be evident. Unfortunately, the present values of μ_i are not sufficiently accurate to indicate either the presence or

absence of such curvature.

The vacancy activation energy is sometimes determined from the temperature dependence of the conductivity of a crystal containing enough divalent ion to completely overwhelm the thermal defects. According to the simple theory, the number of vacancies is then constant, so the increase of conductivity is due entirely to the activation term. However, this method gives high results since the concentration of vacancies actually increases with temperature due to the release of vacancies by the dissociation of complexes. The presence of complexes is demonstrated by the negative curvature of the nearly straight portion of the curves in Fig. 25. It is easily demonstrated that the slope of these curves gives a value of Δh_v^* that is too high. The slope at 226.8°C on the Cd 2-1 curve in Fig. 25 corresponds to an activation energy of 0.33 ev. However, if the increase in the concentration of vacancies with temperature (and a small increase in contribution of interstitials) is taken into account, a Δh_v^* of 0.28 ev is found, in good agreement with Table 12.

e. The "anomalous" conductivity of silver chloride near the melting point It can be seen in Fig. 26 that the conductivity of pure silver chloride according to Ebert and

Fig. 25. σT versus 1000/T for four cadmium doped samples

The numbers in parentheses indicate the cadmium concentration in mole fraction.

The dashed lines indicate measurements below the solubility limit.

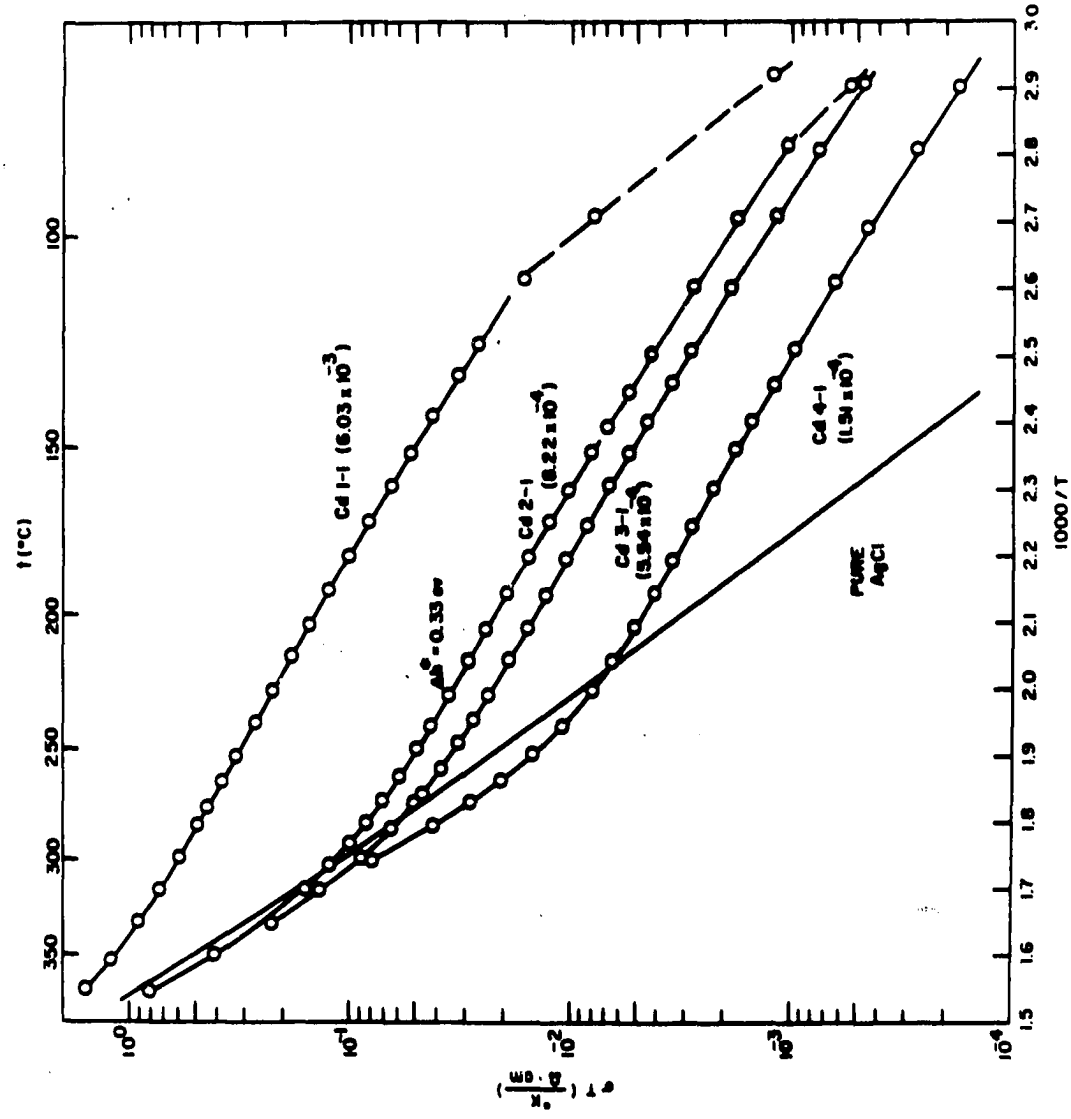
t (°C)
1000/T
Cd 1-1 (6.03 x 10⁻³)
Cd 2-1 (8.22 x 10⁻⁴)
Cd 3-1 (5.54 x 10⁻⁴)
Cd 4-1 (1.54 x 10⁻⁴)
PURE AgCl

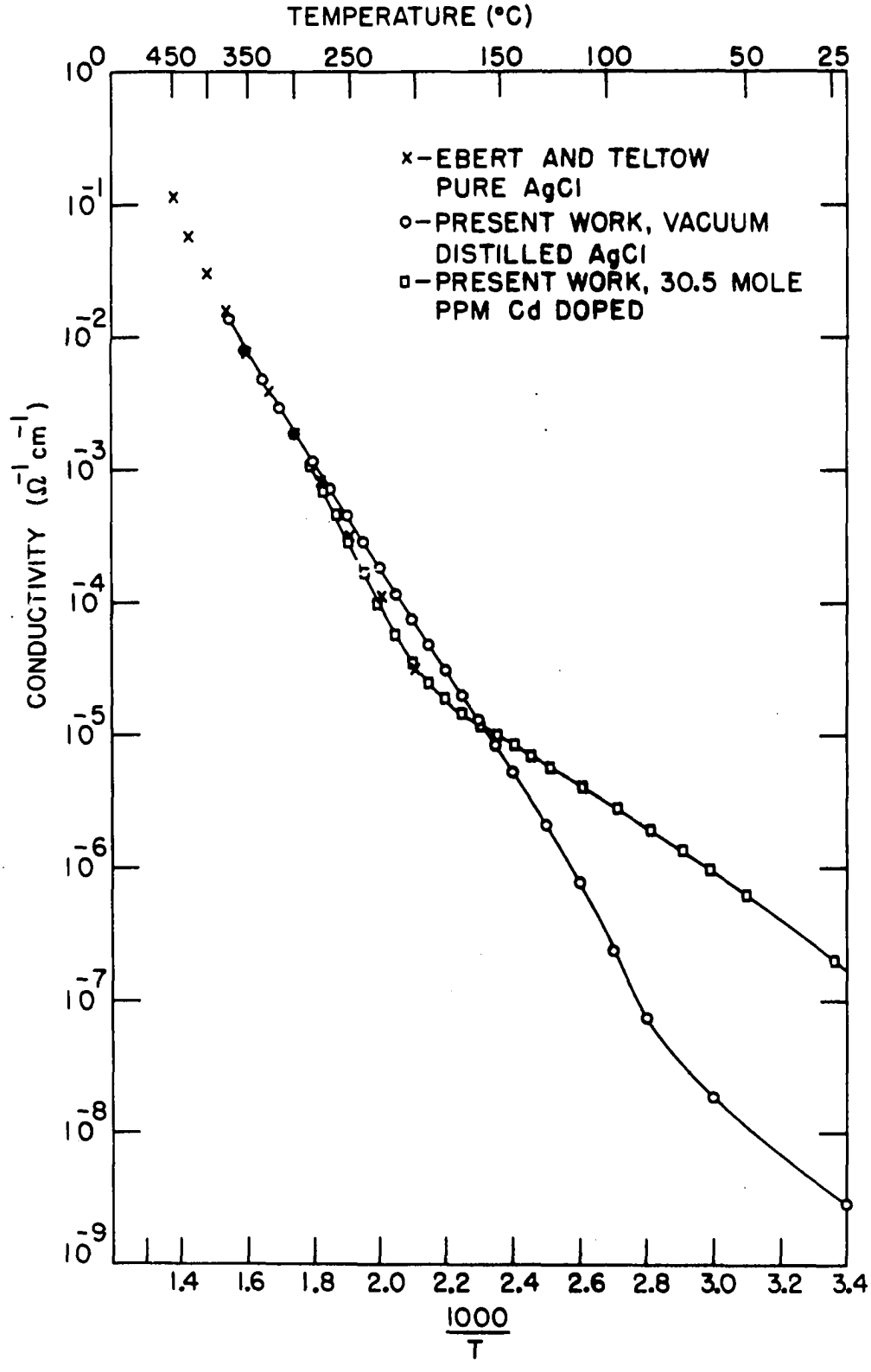

Fig. 26. Conductivity of silver chloride versus 1000/T

Teltow (1) plotted in this manner is represented by a straight line up to a temperature of about 400°C. Above this temperature the conductivity plot exhibits positive curvature. The excess conductivity above the straight line extrapolated from below 400°C has been called the anomalous conductivity. A similar behavior had been observed earlier for silver bromide (8). This behavior has been the subject of much speculation, and it has often been assumed that this rise was due to the onset of Schottky defects. When his dilatation and X-ray measurements indicated that Schottky defects did not occur to any appreciable extent, Fouchaux (20) proposed that the anomalous rise was due to Debye-Hückel interactions and he showed that these interactions predicted a rise of the correct order of magnitude. It appears that this is the correct interpretation.

According to the measurements of the present investigation, the plot of conductivity of pure silver chloride in Fig. 26 is in fact not a straight line below 400°C, but has a positive curvature above 150°C. The conductivity of pure silver chloride is given by Equation 14,

$$\sigma_o = Ne\, x_o(u_v + u_i), \tag{87}$$

where x_o, u_v, and u_i are temperature dependent. There are two

factors which cause the curvature of the plot of σ_o in Fig. 26. The first factor arises because in pure silver chloride the conductivity is the sum of the contribution of two carriers, each with a temperature dependent mobility given by Equation 85. The primary carrier is the interstitial, but the relative contribution of the vacancy increases with temperature from about 4.5 per cent at 203°C to ten per cent at 298°C. The sum of the contributions of the two carriers gives a positive curvature on a logarithmic plot. The second factor is a direct consequence of the Debye-Hückel interactions in pure silver chloride. x_{oo}^2 is the equilibrium constant for the formation of defects, and indeed a plot of log x_{oo} versus 1/T is a straight line (Fig. 21). The actual concentration of defects in the pure silver chloride, x_o, is related to x_{oo} by

$$x_o = \frac{x_{oo}}{\gamma_o} . \qquad (88)$$

But γ_o is given by Equation 34, with x_v replaced by x_o. Since x_o increases with temperature, γ_o decreases with temperature, so x_o increases more rapidly than x_{oo}. This gives rise to the curved plot of x_o in Fig. 21. The curvature of the conductivity plot in Fig. 26 is a reflection of this temperature dependence of x_o. It was roughly estimated that the two factors contribute about equally to the curvature in the range

203-298°C. At temperatures near the melting point, the second factor is relatively much larger.

If in Fig. 26 the conductivity of pure silver chloride in the range 150-250°C is extrapolated with a straight line to the melting point (456°C), the observed conductivity (using the Ebert and Teltow data above 375°C) is about a factor of three higher than the extrapolated value. If x_{oo} (Fig. 21) is similarly extrapolated and x_o is calculated by Equations 34 and 88, it is found that $x_o \simeq 4\ x_{oo}$. At 200°C, $x_o \simeq 1.1\ x_{oo}$ so the Debye-Hückel interactions are sufficient to account for the difference between the extrapolated and observed conductivity rather well. This is especially true if one considers the uncertainties in the extrapolations and the fact that the concentration of defects near the melting point is so large as to be out of the concentration range for which the Debye-Hückel theory is expected to be strictly valid.

B. Copper Doped Silver Chloride

1. General features of the isotherms

The conductivity isotherms for several temperatures are shown in Fig. 27. They qualitatively resemble the isotherms for cadmium doped silver chloride but the minimum for a given

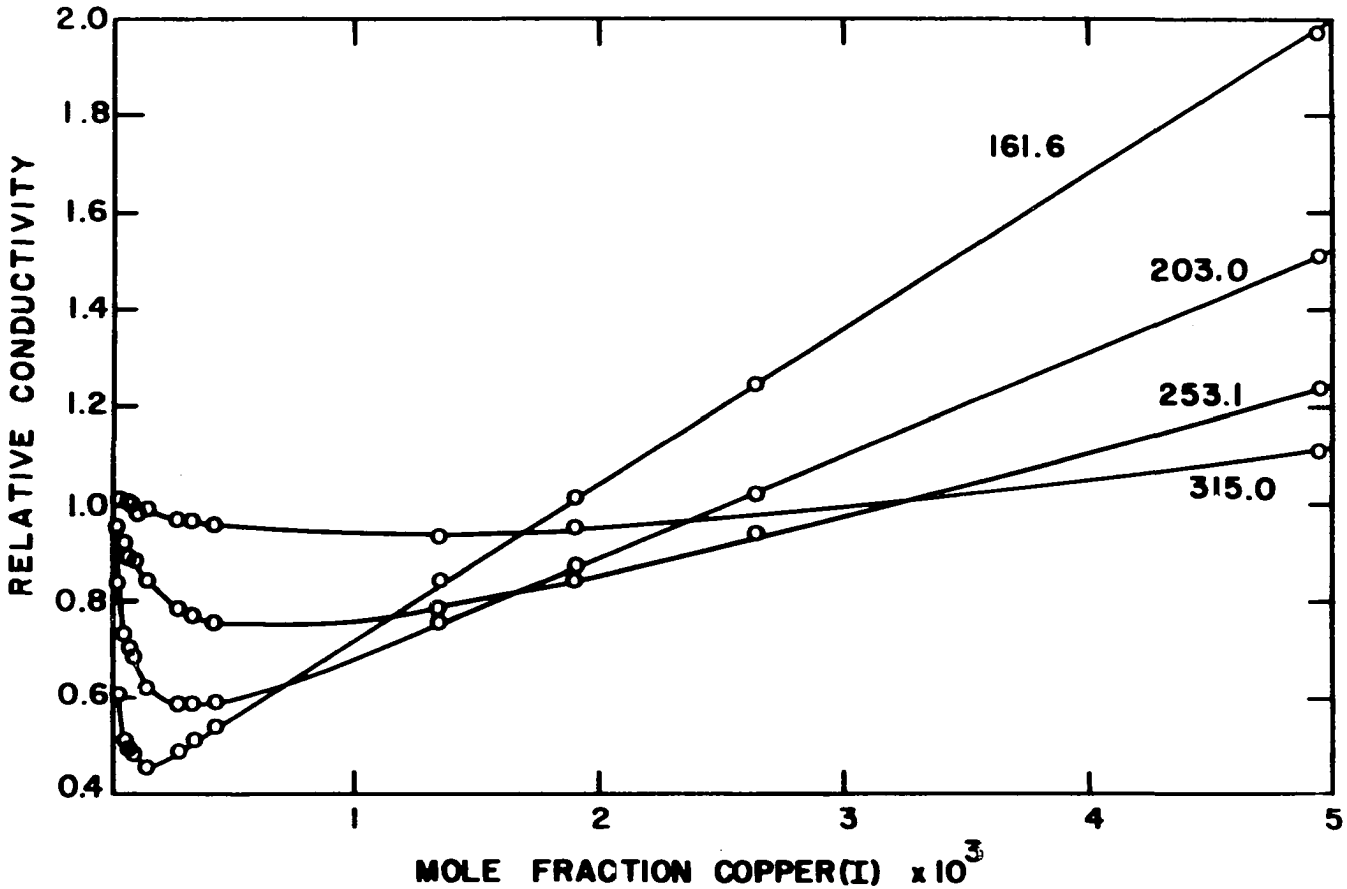

Fig. 27. Relative conductivity isotherms of copper(I) doped silver chloride at several temperatures (^{o}C)

temperature is not so sharp and it occurs at higher concentrations. The minima are definitely not due to traces of Cu(II) since the method of doping used in this investigation was the same as used by Tucker (43) who observed no electron spin resonance. (A resonance was observed after the sample was heated in a chlorine atmosphere.) It is reasonable that this behavior is caused by a fraction of the copper ions entering interstitial positions with the formation of one vacancy per copper interstitial.

2. Results

The data were treated according to the theory in Chapter II (pp. 26-28) with the omission of Debye-Hückel interactions. For consistency, the values for x_{oo} and ϕ were taken from the treatment of the cadmium doped silver chloride data by the simple theory.

The results are presented in Table 13.

3. Discussion

K_I is the equilibrium constant for the reaction

lattice copper ion → interstitial copper ion + vacancy. (89)

The dependence of K_I on copper concentration is probably due to the fact that Debye-Hückel interactions were neglected. Since the products in Equation 89 are charged, increase in

Table 13. Parameters of Cu(I) doped silver chloride

Temperature (°C)	χ [a]	K_I [b,c] (mole fraction)^2	K_I [d] (mole fraction)^2	$\left(\frac{C_i}{C_l}\right)_o$ [e]
253.12	0.81	3.24×10^{-6}	4.98×10^{-6}	0.12
267.34	0.75	5.98×10^{-6}	7.80×10^{-6}	0.15
298.23	0.80	1.22×10^{-5}	1.55×10^{-5}	0.19
315.04	1.01	3.20×10^{-5}	3.56×10^{-5}	0.18

[a]By Equations 44 and 45.

[b]By Equations 49($K_C = 0$), 50, and 51.

[c]Determined at $C = 2 \times 10^{-4}$ mole fraction.

[d]Determined at $C = 1.5 \times 10^{-3}$ mole fraction.

[e]Ratio of the concentration of interstitial copper ion concentration to lattice copper ion concentration at infinite dilution. Based on K_I, footnote c.

defect concentration favors the forward reaction. This is predicted by the Debye-Hückel theory in the decrease of activity coefficient with increase in the ionic concentration. When the activity coefficients are ignored, the effect is manifested in the variation of the equilibrium constant with concentration.

a. The enthalpy of formation The enthalpy change for the reaction given in Equation 89 was determined from the slope of the line in Fig. 28 to be 1.03 ev.

The enthalpy for the analogous reaction

lattice silver ion → interstitial silver ion + vacancy (90)

was 1.48 ev (Table 9).

This difference is easily explained on the basis of the ionic radii. A simple geometrical calculation shows that the copper ion can just fit into an interstitial position but the larger silver ion requires the chloride ions to relax somewhat. The relative ease of the copper interstitial formation is further illustrated by the ratio of interstitial copper ion to lattice copper ion concentration in Table 13.

It is important to note that sodium ions added to silver bromide have no tendency to enter interstitial sites (2) although the sodium ion is about the same size as the copper(I)

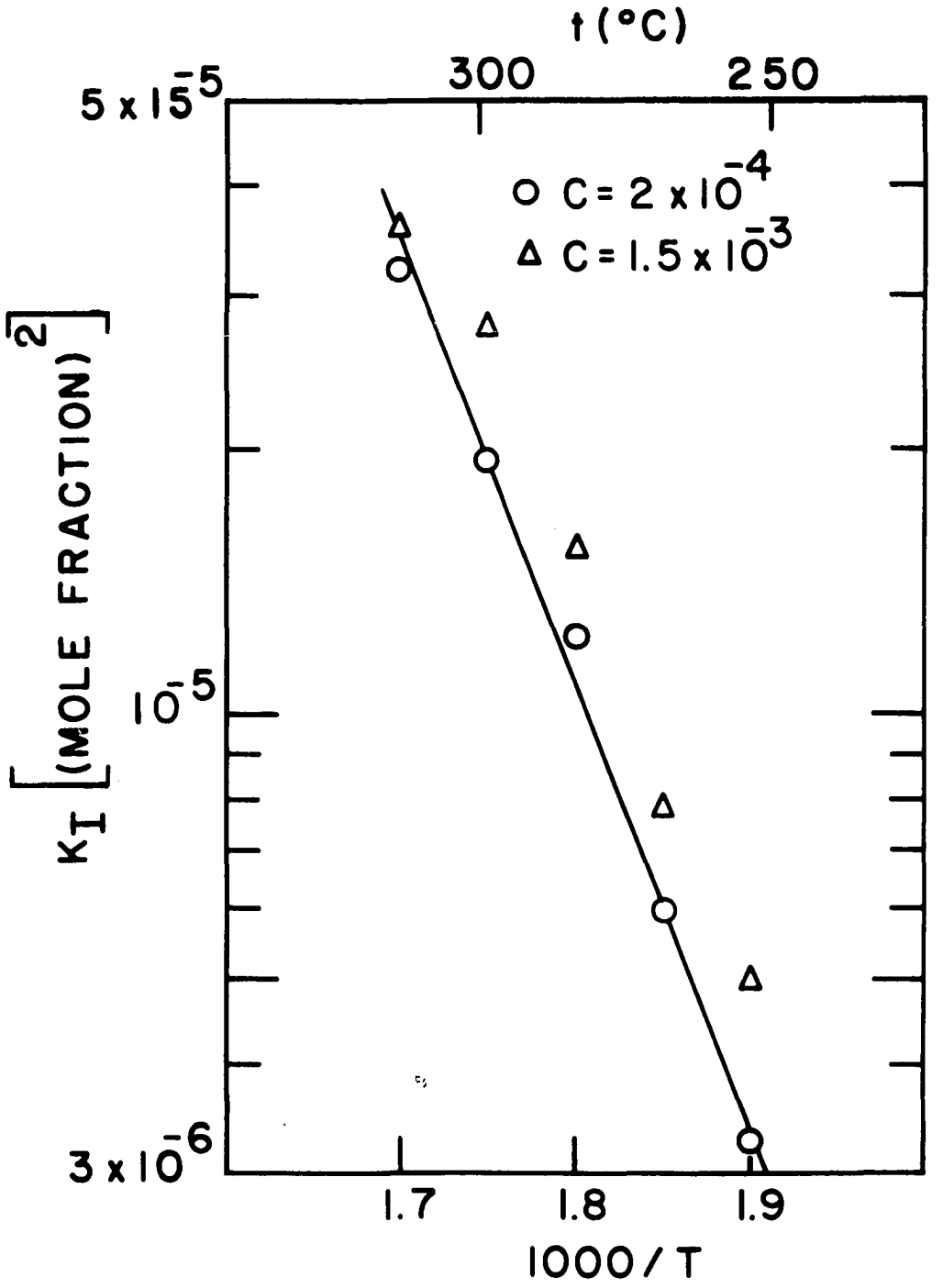

Fig. 28. Temperature dependence of K_I

ion. The explanation for this is the same as the explanation of why sodium chloride exhibits Schottky defects but silver chloride exhibits Frenkel defects. According to the valence bond theory, both copper(I) and silver(I) ions can form hybrid sp^3 orbitals which have tetrahedral symmetry. This coordination is well known in the solution chemistry of these ions. It is proposed that covalent bonding between the sp^3 orbitals and the four adjacent chloride ions tends to stabilize the copper or silver ions in the interstitial position.

Two implications of this proposal are noted. First, the dumbbell interstitialcy proposed by Hove (32) is considered. Hove calculated that the energy of two silver ions straddling a silver lattice site forming a dumbbell in the (1,1,1) plane is about 0.1 ev lower than for an interstitial ion located at the center of symmetry in the interstitial position. Since the existence of the interstitial ion by stabilization through hybrid orbital bonding is dependent on the tetrahedral symmetry, the dumbbell configuration is not likely.

The second implication is that any ion capable of sp^3 hybridization, small enough to fit into the interstitial site, has a tendency to enter the crystal interstitially. Unfortunately, the cadmium ion falls in this category. This

problem is discussed shortly.

b. Activation energy of motion Since within experimental error, χ does not change with temperature, the activation energy for interstitial copper motion must be approximately equal to the vacancy activation energy or about 0.26 ev.

Presumably, a copper ion in an interstitial position can move by the interstitialcy mechanism just as a silver ion. One might first expect a very low activation energy. However, the activation energy must be at least as great as the enthalpy change for the reaction

$$\text{interstitial copper ion} + \text{lattice silver ion} \xrightarrow{\Delta h} \text{lattice copper ion} + \text{interstitial silver ion}^*. \quad (91)$$

The asterisk indicates that the silver interstitial is located next to the copper ion. The above reaction can be approximated by the difference between two reactions for which the enthalpy of reaction has been determined:

$$\text{lattice silver ion} \xrightarrow{1.48\text{ev}} \text{interstitial silver ion} + \text{vacancy} \quad (92)$$

$$\text{lattice copper ion} \xrightarrow{1.03\text{ev}} \text{interstitial copper ion} + \text{vacancy}. \quad (93)$$

This gives $\Delta h = 0.45$ ev, which is probably too large. A silver interstitial located next to a lattice copper ion is

probably at a lower energy than the normal silver interstitial, because the small copper ion can allow the chloride ions to relax to provide a larger interstitial site. There is also uncertainty in the two enthalpies used to calculate Δh, so a value of 0.26 ev is not unreasonable.

C. Experimental Method

1. Purity of silver chloride

If it is assumed that the disagreement in the conductivity of pure silver chloride between the work of Ebert and Teltow (1) and the present investigation is solely due to divalent impurities, it can be estimated that the silver chloride used by these workers contained about 15 mole ppm of polyvalent impurities.

Unfortunately, it is not possible to routinely determine the impurity content of silver chloride at impurity levels below one ppm. However, since the conductivity of silver chloride at lower temperatures is very sensitive to polyvalent cation impurities, a rough estimate of this kind of impurity can be made.

The curve representing the conductivity of the vacuum distilled silver chloride in Fig. 26 has positive curvature down to about 150°C; at this temperature some effect of the

impurities is observed. An extrapolated value of x_o was taken as 0.4 mole ppm. From Equation 19, with an extrapolated $\phi \simeq 40$, $\left[\frac{d(\sigma/\sigma_o)}{dc}\right]_{c\to 0} \simeq -1.25$ per ppm. Since the change in the conductivity at this temperature due to impurities was estimated to be about ten per cent, the total divalent impurity concentration was about 0.1 mole ppm.

Very pure silver chloride has been prepared by Moser, et al. (76) by the zone refining process. The low temperature conductivity of material obtained by this method is compared with the present data in Fig. 29. Apparently the material produced by zone refining is of higher purity although some of the low temperature conductivity in the present work may be influenced by strain since the samples were not annealed. The starting material used for the zone refined silver chloride was of significantly higher purity than the starting material used in the present investigation.

Zone refining does have some basic advantages over vacuum distillation. However, occasionally systems are encountered in which the distribution coefficient of an impurity is so close to unity that it cannot be removed by zone refining. This is the case for several impurities in potassium chloride (56). Vacuum distillation has been applied to this

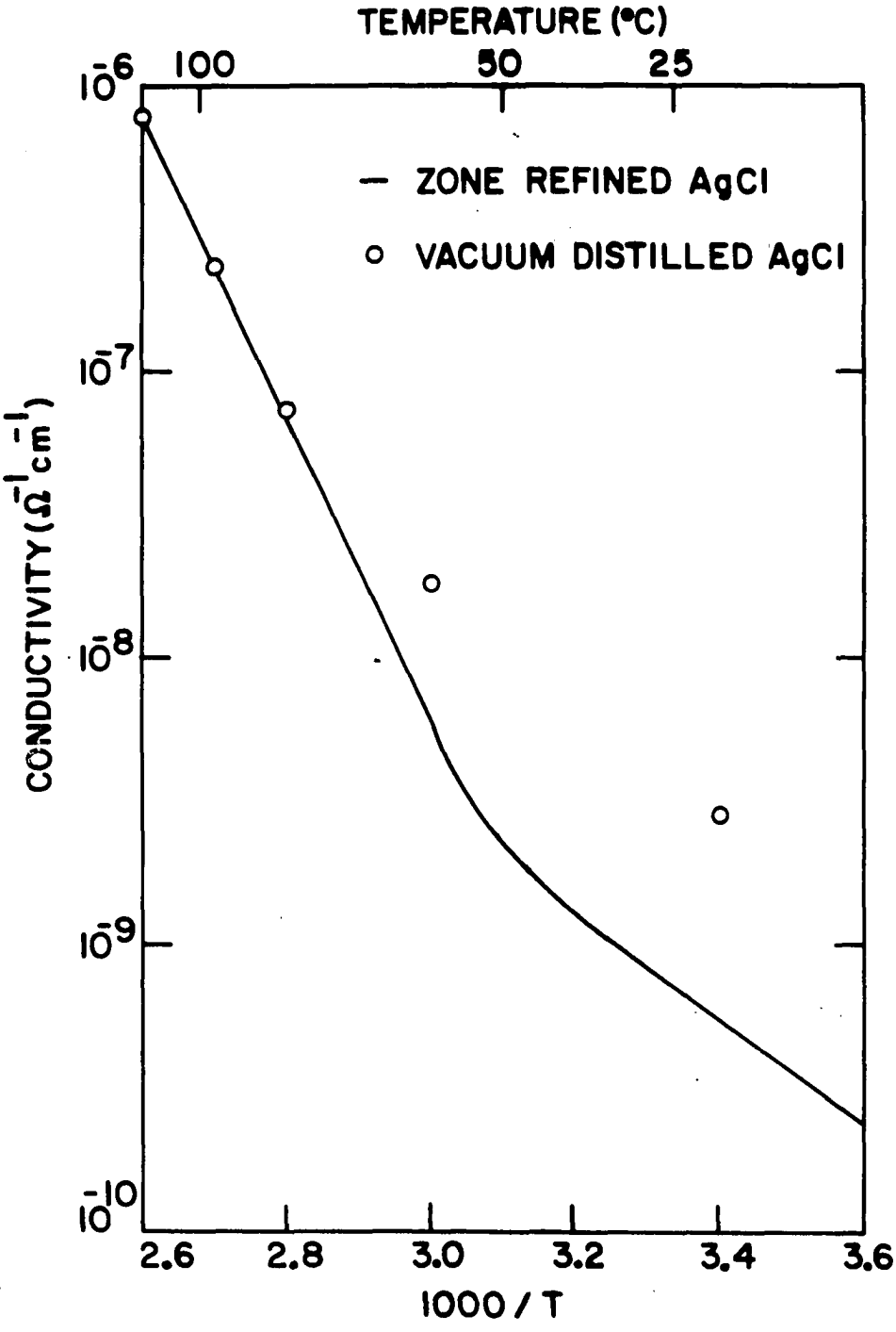

Fig. 29. Comparison of the conductivity of vacuum distilled silver chloride from this investigation with the conductivity of zone refined silver chloride by Moser, et al. (76)

problem with some success (77). In view of the successful application of vacuum distillation in the present investigation, it appears that vacuum distillation may be an alternate to zone refining worthy of consideration.

It should be noted that silver chloride which is to be doped must be free of water or hydroxide ion. It is known that anhydrous cadmium chloride cannot be prepared by heating the hydrated salt since the oxide is formed. If this occurred in silver chloride, the oxide would charge-compensate for the cadmium and the assumed creation of a vacancy for each cadmium ion would not occur.

2. Possibility of cadmium interstitials

The possibility that a fraction of the cadmium ions in cadmium doped silver chloride may enter the crystal interstitially has already been noted. The reaction for the formation of cadmium interstitials is

lattice cadmium ion → interstitial cadmium ion + vacancy. (94)

Since the theory did not take into account possible additional vacancies from this source, the results of this investigation would be affected if this reaction occurred to any appreciable extent. The possibility that the occurrence of this reaction had caused a false temperature dependence of K_2 was consid-

ered, but it does not appear that this was the case. Nevertheless, the use of cadmium as a dopant is common, so it seems worthwhile to consider the possibility of cadmium interstitial formation.

In solution, the cadmium ion forms a number of tetrahedrally coordinated complexes, including the halogen complexes. Furthermore, the cadmium ion, which is nearly the same size as the copper(I) ion, can easily fit into an interstitial position. However, the cadmium interstitial would have a +2 charge as opposed to the +1 of the copper interstitial and would interact strongly with vacancies to repress the reaction in Equation 94. Therefore, it is expected that if cadmium interstitials occur, the enthalpy of formation is high so they would be observed only at high temperatures.

Hanlon (40) has measured the diffusion coefficient of cadmium as a function of concentration. The initial rise of the diffusion coefficient with increasing concentration and the saturation at high concentrations establish that the primary mechanism is the diffusion of lattice cadmium ions by complex formation. If the diffusion were solely by interstitial cadmium ions, the diffusion coefficient would be expected to decrease with increasing concentration. However,

a small fraction of cadmium interstitials would not have been detected. The increase in the slope of the log D versus reciprocal temperature curve at about 300°C, observed in silver chloride by Reade and Martin (33) and in silver bromide by Hanlon, is strong evidence that a new mechanism becomes effective at higher temperatures. The diffusion of cadmium interstitials is the most reasonable high temperature mechanism.

Density measurements of cadmium doped silver chloride at room temperature (78) do not exclude the formation of cadmium interstitials at high temperatures.

Ebert and Teltow (1) have studied the relative conductivity of both cadmium doped and lead(II) doped silver chloride. Because of its size, lead cannot form an interstitial. The slight differences in the isotherms for the two systems can be interpreted on the basis that lead introduces relatively fewer vacancies than does cadmium. However, the larger lead ion tends to form stronger complexes, and it may be that the differences between the isotherms are due to differences in the degree of association.

The absence of cadmium interstitials has not been proved and there are indications that they exist. An investigation of the temperature dependence of the diffusion of radioactive

calcium into pure silver chloride would be desirable. The ionic radius of calcium is 0.99Å compared to 0.96Å for cadmium, and the calcium ion has little tendency to form sp^3 hybrid orbitals. It is expected that a plot of log D versus reciprocal temperature for the calcium diffusion would not exhibit a change of slope at high temperatures. This would strongly indicate that the diffusion of cadmium interstitials is the high temperature mechanism for cadmium diffusion. It would at the same time test the theory of stabilization of interstitials by hybrid orbital bonding.

A study of the conductivity of silver chloride doped with strontium (or calcium) would also be of interest since there would be no possibility of interstitial strontium ions. If the solubility of calcium in silver bromide (8) is used as a guide, only concentrations below one mole per cent could be used. Accurate determination of the strontium concentration at low levels could be accomplished by activation analysis.

D. Discussion of the Present Application of the Debye-Hückel Theory

The approximations and assumptions involved in the Debye-Hückel theory for solutions have been analysed by a number of

workers; summaries with references have been given by Fowler and Guggenheim (79, Chapter 9) and Harned and Owen (80, Chapter 2). Here, the application of the Debye-Hückel theory to the present problem is considered from a more practical viewpoint.

1. Concentration range

It is well known that in aqueous solutions, the Debye-Hückel theory is applicable only to very dilute solutions. If for 1-1 electrolytes, the separation parameter, R, is arbitrarily adjusted, good agreement with experiment can be obtained up to a concentration of about 0.01 M. In silver chloride, a 0.01 M solution of defects corresponds to a mole fraction of 2.6×10^{-4}. It might be expected, however, that the range of applicability in silver chloride would be less than this. The dielectric constant of water is about 80 compared to 15 for silver chloride. It can be predicted from a consideration of the approximations involved in the solution of the Poisson-Boltzmann equation (79, p. 390) and is observed experimentally that the range of applicability decreases as the dielectric constant of the solvent decreases. In the Debye-Hückel interactions treatment of this investigation, concentrations up to 8.5×10^{-4} mole fraction were used in

the calculations. This is justified by the fact that the calculated curves at several times this concentration did not deviate badly from the experimental points (Fig. 20).

In aqueous solutions, the Debye-Hückel theory predicts activity coefficients that are too small at concentrations above the range of applicability. If the Debye-Hückel theory deviated from reality in the same manner in silver chloride, it would be expected that the calculated conductivity isotherms would be too high (Fig. 20). However, the fact that the calculated curve is too high can also be explained qualitatively by the neglect of the present treatment to take into account the effect of the Debye-Hückel charge cloud on the mobility of the vacancy.

It is surprising that the Debye-Hückel theory holds so well at higher concentrations. The mean thickness of the Debye-Hückel charge cloud is given by $1/\kappa$. An indication of the range of $1/\kappa$ for several concentrations is given in Table 14. At distances on the order of the nearest neighbor distance, the interionic forces can no longer be assumed to be coulombic. Strictly coulombic forces were assumed in the Debye-Hückel derivation of the relation for the activity coefficient.

Table 14. Range of $1/\kappa$

Mole fraction cadmium	$1/\kappa$ (Å)
3.0×10^{-5}	40 - 70
8.5×10^{-4}	14 - 15
6.0×10^{-3}	4 - 6

Probably there are factors for which the Debye-Hückel treatment has not accounted, which fortuitously cancel errors. For instance, no account has been taken of the effect of the cadmium dopant and the accompanying vacancies on the mobility of a defect. It is reasonable that the addition of cadmium ions causes a general loosening of the lattice which increases the mobility of the carrier by a decrease of the potential barrier. Although the activity coefficient may in fact be larger and the concentration of defects less than predicted by the Debye-Hückel treatment, the conductivity could be close to the value predicted by the Debye-Hückel theory because of the concentration dependent mobility.

2. The separation parameter, R

Strictly, R is definable only in systems having two kinds of ions. In the present application there are three: vacancies, interstitials, and cadmium ions. Hence, there

are three different closest approach distances: 1) cadmium ion-vacancy, 2) cadmium ion-interstitial, and 3) interstitial-vacancy. R was set equal to the cadmium ion-vacancy distance in the complex configuration or 3.9Å. This procedure should not lead to serious errors. An interstitial and vacancy which are separated by less than 2.4Å annihilate to form a normal silver ion. This sets a minimum value for the separation parameter for this pair. Furthermore, the interstitial-vacancy interactions are most predominant at low doping concentrations where the choice of R is not critical since R appears in Equation 34 as κR and κ is small at low concentration. At higher doping concentrations, the number of interstitials is decreased to a small fraction of the total defects, so the interstitial-vacancy and interstitial-cadmium ion interactions are not important. In addition, the cadmium ion and the interstitial have like charges and have a low probability of being located at the 2.4Å minimum approach distance for this pair.

Another problem is the real physical significance attached to R. In solutions, R is used as an adjustable parameter to give better agreement between experiment and theory at higher concentrations than is possible by the limiting law

(R = 0). Values of R found by adjustment to give best agreement are sometimes much smaller than the possible closest approach of the ions; for example, R = 0.4Å for potassium nitrate and R = 0.0Å for potassium iodate (71, p. 402). According to Fowler and Guggenheim (79, p. 403), R "is not a real mean ionic diameter but rather a parameter correcting for a whole variety of theoretical imperfections". The nitrate and iodate ions are planar and easily polarized, and it is conceivable that induced dipole interactions lower the free energy of these ions to a greater extent than predicted by the Debye-Hückel theory. This would lead to the low values of R. Similar arguments can be advanced for other large ions for which R approaches zero.

Electrolytic solutions of simple ions usually yield more reasonable values for R; for example, for solution of potassium chloride, R = 3.8Å. This gives confidence that in the present application, R can be roughly regarded as a separation parameter, but it would not be surprising if the best value for R is somewhat different than the vacancy-cadmium ion distance.

In practice, a change of R from 3.9Å to 2.9Å changed values of x_{oo}, μ_v and μ_i by only a few per cent at most. The

activation energy for the interstitial is affected more strongly, as is the binding energy for the complex. However, the affect is not sufficient to change any of the basic conclusions.

3. Effect of Debye-Hückel interactions on mobility

If an ion moves through a solution under the influence of an electric field, it must continuously build up its atmosphere in front of it while the atmosphere in back of it dies out. Since this process is not instantaneous, there is an asymmetric charge distribution which tends to retard the motion of the ion. This influence on the mobility is called the asymmetry effect. A second factor which reduces the mobility is the tendency of the applied field to move the charge atmosphere, with its associated molecules of solvent, in the direction opposite to the motion of the ion. This is called the electrophoretic effect. The dependence of the mobility on concentration due to the above factors has been derived by Onsager (81).

In the treatment of the various defects in ionic solids as charged particles in a uniform dielectric medium, the electrophoretic term obviously has no meaning and is dropped.

According to the Onsager theory, the concentration

dependence of the mobility of either ion of a 1-1 electrolyte due to the asymmetry effect is

$$\mu = \mu' \left(1 - \frac{e^2 \kappa}{3D\kappa T(2 + \sqrt{2})}\right) \qquad (95)$$

where μ' is the mobility at infinite dilution. This correction factor has been applied by Teltow in his treatment of the conductivity of cadmium doped silver bromide (8). Lidiard (75) has used an extended form due to Pitts (82) in his treatment of the Debye-Hückel interactions in ionic solids.

The use of Equation 95 is correct only when there are two ions present. Except at the extremes of the pure material and heavily doped material, three "ions" are present in appreciable concentrations in the doped silver halides. The problem of solutions of electrolytes containing more than two ions has been treated by Onsager and Fuoss (83). A more workable solution has been obtained by Onsager and Kim (84); nevertheless, the relations for three ions are complicated.

It was estimated by the use of Equation 95 that the asymmetry effect decreases the mobility by two to five per cent, depending on temperature in the pure silver chloride, and about 15 per cent in silver chloride containing 8.5×10^{-4} mole per cent cadmium. Hanlon's (40) diffusion measurements indicate that the mobility of a cadmium ion-vacancy

complex in silver bromide increases by a factor of two with the addition of one mole per cent of cadmium. A large part of this increase must be due to an increase in the vacancy mobility. If the effect is linear in concentration of cadmium and of the same magnitude in silver chloride, the increase in mobility due to lattice distortions is of the same magnitude as the decrease due to the asymmetry effect. In view of this cancellation of errors and the complexity involved in correctly calculating the asymmetry effect, the assumption of constant mobilities in the present investigation is justified.

VII. SUMMARY

Vacuum distilled silver chloride with a residual polyvalent impurity of 0.1 ppm was prepared. Measurements of the conductivity of single crystals of this material doped with 0.003 to 0.6 mole per cent of cadmium or copper(I) and of crystals of the pure material were made in the temperature range 25-372°C. In the range 150-300°C measurements were accurate to ± 1.5 per cent.

The cadmium concentration was determined by atomic absorption spectrophotometry and the copper concentration by a spectrophotometric method using neocuproine reagent. These determinations were accurate to ± five per cent. Activation analysis procedures were developed for the determination of both cadmium and copper. Good results by this method were obtained for the cadmium analysis at all concentrations, but only at high concenerations for the copper analysis.

The existence of Debye-Hückel interactions between vacancies and interstitials in pure silver chloride and between cadmium ions and these defects in doped silver chloride was demonstrated. The so-called anomalous conductivity of pure silver chloride near the melting point was explained on the basis of Debye-Hückel interactions.

A number of parameters of defect formation and motion were obtained by the analysis of the isotherms of the conductivity of cadmium doped silver chloride versus concentration at temperatures in the range 203-298°C. The mole fraction of Frenkel defects, x_o, was given by $x_o = x_{oo}/\gamma_o$, where x_{oo}, the hypothetical mole fraction of defects in the absence of Debye-Hückel interactions, obeyed the relation $x_{oo} = \sqrt{2}\exp(5.2 - 1.48\text{ev}/2kT)$. The activity coefficient, γ_o, given by the Debye-Hückel theory, ranged from 0.91 at 203°C to 0.77 at 298°C. The mobilities in cm^2/V sec of the vacancy and interstitial were given by $\mu_v = 52.2/T \exp(-0.26\text{ev}/kT)$ and $\mu_i = 6.65/T \exp(-0.045\text{ev}/kT)$, respectively. The binding energy of the cadmium ion-vacancy complex was 0.6 ev.

In view of the limited concentration range to which the Debye-Hückel theory is applicable and the uncertainty in the effect of dopant on mobility, accurate measurements of the dependence of the conductivity on divalent cation concentration in the range 0.0002 to 0.01 mole per cent would be desirable in order to determine more accurate values for the defect parameters. Preferably calcium or strontium would be used to avoid the possibility of interstitial divalent ions.

The conductivity isotherms of the copper(I) doped silver

chloride indicated appreciable interstitial copper ion formation; the equilibrium constant for the reaction

lattice copper ion $\overset{K_I}{\rightarrow}$ interstitial copper ion + vacancy

was given in units of mole fraction by $K_I = \exp(10.0 - 1.03$ ev/kT) in the temperature range 253-315°C. The mobility of the copper interstitial in this range was about 0.85 that of the silver ion vacancy.

VIII. LITERATURE CITED

1. Ebert, I. and Teltow, J., Ann. Physik 15, 268 (1955).

2. Teltow, J., Z. physik. Chem. 195, 197 (1950).

3. Frenkel, J., Z. Physik 35, 652 (1926).

4. Schottky, W., Z. physik. Chem. B29, 335 (1935).

5. Tubandt, C., Leitfahigkeit and Uberfurhungszohlen in festen Elecktrolyten. In Wien, W. and Harms, F., eds. Handbuch der Experimentalphysik. Vol. 12. Pt. 1. pp. 383-469. Leipzig, Akademische Verlagsgesellschaft M. B. H. (1932).

6. Tubandt, C., Z. anorg. allgem. Chem. 115, 113 (1920).

7. Koch, E. and Wagner, C., Z. physik. Chem. B38, 295 (1937).

8. Teltow, J., Ann. Physik 5, 63, 71 (1949).

9. Kurnick, S. W., J. Chem. Phys. 20, 218 (1952).

10. Mitchell, J. W., Phil. Mag. 40, Series 7, 667 (1949).

11. Lawson, A. W., Phys. Rev. 78, 185 (1950).

12. Strelkow, P. G., Physik. Z. Sowjetunion 12, 73 (1937). [Original not available; cited in Lawson, A. W., Phys. Rev. 78, 185 (1950).]

13. Stasiw, O., Z. Physik 127, 522 (1950).

14. Christy, R. W. and Lawson, A. W., J. Chem. Phys. 19, 517 (1951).

15. Berry, C., Phys. Rev. 82, 422 (1951).

16. Kobayashi, K., Phys. Rev. 85, 150 (1952).

17. Zeiten, W., Z. Physik 146, 451 (1956).

18. Layer, H. and Slifkin, L., J. Phys. Chem. 66, 2396 (1962).

19. Nicklov, R. M. and Young, R. A., Phys. Rev. 129, 1936 (1963).

20. Fouchaux, R. C. Measurements of thermal expansion and thermal equilibrium defects in pure silver chloride. U. S. Atomic Energy Commission Report TID-19499 [Technical Information Service, AEC]. (1963).

21. Compton, W. D., Phys. Rev. 101, 1209 (1956).

22. Compton, W. D. and Maurer, R. J., Phys. and Chem. Solids 1, 191 (1956).

23. Friauf, R. J., Phys. Rev. 105, 843 (1957).

24. Miller, A. S., Ionic conductivity and diffusion in silver bromide. Astia Document AD 126-522 [Air Force Office of Scientific Research (ARDC)]. (ca. 1957).

25. Miller, A. S. and Maurer, R. J., Phys. and Chem. Solids 4, 196 (1958).

26. McCombie, C. W. and Lidiard, A. B., Phys. Rev. 101, 1210 (1956).

27. Bardeen, J. and Herring, C., Diffusion in alloys and the Kirkendall Effect. In Atom movements. pp. 87-111. Cleveland, Ohio, Amer. Soc. Metals. (c1951).

28. Lidiard, A. B., Ionic conductivity. In Flugge, S., ed. Handbuch der Physik. Vol. 20. pp. 246-349. Berlin, Springer Verlag. (1957).

29. Compaan, K. and Haven, Y., Trans. Faraday Soc. 54, 1498 (1958).

30. Friauf, R. J., J. Phys. Chem. 66, 2380 (1962).

31. Lidiard, A. B., Nuovo Cimento 7, Series 10, Suppl. 2, 620 (1958).

32. Hove, J. E., Phys. Rev. 102, 915 (1956).

33. Reade, R. F. and Martin, D. S., Jr., J. Appl. Phys. 31, 1965 (1960).

34. Noetling, J., Z. physik. Chem. 38, 154 (1963).

35. Murin, A. and Taush, Y., Doklady Akad. Nauk. S.S.R. 80, 579 (1951).

36. Tannhauser, D. S., Phys. and Chem. Solids 5, 224 (1958).

37. Lidiard, A. B., Phil. Mag., Series 7, 46, 815 (1955).

38. Schone, E., Stasiw, O. and Teltow, J., Z. physik. Chem. 197, 145 (1951).

39. Teltow, J., Phil. Mag. Series 7, 46, 1026 (1955).

40. Hanlon, J. E., J. Chem. Phys. 32, 1492 (1960).

41. Watkins, G. D., Phys. Rev. 113, 91 (1958).

42. Watkins, G. D., Phys. Rev. 113, 79 (1958).

43. Tucker, R. F., Phys. Rev. 112, 725 (1958).

44. Abe, H., J. Phys. Soc. Japan 12, 435 (1957).

45. Daehler, Max, Jr. Electron spin resonance of Mn^{2+} in AgCl. Unpublished Ph.D. thesis. Madison, Wisconsin, Library, University of Wisconsin. (1963).

46. Howard, R. E. and Lidiard, A. B., Phil. Mag. 2, Series 8, 1462 (1957).

47. Haga, E., J. Phys. Soc. Japan 13, 1090 (1958).

48. Haga, E., J. Phys. Soc. Japan 14, 992 (1959).

49. Haga, E., J. Phys. Soc. Japan 14, 1176 (1959).

50. Patrick, C. and Lawson, A. W., J. Chem. Phys. 22, 1492 (1954).

51. Christy, R. W., Fukushima, E. and Li, H. T., J. Chem. Phys. 30, 136 (1959).

52. Suzuki, Y., Endo, S. and Haga, E., J. Phys. Soc. Japan 14, 729 (1959).

53. Christy, R. W., J. Chem. Phys. 34, 1148 (1961).

54. Leddicotte, G. W., Anal. Chem. 36, 419R (1964).

55. Raleigh, H. D. Activation analysis. U. S. Atomic Energy Commission Report TID-3575 [Technical Information Service, AEC]. (1963).

56. Anderson, S., Wiley, J. S. and Hendricks, L. J., J. Chem. Phys. 32, 949 (1960).

57. Sullivan, W. H. Trilinear chart of nuclides. Washington, D. C., U. S. Govt. Print. Off. (1957).

58. Dekker, A. J. Solid state physics. Englewood Cliffs, N. J., Prentice Hall, Inc. (1961).

59. Seitz, F. The modern theory of solids. 1st ed. New York, N. Y., McGraw-Hill Book Company, Inc. (1940).

60. Debye, P. and Hückel, E., Physikal. Zeit. 24, 185 (1923).

61. Hodgman, C. D., ed. Handbook of chemistry and physics. 36th ed. Cleveland, Ohio, Chemical Rubber Publishing Co. (1954).

62. Hildenbrand, D. L. and Potter, N. D., J. Phys. Chem. 67, 2231 (1963).

63. Guthrie, A. and Wakerling, R. K. Vacuum equipment and techniques. New York, N. Y., McGraw-Hill Book Company, Inc. (1949).

64. Gusarov, A. V. and Gorokhov, L. N., Vestn. Mosk. Univ., Ser. 2, Khim 17, 14 (1962). [Original not available; abstracted in Chem. Abstr. 58, 4005c (1963).]

65. Stöber, F., Z. Kristallogr. 61, 229 (1925).

66. Spedding, F. H., Newton, A. S., Warf, J. C., Johnson, O., Nottorf, R. W., Johns, I. B. and Daane, A. H., Nucleonics 4, 4 (1949).

67. Fritz, J. S., Abbink, J. E. and Payne, M. A., Anal. Chem. 33, 1381 (1961).

68. Kraus, K. A. and Nelson, F., Proc. Intern. Conf. Peaceful Uses Atomic Energy, Geneva, 1955, 7, 113 (1956).

69. Diehl, H. and Smith, G. F. The copper reagents: cuproine, neocuproine, bathocuproine. Columbus, Ohio, The G. Frederick Smith Chemical Company. (c1958).

70. Gilat, J. and Gurfinkel, Y. Self-shielding effects in activation analysis. Israel Atomic Energy Commission Report IA-756 [Israel Atomic Energy Commission, Rehovoth]. (1962).

71. Worthing, A. G. and Geffner, J. Treatment of experimental data. New York, N. Y., John Wiley and Sons, Inc. (c1943).

72. Smith, G. C. Thesis to be submitted to Cornell University, Ithaca, N. Y. [Original not available; xeroxed copy of Figs. 4, 16, and 18 secured from Ithaca, N. Y., Department of Physics, Cornell University.]

73. Yamashita, J. and Kurosawa, T. Formation energy of lattice defects in silver chloride cyrstals. Symposium Phot. Sensitivity, Hakone, Japan. (1953) preprint. [Original not available; abstracted in Chem. Abstr. 48, 5697e (1954).]

74. Bailey, R. C. A calculation of the binding energy of a cadmium-silver vacancy complex in AgCl and AgBr. Unpublished Masters thesis. Ames, Iowa, Library, Iowa State University of Science and Technology. (1964).

75. Lidiard, A. B., Phys. Rev. 94, 29 (1954).

76. Moser, F., Burnham, D. C. and Tippins, H. H., J. Appl. Phys. 32, 48 (1961).

77. Anderson Physical Laboratory, Progress report on chemistry . U. S. Atomic Energy Commission Report TID-14651 [Technical Information Service, AEC]. (1961).

78. Junghauss, H. and Staude, H., Z. Electrochem. 57, 391 (1953).

79. Fowler, R. and Guggenheim, E. A. Statistical thermodynamics. Cambridge, University Press. (1960).

80. Harned, H. S. and Owen, B. B. The physical chemistry of electrolytic solutions. 3rd ed. New York, N. Y., Reinhold Publishing Corporation. (c1958).

81. Onsager, L., Physikal. Zeit. 28, 277 (1927).

82. Pitts, E., Proc. Roy. Soc. (London) A217, 43 (1953).

83. Onsager, L. and Fuoss, R. M., J. Phys. Chem. 36, 2689 (1932).

84. Onsager, L. and Kim, S. K., J. Phys. Chem. 61, 215 (1957).

IX. ACKNOWLEDGMENTS

The author wishes to express his appreciation to R. N. Kniseley, E. L. Dekalb, and J. F. Wolcott for their assistance with the atomic absorption measurements; to G. Wells for helpful suggestions in the design and for the construction of some of the equipment used in this investigation; to members of the laboratory glass shop for their cooperation in performing some unusual glass blowing; and to C. A. Lenhardt and L. G. Cilindro of this group for assistance with the construction of the vacuum still and performing some early experiments in activation analysis, respectively.

Especially he wishes to thank Dr. D. S. Martin for his advice, helpful suggestions and patience; Dr. D. W. Lynch for a number of valuable discussions; and his wife, Jan, who spent many, long hours assisting with the activation analysis, assisted in the preparation of the manuscript, and helped bear the disappointments met along the way.